Flood frequency analyses based on streamflow time series, historical information & paleohydrological data

Anna Haaland Aano

Thesis submitted for the degree of
Master of Science in Natural Hazards
60 credits

Department of Geosciences
The Faculty of Mathematics and Natural Sciences

UNIVERSITY OF OSLO

June 2017

Flood frequency analyses based on streamflow time series, historical information & paleohydrological data

Anna Haaland Aano

Thesis submitted for the degree of
Master of Science in Natural Hazards
60 credits

Department of Geosciences
The Faculty of Mathematics and Natural Sciences

UNIVERSITY OF OSLO

June 2017

2017

Flood frequency analyses based on streamflow time series, historical information and paleohydrological data

Anna Haaland Aano

http://www.duo.uio.no/

Trykk: Reprosentralen, University of Oslo

Sammendrag

Beregning av dimensjonerende flomverdier (20-1000-årsflommer) er et krav ved bygging av dammer, infrastrukturer og arealplanlegging. Robuste og pålitelige beregninger er viktig for korrekte risikovurderinger og for å ta best mulige beslutninger. En av de anbefalte metodene for å beregne dimensjonerende flommer er basert på årlige maksimalverdier fra en tidsserie med vannføring. Disse seriene tilpasses så en statistisk fordeling, vanligvis den generelle ekstremverdifordelingen (GEV-fordeling). En utfordring med denne tilnærmingen er at man som regel har relativt korte tidsserier med vannføring, de fleste er kortere enn 50 år. Estimat av en 200- eller 1000-årsflom er derfor basert på ekstrapolering av data, noe som inneholder store usikkerheter i beregningene. For å utvide datagrunnlaget for estimering av dimensjonerende flommer er det i denne studien benyttet informasjon om flommer fra før systematiske observasjoner av vannføring ble igangsatt; (i) historiske flomkilder (f.eks. flomsteiner) og (ii) paleohydrologi – flominformasjon fra sedimentprøver er undersøkt.

I dette studiet er kjerneprøve FLS113 (18.0 cm lang, representerer omtrent de siste 65 årene) og FLS213 (516 cm lang, representerer trolig de siste 10 000 årene) fra Flyginnsjøen brukt. Ved å studere sedimentene i FLS113 kan man finne igjen karakteristiske flomlag for når Glomma var i flom og vannføringen oversteg terskelen, som i dag er beregnet til 1500 m^3/s. Resultatene viser at det er en sammenheng mellom bifurkasjonshendelser i Glomma ved Kongsvinger og sedimentlag i kjerneprøver fra Flyginnsjøen. Dette gir grunnlag for å bruke paleohydrologi til å forlenge flomhistorien og dermed basere flomfrekvensanalysen på lengre datagrunnlag utover det instrumentelle målinger kan gi.

De tidligste instrumentelle målingene startet rundt 1870. Historisk informasjon brukt i dette studiet legger til ni flommer i perioden 1650-1850 og paleohydrologisk informasjon legger til 155 flommer siden år 1200. Nye flomfrekvenskurver er laget på bakgrunn av denne utvidede flominformasjonen og man kan, ved å sammenligne disse med tidligere flomfrekvenskurver, se at det utgjør en forskjell. I diskusjons-kapittelet diskuteres det hvorvidt de ulike informasjonskildene og lengden på perioden med informasjon, har av betydning for flomfrekvensanalysene.

Resultatene viser generelt at ved å inkludere historiske flomhendelser øker vannføringen for forventede gjentaksintervaller, mens ved å inkludere paleohydrologisk flomdata minker vannføringen for forventede gjentaksintervaller, sammenlignet med flomfrekvensanalyser basert på systematisk data.

Bruken av historisk informasjon i flomfrekvensanalyse anses å være av verdi, da beregningene blir gjort på utvidet grunnlag om flomhistorien. Spesielt er det nyttig i beregninger av lengre gjentaksintervaller der det kun finnes korte instrumentelle måleserier. Å bruke paleohydrologisk flominformasjon i flomfrekvensanalyse er en nyere og meget spennende metode som det trengs å forskes mer på.

Abstract

Estimation of design floods (20 – 1000-years floods) is a requirement when building dams, infrastructure and areal planning. Therefore, to make the best decision possible, it is important to have robust and reliable estimations of the flood risk. One of the recommended methods to estimate the design flood is based on yearly maximum values from a long time series with water discharge. Then these yearly time series are fitted to a statistical distribution, most commonly the general extreme value (GEV) distribution. One of the challenges is the relatively short time series of values of discharge, rarely larger than 50 years. Estimate of a 200- or a 1000-years flood is therefore based on extrapolation from the data, and these estimations can contain large uncertainties. To extend the flood records the design floods are based upon, it is in this study obtained flood information from the period before the systematic measurements started; (i) historical flood information (e.g. flood monuments) and (ii) paleohydrology – flood information from sediment cores are investigated.

In this study, sediment cores FLS113 (18.0 cm long, representing the last approximately 65 years) and FLP213 (516 cm long, representing the last 10 000 years) from Flyginnsjøen are used. By studying core FLS113 one can find characteristic flood layers for when Glomma was flooded and the water discharge exceeded the threshold, which today is approximately 1500 m^3/s. The results show that there is a relationship between bifurcation events in Glomma at Kongsvinger and the sediment layers in cores from Flyginnsjøen. This provides the basis for using paleohydrology to extend the flood history and therefore base new flood frequency analyses on longer data records than what instrumental measurements can provide.

Instrumental measurements started around 1870. Historical information used in this study adds nine floods in the period 1650-1850 and paleohydrological information adds 155 floods since year 1200. New flood frequency analyses are made based on this extended flood information, and one can, by comparing these with previous flood frequency analysis, see that this makes a difference. In the discussion-chapter, it is discussed how the different types of information sources and the length of the period with information influences the flood frequency analysis.

The results show that by including the historical flood history, the water discharge for design floods will generally increase, and by including paleohydrological flood information, the water discharge for design floods will generally decrease, compared to flood frequency analyses based on modern, instrumental data.

The use of historical information in flood frequency analysis is assessed to be valuable, because the estimated are done on an extended flood record. It is useful especially for short record lengths and long return periods. The use of paleohydrological information in flood frequency analysis is a newer and interesting method that needs further research.

Preface

When I was only two and a half years old, my family and I went to Hunderfossen – an amusement park located next to Gudbrandsdalsågen in Oppland. I do not remember much from this vacation, but I was so disappointed to find out that half of the park was closed because large amount of water covered big parts of the park. Gudbrandsdalsågen makes, together with Mjøsa and Vorma, the west part of Glomma's catchment. The time was July 1995, and the cause of the water was Vesleofsen – as the flood was named. This is the largest flood that has happened in Norway since instrumental measurements started in the 1850s, and is believed to be one of the biggest floods in Norwegian history. Maybe my interests for floods started here …

Or maybe it started even before I was born. My family name actually means "the river", as my ancestors lived by a river in western Norway.

Anyway: I really want to thank all my supervisors;
Kolbjørn Engeland – thank you for being patient, kind and for guidance through this year. Thank you for everything you taught me through our conversations, meetings and for answering all my e-mails.

Eivind Støren – thank you for teaching me all I needed to know about CT-scanning, and how this can be used to obtain flood information from sediment cores. Thank you for the week we spent together in the EARTHLAB at the University in Bergen, and your attendance on the meetings through skype.

Chong-Yu Xu & Nils Roar Sælthun – thank you for good feedback, and thank you for the time we spent together in Wuhan, China, where I got to present my work and where I learned a lot about a lot!

I also want to thank Erik Holmqvist and Lars-Evan Pettersson for information about bifurcation events in Glomma at Kongsvinger and also Norsk Skogmuseum (The Norwegian Forest Museum) for information about the flood monument at Elverum.

I have been lucky and glad to have had four supervisors guiding me and providing me help, but there were also some challenges due to this – I had to relate to several supervisors (sometimes with different opinions) located in two cities, and I did my best as a middle(wo)man.

Challenges due to the study have also been present; combining more than one field of disciplines, and the combination of three information sources, each with different lengths and level of details have been challenging. This year's work has been extensive; I have done CT-scanning in Bergen, attended a study trip to Wuhan where I presented my master thesis and went to relevant excursions, obtained historical flood information, learned how to use statistical program (R: The R Project for Statistical Computing) in flood frequency analysis, and I have become more independent and more confident with my own work. Despite the challenges, I am happy with my results, and the learning outcome of this year has been huge.

There have been periods with adversity and times I felt stuck during my master thesis. I really want to thank my supportive family and all my friends who have been cheering for me and encouraged me the whole time! This master-thesis-writing-year has had its ups and down, and I really appreciate all the help and supportive words I have got!

Anna

List of contents

Sammendrag v
Abstract vi
Preface vii
List of contents viii
List of figures ix
List of tables xi
1 Introduction 1
1.1 Societal relevance of floods – motivation for the thesis 1
1.2 Flood estimation method 2
1.3 Objectives 4
1.4 Outline of the thesis 4
2 Theoretical background 5
2.1 Floods and flood regimes in Norway 5
2.2 Flood conditions in Norway 7
2.3 Transportation of sediments 9
2.4 Flood frequency analysis (FFA) & paleohydrology 10
3 Study site and data 12
3.1 Glomma, Vingersjøen and Flyginnsjøen 12
3.2 Flood data 16
3.2.1 Instrumental data 16
3.2.2 Historical data 20
3.2.3 Paleohydrological data – sediment cores 22
4 Methods 26
4.1 Instrumental data & bifurcation events 26
4.2 Historical data analysis 28
4.3 Paleohydrology – sediment analysis 29
4.4 Use of historical and paleohydrological data in flood frequency analysis 32
4.4.1 Flood frequency analysis 33
4.4.3 Return level graphs 36
5 Results 38
5.1 Instrumental flood information 38
5.2 Historical data analyses 38
5.3 Paleohydrology – sediment cores 40

5.4 Flood frequency analysis – return levels 50
6 Discussion 58
6.1 Paleohydrological flood information; bifurcation events & flood layers 58
6.2 Historical flood information 62
6.3 Systematic data 64
6.4 Combining systematic-, historical- and paleohydrological flood information 65
6.4.1 Comparing 1000-year floods 66
7 Conclusion 67
Appendix 69
References 70

List of figures

Figure 1) Map showing flood affected areas during Storofsen in 1789 (NVE, 2011). 1
Figure 2) Schematic description of the response time in a river in Western Norway (Øyungen) and a river in Eastern Norway (Glomma) (Sælthun, 1999). 5
Figure 3) The main flood regimes in Norway; green refers to snowmelt floods, red refers to rainfall floods, yellow refers to combination floods (and purple refers to glacier floods) (Stenius et al., 2014). 6
Figure 4) Precipitation frequency and mean precipitation sum in Southern Norway, due to circulation type SE (two upper maps) and circulation type SW (two lower maps) (Hanssen-Bauer et al., 2009). 8
Figure 5) The Hjulström-diagram shows the relationship between the size of sediments and the velocity required to lift a particle of a certain size (GEOCACHING, 2011). 9
Figure 6) Study site, showing Glomma's catchment, 2.604 Elverum station and 2.2 Nor station at Kongsvinger (NVE, 2017). 12
Figure 7) Map over soils in Kongsvinger area (NGU, 2017). 13
Figure 8) Map showing Kongsvinger-area. The green arrows illustrate Glomma's normal waterflow, while the red arrows illustrate Glomma's interaction with Vingersjøen and Flyginnsjøen during bifurcation (Steffensen, 2014). 14
Figure 9) The map shows the saddle point (the lowest point) between Glomma and Vingersjøen. The "normal" water level (07.07.1967) shows the waterflow during normally conditions. The flood water level (03.06.1967) shows the waterflow during bifurcation, when water exceeds the threshold and flow over to Flyginnsjøen (Støren, 2017). 15
Figure 10) Bifurcation events in Glomma at Kongsvinger from 1950-2013 (Pettersson, 2001; updated by Aano, 2017). Years on x-axis and transferred water amount (mill m^3) is shown on the y-axis. For the years with both spring- and autumn floods (1957 & 1987), only the spring flood is represented. 18
Figure 11) AMS-values from 2.604 Elverum (unregulated period, 1971-1936). Years on x-axis, discharge (m^3/s) on y-axis). 19
Figure 12) AMS-values from 2.604 Elverum (regulated period; 1937-2015). Years on x-axis, discharge (m^3/s) on y-axis). 19
Figure 13 A) Flood monument at Grindalen (Sælthun, 2016) and B) flood monument at Elverum Forest Museum (Wikipedia, 2017). 20
Figure 14) Age (x-axis) and flood heights (cm) (y-axis) of the historical floods from Elverum flood monument (Nesje et al., 2001). 21

Figure 15) Picture of sediment core FLS113 (18.0 cm long), bottom side to the left, top to the right. The green on the top and bottom of the core is flower oasis..... 22
Figure 16 A-D) Picture of sediment core FLP213 (516.0 cm long). 22
Figure 17) Sediment core FLS113 with selected proxies and a picture of the core (Steffensen, 2014). The x-axis shows the depth of the core (age increases with depth), and the y-axis shows the concentration of Potassium (K), Calcium (Ca), Titanium (Ti), Iron (Fe), Rubidium (Rb) and Strontium (Sr) (all with unit kcps), and BW (black-and-white-scale, from 0-225, where 0 is black and 225 is white)... 23
Figure 18) Results from measurements on sediment core FLP213 (Steffensen, 2014).. The graphs ^{14}C and SediGraph show where in the core the samples are taken. The BW-graph shows the black-and-white picture, from 0-225, where 0 is black. The y-axis of the XRF-data (K-Sr) have unit kcps. MS is in SI-unit, LOI is in % and DBD and WC is in unit gram per cm^3. 24
Figure 19) Number of floods through Holocene, with thresholds Potassium (K) P94 (blue) and Titanium (Ti) P94 (red). 25
Figure 20) Rating curve between the discharge (m^3/s) in Glomma at Kongsvinger (x-axis) and the water level (m) in Vingersjø (y-axis) made by Pettersson. 27
Figure 21) Curve showing relation between the discharge (m^3/s) at Nor/Nors Bru (x-axis) and the water level (m) in Vingersjøen (y-axis) made by Pettersson. 27
Figure 22) The graph shows the relationship between the AMS-values at Elverum station (blue) and Nor station (red), and the difference between them (grey). 28
Figure 23) Regression line between the AMS-values at 2.604 Elverum (x-axis) and 2.2 Nor (y-axis)..... 29
Figure 24) Model showing the relation between sediment layers, the change in the parameter and the rate of change over time (Støren et al., 2010). 30
Figure 25) Illustration of how to include historical flood information in the Bayesian approach. The number of years in historical period (h) is in this example 100, the number of observation from systematic data (N) is 20 and the perception threshold (x_0) is 6842 m^3/s (Dirceu & Stedinger, 2005).. 34
Figure 26) Rating curve from Elverum flood monument showing the relationship between discharge values (x-axis) and water levels (y-axis). The six red points refers to the known flood sizes (discharge values)..... 39
Figure 27) Picture of sediment core FLS113 with cm-scale. 40
Figure 28) Age-depth model (based on FLS213) shows the relationship between the depth in the core and the age. Error bars show the uncertainties which increases with increasing depth. 41
Figure 29 A) Sediment core FLS113 from Avizo 3D. White is dense layers, black is low-density layers. B) 3-dimensional CT-image of sediment core FLS113 showing near horizontal high-density layers (green/yellow) deposited in a low-density background matrix (blue). 42
Figure 30) Relationship between bifurcation events (blue) and sediment layers with threshold RoC P92 (red). Error bars indicate age uncertainty on the sediment layers. 43
Figure 31) Greyscale values along the spline line in FLS113, and the bifurcation events plotted together. The x-axis shows the depth in the core, the right y-axis shows the greyscale values, and the left y-axis shows the transferred water amount of the bifurcation events..... 44
Figure 32) Close-up pictures of potential flood layers in sediment core FLS113, obtained by Avizo 3D. Yellow refers to the densest layers, while orange/dark red refers to less dense layers. The density threshold in picture B) is set higher than in picture A). 45
Figure 33) Close-up picture of sediment core FLS113 at approximately 9-10 cm depth, showing potential flood layers corresponding to the floods in spring 1987, and the floods in spring and autumn 1986 (Støren, 2017). 45
Figure 34) Graph showing the return levels using systematic data from 2.604 Elverum (black) from 1871-1936 and historical flood information (green and red). 51

Figure 35) Graph showing return levels using systematic data from 2.604 Elverum from 1871-1936 (black), paleohydrological flood information (blue) and combined flood information (turquois). 51
Figure 36) Return level graph will all flood information sources; systematic data (black), historical data (green and red), paleohydrological flood information (blue) and combined flood information (turquois). 52
Figure 37) Return level plot, using AMS-values from 2.604 Elverum for the period after the regulations. Systematic data (black), historical information (green and red), paleohydrological flood information (blue) and combined flood information (turquois). 53
Figure 38) Return level plot, using AMS-values from 2.604 Elverum for the whole period. Systematic data (black), historical information (green and red), paleohydrological flood information (blue) and combined flood information (turquois). 54
Figure 39) Return levels using systematic data from 2.604 Elverum from the last 60 years (black) and historical data (green and red) and flood information from paleohydrological data (blue) and combined flood information (turquois). 55
Figure 40) Return level plot, using systematic data from 2.604 Elverum for the last 30 years (black), historical data (green and red), flood information from paleohydrological data (blue) and combination of these sources (turquois). 56
Figure 41) This figure shows return levels of design flood Q20, Q200 and Q100 using unregulated systematic data from 2.604 Elverum, and additional flood information sources, as well as estimations made by Pettersson (2000). 57
Figure 42) CT-scan of sediment core FLS113. On the left side, the depth in cm, and on the right side, the corresponding ages. 59
Figure 43) Return levels where Storofsen have been given different sizes, to see how/if this (extreme) flood influence the return levels significantly. Storofsen as a 100-year flood (black), as a 1000-year flood (red), as a 5000-year flood (green), as a 10 000-year flood (blue) and excluded (turquoise). 63

List of tables

Table 1) Hydrological stations in Kongsvinger area (Pettersson, 2001; NVE, 2017). 17
Table 2) Bifurcation events in Glomma at Kongsvinger from 1950 to 2013 (Pettersson, 2001; updated by Aano, 2017). 18
Table 3) Layout of CT-table. 32
Table 4) Table showing year, transferred water amount, duration, maximum discharge and dates for the bifurcation events from 2000-2013. 38
Table 5) Table showing year, heights, and estimated discharge values at Elverum and Nor stations. .. 39
Table 6) CT-tables for the different thresholds (RoC P94, RoC P92, RoC P90, greyscale P94, greyscale P90), correlation between the different thresholds and the bifurcation events and the CSI-values. 46
Table 7) Correlation (and corresponding p-value for the best correlation) for running windows (3-, 4-, 5- and 10-years running windows). 47
Table 8) Sediment layers detected using RoC P92 of greyscale as the threshold. Column 1 shows the number of dense layers, column 2 shows the greyscale values and column 3 shows the age (from age-depth-model) of these layers. 48
Table 9) Table showing the tuned alternative, based on threshold RoC P92 of greyscale vales. 49
Table 10) CT-table and CSI-value for tuned alternative. 50

Table 11) Design floods with corresponding discharge values, using different types of flood information. Units: m3/s. Highest values are marked with bold text and lowest values are marked with italic text. 52
Table 12) Design floods with corresponding discharge values, using different types of flood information. Units: m3/s. Highest values are marked with bold text and lowest values are marked with italic text. 53
Table 13) Design floods with corresponding discharge values, using different types of flood information. Units: m3/s. Highest values are marked with bold text and lowest values are marked with italic text. 54
Table 14) Design floods with corresponding discharge values, using different types of flood information. Units: m3/s. Highest values are marked with bold text and lowest values are marked with italic text. 55
Table 15) Design floods with corresponding discharge values, using different types of flood information. Units: m3/s. Highest values are marked with bold text and lowest values are marked with italic text. 56
Table 16) Design levels based on Storofsen with different sizes and where Storofsen is excluded from the flood frequency estimations. The highest numbers are written in bold text, and the lowest numbers are written in italic. 63
Table 17) Return level estimation at Kongsvinger (Pettersson, 2000). 65
Table 18) Return levels for the 1000-year flood using different length of systematic data and different types of additional flood information sources. The highest values are written in bold text, while the lowest values are written in italic. 66

1 Introduction

Floods are one of the most common natural hazards; they happen all over the globe, and are some of the most devastating geohazards in the world. The consequences can be disastrous, and floods affect the economy, environment, infrastructure, animals and people. According to United Nations Environmental Program's (UNEP) climate program IPCC (International Panel on Climate Change), the extreme weather is expected to increase in the future (IPCC, 2012). To improve the estimation of critical flood sizes is therefore crucial.

1.1 Societal relevance of floods – motivation for the thesis

During floods, infrastructure like roads and bridges, dams, farms, houses and automobiles can be destroyed. People become homeless and are often in need of urgent shelter. Drinking water can be polluted, and lead to sickness for people who drink it. The emergency services like firemen, policemen and medical care need to help the affected people. All these things come at a heavy cost to people and the government in the affected area. It usually takes years for flood damaged and affected communities to be re-built and the business to come back to normal.

Year 2011 was a major flood year in many parts of the world, and in the USA alone, the floods in 2011 (represented in hydrological year, which is from October until the next September) costs the country more than 9.1 billion US Dollars and caused 113 fatalities (NWS Internet Services Team, 2015).

Flood is becoming a matter of increased concern for the UK as well, and river flooding alone cost Britain about £475 million each year (CEH, 2016).

The catastrophic flood that happened in China in 1931 is probably the worst flood in living memory. The number of fatalities have not been verified, but Chinese authorities claim that approximately 140 000 people lost their lives in this devastating flood, and economic damage was 566 000 000 USD (Yen, 1993).

In Norway, flooding is the natural hazard that leads to the biggest economic losses, year after year (Roald, 2013). The flood that happened in July 1789 is probably the largest flood in Norwegian history, and it affected huge parts of mid- and east-Norway (see map, Figure 1). Storofsen, as the flood is called, caused 61 fatalities and disastrous destructions on infrastructure, farms and crops, causing huge economic losses (Sælthun, 1999). Approximately 1500 farms got tax reduction because of the flood damages (NVE, 2016).

The floods in Glomma in spring 1966 and 1967 were both characterized as 100-year floods (Roald, 2013). The cold winter in 1966/67 followed by an abrupt increase in temperature resulted in the biggest spring flood since 1934 (Roald, 2013). The flood in 1967 caused huge damage; 15 000 acres were flooded, approximately 1200 houses had water damages, and the extent of damage was calculated at 35 million NOK (Roald, 2013).

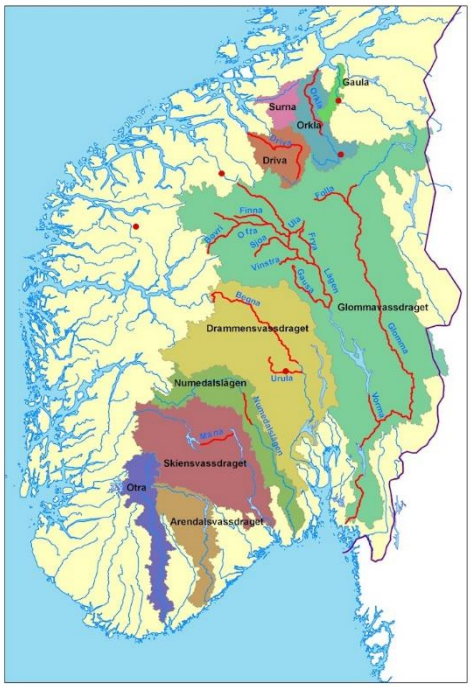

Figure 1) Map showing flood affected areas during Storofsen in 1789 (NVE, 2011).

The great flood in Eastern Norway in spring 1995, called Vesleofsen, is the biggest flood since the instrumental measurements started in the 1850s. This flood caused 1 fatality and the extent of damage has been estimated at up to 1.8 billion NOK (Roald, 2013).

Recent years have seen some particularly extreme flooding events, and storms are only getting more frequent and more severe with climate change. The estimation of design floods is therefore of huge importance and becoming a matter of increased concern (Engeland et al., 2017; Vormoor et al., 2016).

1.2 Flood estimation method

Estimation of design floods (20–1000-year floods) is a requirement when building dams, infrastructure and areal planning. TEK 10 (2016) is a guidance made for technical requirements for construction work. One of the chapters deals with flooding processes and indicates the level of safety to be taken into account when building in hazard prone areas (TEK 10, 2016). Therefore, to make the best decision possible, it is important to have robust and reliable estimates of the flood risk.

The recommended method for the estimation of flood sizes with a given return period is called flood frequency estimation (Midttømme et al., 2011). Flood frequency analyses can be performed using observed instrumental data based on single measurement series or a selected series within the same region, which is analysed together to decide a regional distribution function. Using flood frequency analyses, the distribution which is best fitted to the data, is used – especially for the large floods. This is done based on assessments of several distributions. Usually the Gumbel distribution (EV1) is used – a two-parameter distribution, or the General Extreme Value (GEV) distribution – a three-parameter distribution. To obtain a picture of the regional pattern of flood distributions and to control that the measurement series do not give extreme distribution, it is necessary to do several flood frequency analyses for several stations in the area (Midttømme et al., 2011).

The flood frequency estimation today is usually based on systematic streamflow data from gauging stations. The longest series in Norway contains maximum 145 years of data, but most series contain less than 50 years of measurements. The water level and the water flow are important and necessary for estimation of flood frequency, and to evaluate the risk of extreme flooding in the future. Design flood sizes are used as the basis for areal planning (TEK 10, 2016) and dam safety (500-1000-year floods). The GEV-distribution can be adapted to the flood data to give an estimated exceedance probability and return levels for floods. Based on regular measurements of water discharge in a river, one can see how common a specific flood of a certain size is.

A flood frequency curve shows the relationship between flood size and the exceedance probability or return period of a flood. In areas where long flow records are available, the flood frequency curve can be estimated using flood peak data from this site alone. More commonly, where the site is either un-gauged or has insufficient flow records for design, the flood frequency curve is estimated using data pooled from a group of comparable sites. Methods are presented for selecting appropriate gauged sites for pooling and for combining the data (Sælthun, 1997; CEH, 2016).

Challenges linked to flood danger, areal planning, infrastructure, water politics and water supply are usually built and estimated on a basis that presupposes stationarity in the hydrological circle. One assumes that the period with instrumental data is also representative for the future. But in a changing climate, this is a problematic prerequisite (Milly et al., 2008), particularly as the period for these calculations, may has been a period with minor changes compared to what is expected in future (IPCC, 2007). The consequences of a changing climate are that the estimations of expected flood sizes and return levels are not representative of longer time perspectives (Støren & Paasche, 2014). Given the

expected variations (non-stationarity) of flood magnitudes in the future, new approaches are needed for the analyses of non-stationary series (Wilson et al., 2011). The flood frequency analysis presupposes stationarity, but the processes are believed to be non-stationary. This is, therefore, a drawback with the conventional flood frequency analysis approach (Wilson et al., 2011).

Another challenge due to the flood frequency estimation is the short data series used to estimate return levels for big floods. Even 145 years of data can lead to an important estimation uncertainty when estimating a 500- or a 1000-year flood. Limited data is the major drawback of this approach. Despite the accuracy of this type of data, the challenges of predicting future scenarios based on few and short time series are difficult and uncertain.

Extrapolation is used where data is limited or missing. It is hard to do good extrapolation based on limited measurements, and the probability of failure or misinterpretation is substantial. Extrapolating should be avoided if possible, because the uncertainty increases with increasing return period. If it is necessary to extrapolate after all, this should be done only as far as necessary and preferably only up to double the length of the record (Wilson et al., 2011). Limited data is the main drawback with flood frequency analysis. Therefore, there is a great need to extend the data basis beyond the information the instrumental data can provide.

Adding historical flood information is one way to extend the flood records. Historical flood information can be obtained from, for example, flood marks on stones or buildings, old documents, tales and stories (Roald, 2013). This type of information is often subjective and can be inaccurate. Flood marks give water levels of floods, while systematic information provides discharge values. When the exact flood discharge is unknown, the information if a flood was above or below a specific perception threshold can be used as valuable, additional flood information (Kjeldsen, 2014). Several researchers have shown that just knowing that a flood exceeded a specific perception threshold can add significant value to the flood frequency analysis (e.g. Stedinger & Cohn, 1986; Cohn & Stedinger, 1987; Payrastre et al., 2011). Different quantitative methods have attempted to extract the information contained in historical data using a variety of approaches – where the most common approach is to consider a perception threshold for a historical period, with the assumption that each flood exceeding this threshold has been recorded (e.g. NERC, 1975).

Historical data add valuable information about the flood history before the systematic measurements started. Using historical information can lengthen the flood records from approximately 145 years to 300-400 years of flood history.

Another source of information is the flood history saved in sediments at the bottom of lakes. During a flood, sediments can be transported and later deposited. If the conditions are right, flood sediments can be kept and preserved at the bottom of lakes and flood plains undisturbed for thousands of years. Sediment cores from certain lakes might therefore be used as flood archives, containing characteristic layers representing the floods. Such paleohydrological data can lengthen the flood history thousands of years. An important complication when considering paleohydrological flood data is the impact of a changing environment (i.e. changes in climate and land-use, or river engineering works) on the characteristics of the flood series, and how to include this impact in future predictions (i.e. Gilli et al., 2013; Kjeldsen, 2014; Støren & Paasche, 2014).

1.3 Objectives

The primary objective of this study is to assess how combinations of systematic flood records, flood information from historical sources, and paleohydrological information improve flood frequency estimation. Standard flood frequency methods usually use systematic data only, and in a few cases historical flood information, so this is a relatively new and innovative study, which desirably will improve the flood frequency analysis.

To answer the primary objective, three sub-objectives must be done;

1) Investigate if historical flood information used to lengthen the flood records can improve the design flood estimations. To do so, the following must be done;
    a. Identify flood levels from historical information, and estimate corresponding discharge values.
    b. Add this information into flood frequency analysis.
2) Investigate if paleohydrological information can be used to lengthen the flood record. To do so, the following must be done;
    a. Identify if there is a link between sediment layers in cores from lakes, and flood events, and subsequently use this link to estimate the rate of flood occurrences from paleohydrological data.
    b. Add this information into flood frequency analysis.
3) Calculate design flood sizes combining information from instrumental data (direct streamflow observations) with historical flood information and paleohydrological information.

The unique contribution of this study is to combine the three different information sources in flood frequency estimations. The difference in lengths and levels of details of these sources is challenging; (i) instrumental data is considered accurate, but cover a short time period, (ii) historical information is less accurate, but covers a longer time period, and (iii) paleohydrological data is also less accurate, but can cover thousands of years of history.

1.4 Outline of the thesis

This thesis will answer the questions presented in the introduction chronological and systematic, based on chaptering.

Chapter 1 introduces societal relevance of floods, why flood frequency analysis is important, the main methods used and the objectives of the thesis. Chapter 2 contains theoretical background explaining the main flood regimes in Norway and the processes causing floods, the function of running water (flood), why this is important and how it can be used in the study of sediment cores. The extended flood frequency analysis is also explained theoretically in this chapter. Chapter 3 introduces the study site which is Glomma (mainly upstream Kongsvinger), the lakes Vingersjøen and Flyginnsjøen. Chapter 3 also presents the three types of data used in the thesis; instrumental data, historical data and paleohydrological data. Chapter 4 explains the methods used to analyze the data, and in chapter 5 the results are presented and explained. In chapter 6 the results are discussed, and in chapter 7, conclusions are listed. At the end, references and appendix containing tables, figures and scripts from R are shown.

2 Theoretical background

2.1 Floods and flood regimes in Norway

There is no unambiguous definition of flood, but one common way to describe flood is "when a large amount of water covers an area of land that is usually dry" (Roald, 2013).

It is the climatic and physiographic conditions in the catchments that influence the flood conditions. As a main rule, it is rainfall that causes flooding – especially high-intensity rainfall with duration corresponding to the concentration period of the watercourses (Midttømme et al., 2011). The concentration period varies from a couple of minutes in urban areas to weeks in big catchments like Glomma or lakes with narrow outlets. Snowmelt can also cause flooding in many parts of the country, but when the damaging floods occur, it is usually caused by rainfall or a combination of rainfall and snowmelt. One exception in Norway is Finnmarksvidda, where the elevation differences are small, and where an increase in temperature will result in intense snowmelt covering huge areas at the same time.

Nevertheless, the largest floods in Norway usually occur when rainfall is combined with other adverse conditions like snowmelt, saturated ground because of previous rainfall or frozen ground (which make the ground impermeable) and catchment properties, such as lake percentage and amount of soils (Midttømme et al., 2011).

The main flood types in Norway can be characterized as either spring/summer floods or autumns/winter floods (Stenius et al., 2014), and should therefore be treated statistically different. The flood regimes in Norway are based on which season the biggest floods normally appear.

Spring/summer floods are when the largest flooding usually occurs during May-June. These floods are mainly caused by snowmelt, but often in combination with rainfall. They have relatively long durations and large volumes. The size of the flood increases slowly with increasing return period (Midttømme et al., 2011).

Autumn/winter floods are when the largest flooding usually occurs in September-November. These floods are mainly dominated by rainfall. They often have shorter duration, which is mainly caused by intense rainfall. The size of the flood normally increases relative to increasing return period. The rainfall floods have a more pronounced course than the snowmelt floods (Figure 2), and the difference between culmination discharge and daily average discharge is usually higher than in pure snowmelt floods (Stenius et al., 2014).

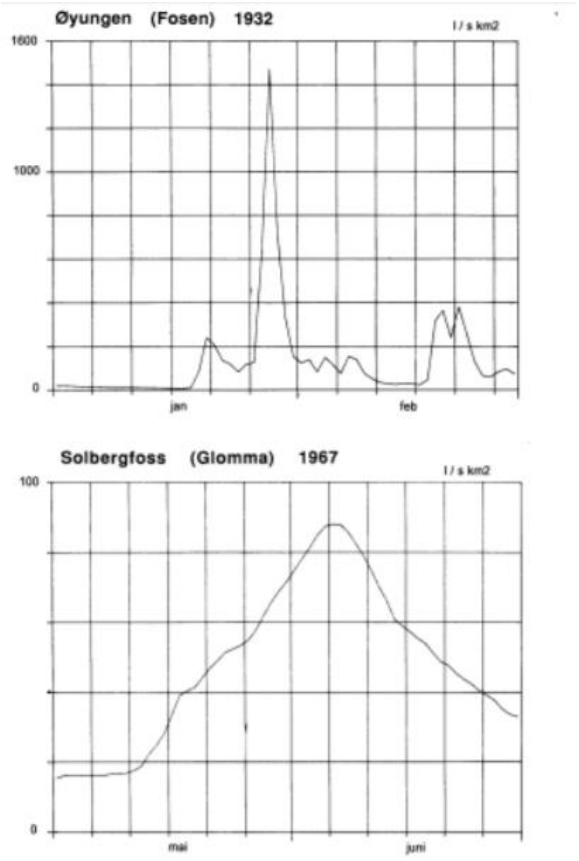

Figure 2) Schematic description of the response time in a river in Western Norway (Øyungen) and a river in Eastern Norway (Glomma) (Sælthun, 1999).

Other types of floods are for example urban floods, flash floods, ice jam floods, landslide-induced floods and dam-break floods (Killingtveit, 1996). Nevertheless, in this study the focus is floods in big catchment, so further in this thesis the focus will be on rainfall floods, snowmelt floods and the combination of these two. The largest floods in Norway are the ones caused by a combination of both snowmelt and heavy precipitation (Roald, 2013; Eikenæs et al., 2000). This was the case with two of the largest floods known in Norwegian history – Storofsen (1789) and Vesleofsen (1995).

Even if an area is characterized by a certain flood season or flood causing feature, such as spring flood or autumn flood, this does not mean that one or more floods will not occur in other parts of the year. It mainly indicates the dominating flood season or flood causing effect, but there can, of course, occur other types of floods from time to time (Stenius et al., 2014).

The differences in characterization in the rivers in western- and eastern Norway are part of the reason for the different main flood types occurring. The rivers in the west usually have small catchments and short river channels. Heavy precipitation will then often result in flooding of these rivers, so the western and coastal parts of Norway are most prone to rainfall floods.

Snowmelt floods happen regularly all over Norway. They happen when the snow in the mountains starts to melt due to temperature increase. The snowmelt-floods dominate the big catchments in the central parts of eastern Norway, where the rainfall floods are less important. The rivers in the east have bigger catchments and longer river channels, so flooding here is a slower process. When snow melts and eventually fills up the rivers, flooding may occur. A significant factor here is the amount of snow that falls during winter time, which is of great importance for the snow magazines and the amount of snow available when spring comes and the temperature increases. Large amounts of snow in the magazines leads to more available snow to melt and thus presents a bigger risk for flooding.

Figure 3 shows the distribution of the different types of flood types in Norway. Red refers to rainfall floods and yellow refers to combination floods which are most common in the coastal areas. Green refers to snowmelt floods which are most common in the inland and the eastern parts of Norway. Purple refers to glacier floods which are most common in the inland.

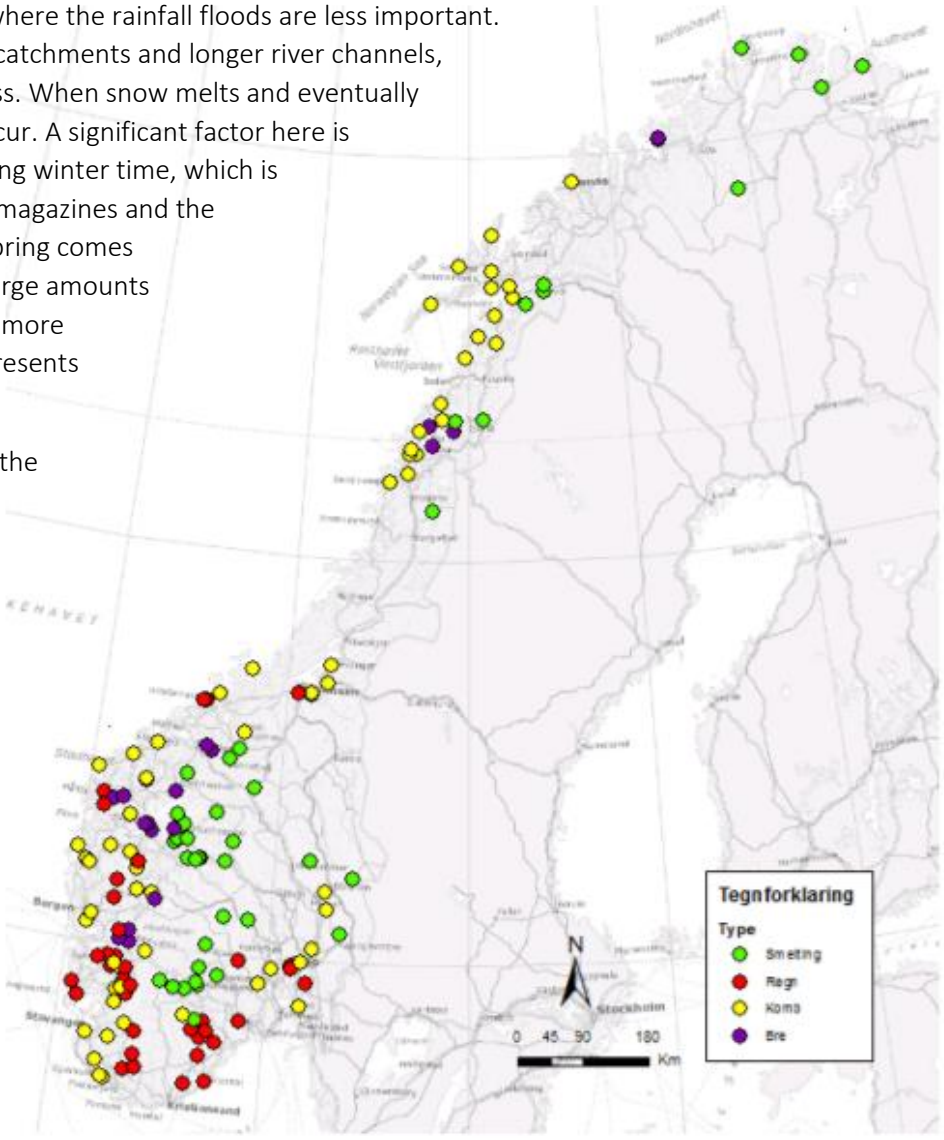

Figure 3) The main flood regimes in Norway; green refers to snowmelt floods, red refers to rainfall floods, yellow refers to combination floods (and purple refers to glacier floods) (Stenius et al., 2014).

2.2 Flood conditions in Norway

Because precipitation is the main cause of flooding, precipitation distribution is significant. Figure 4 shows the precipitation frequency in Norway, depending on the wind direction. The two upper maps show the precipitation frequency with circulation type SE (south-east), while the two lower maps show the precipitation frequency with circulation type SW (south-west). There is a clear difference between the distribution of precipitation in Norway, and the mountains separating west from east play a key role for precipitation distribution and therefore the regional flood pattern. Humid air coming from the west is forced upward because of the mountains – and result of this is release of humidity as precipitation. A large amount of precipitation is, thus, not unusual in Western Norway. Heavy rain in small catchment makes the rivers flood. The large catchments in Eastern Norway have a longer response time, making snowmelt (continuous adding of water to the rivers over a larger expand of time) the main reason for floods (Sandersen et al., 1997; Støren et al., 2010).

The weather pattern in Norway explains why rainfall floods are more common in the coastal areas than in the inland. The weather and precipitation condition in Norway is strongly influenced by the strength of the westerlies. An indicator for this wind relation is called the North Atlantic Oscillation (NAO). The NAO describes the pressure differences between the low pressure over Iceland and the high pressure over the Azores. The influence the NAO has on the climate in Norway is most distinct during winter, but can be tracked throughout the year (Hanssen-Bauer et al., 2009). In periods with positive NAO-index, the westerly storm tracks will be routed towards Scandinavia, warm and humid higher air masses will occur at the west coast of Norway and cause heavy precipitation and strong wind, whereas Eastern Norway will be in a rain-shadow, receiving less precipitation. During other circulation patterns the precipitation will be distributed differently. When the wind comes from southeast, there will be more precipitation in the eastern and southern parts of Norway, than in the western parts (Uvo, 2003; Hanssen-Bauer et al., 2009).

If the atmospheric circulation pattern changes, even slightly, it will have huge influence on the precipitation distribution in Norway. Therefore, potential future changes in the low-pressure systems or the atmospheric circulation will be of great significance for the future precipitation distribution and the precipitation development in Norway (Hanssen-Bauer et al, 2009). Precipitation has been measured in Norway in many years – some places the records extend more than 150 years back in time, and they are distributed all over the country. When hydropower became of interest in the late 19th century this nationwide network of precipitation measuring stations was established. Even if there are many measuring stations all over the country – all the places are not evenly covered. Another possible source of error is the elevation of the measure gauges. It is easier to place them in the lowland, and this is also the reason that there are few gauges in the mountains (Hanssen-Bauer et al, 2009).

Since 1900, the yearly precipitation rate in Norway has had an increase of approximately 18 % (Hanssen-Bauer et al., 2015). The increase is highest during spring and less during summer. Heavy precipitation also seems to occur more often and at higher frequency than before. The annual middle temperature in Norway (reference period 1971-2000) was + 1.3°C. There has been an increase in the annual middle temperature of ca 1°C from 1900-2014. In this time interval, there have been periods with both increasing and decreasing temperatures, but the last 40 years have been dominated by a distinct increase in temperature (Hanssen-Bauer et al., 2015). This temperature increase has resulted in increased water discharge in winter times and earlier snow melt in spring time. Nevertheless, the rivers' response on the climate changes is not fully known, because instrumental data are rare in both time and space (IPCC, 2012).

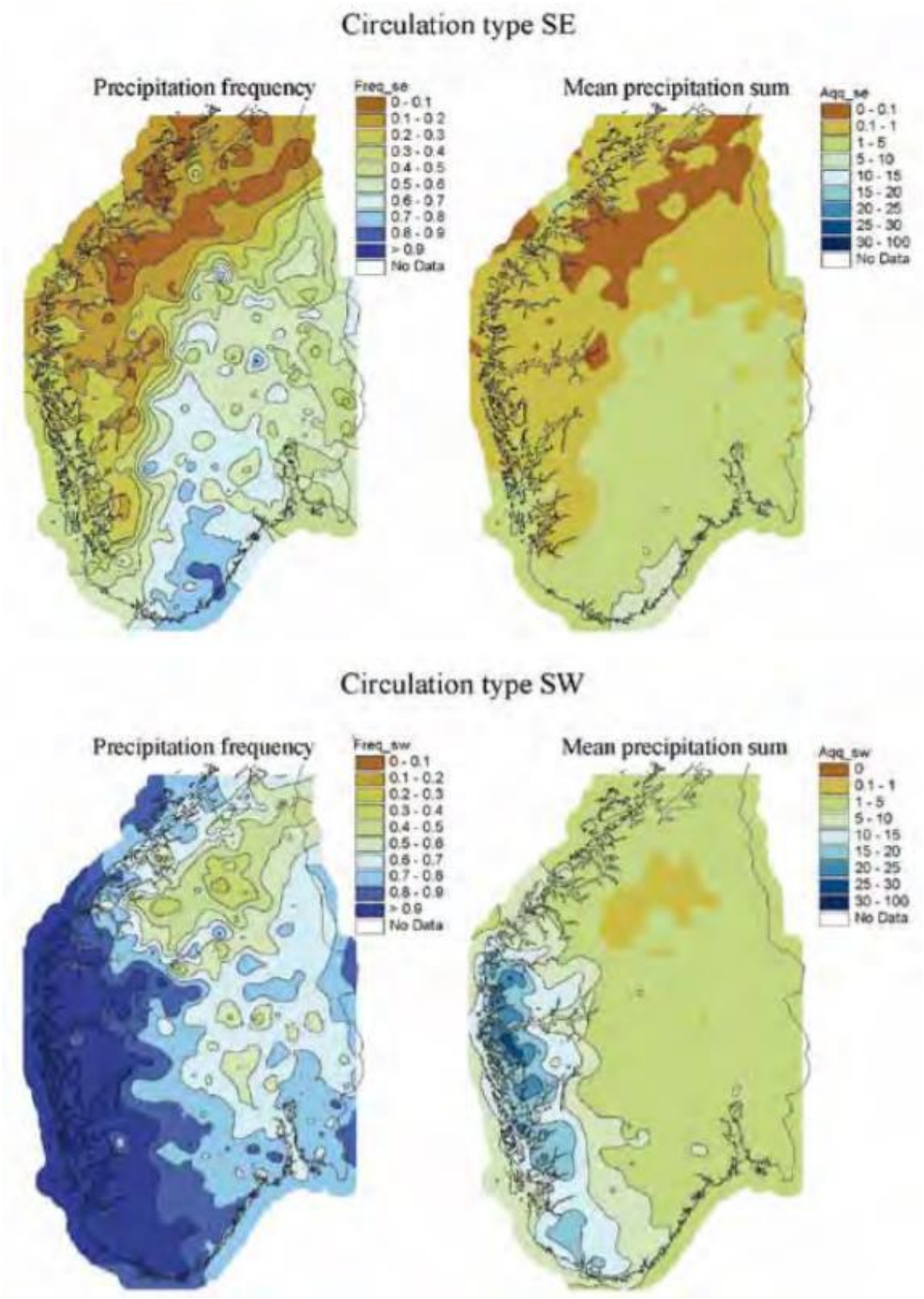

Figure 4) Precipitation frequency and mean precipitation sum in Southern Norway, due to circulation type SE (two upper maps) and circulation type SW (two lower maps) (Hanssen-Bauer et al., 2009).

Even though the amount of rainfall, winter precipitation and snowmelt play the biggest roles when it comes to flooding in Norway, there are also some other factors of significance. Initial conditions in the catchment, in particular for snow, soil- and groundwater can influence the flood magnitudes. If the ground is frozen, this prevents water from infiltrating, and leave it flowing on the ground, increasing the chance for floods. The catchment properties are also of importance, and anthropogenic influence plays a role. Asphalt makes the ground impermeable (just like frost), deforestation prevents trees from taking up water, and regulation in rivers can attenuate the effect of flooding. Dams are built along rivers to reduce the risk of flooding. Dams can store water, and this way prevent flooding, but the big floods are nevertheless hard to avoid, even with structures like dams.

2.3 Transportation of sediments

Floods are usually sudden events where the waterflow can increase abrupt and a lot in a short span of time. Running water has three basic functions; erosion, transportation and sedimentation. Erosion is the action of water that removes soil, rock or dissolved material. Transportation is the movement of material, in this case by running water. Transportation can happen in three ways; physical processes of traction (dragging), suspension (being carried) and saltation (bouncing), and the chemical process of solution. The amount of sediments that will be transported to the lake during a flood depends on several factors; among them the rate of precipitation, the distribution of precipitation over the catchment, the amount of runoff and its intensity, the speed of transportation and the distance from the flood to the main river. Another significant factor for sediment transport is the flow rate of the water. If the velocity is high, the water can carry higher amount of sediments, and bigger grains. Then large particles, like sand and even bigger, can be transported. A decrease in water discharge can lead to deposition of sediments, which again can lead to, under the right conditions, that the sediment layers will be preserved for a long time, without being interrupted by erosion from later floods. The biggest and heaviest grains are deposited first, and the smaller and lighter grains are transported further and deposited later. Figure 5 shows the relationship between the size of sediments and the velocity required to erode, transport and deposit it. The critical erosion curve shows the minimum velocity required to lift a particle of a certain size. This diagram is called the Hjulström-diagram, and was developed by a Swedish geographer named Henning Filip Hjulström.

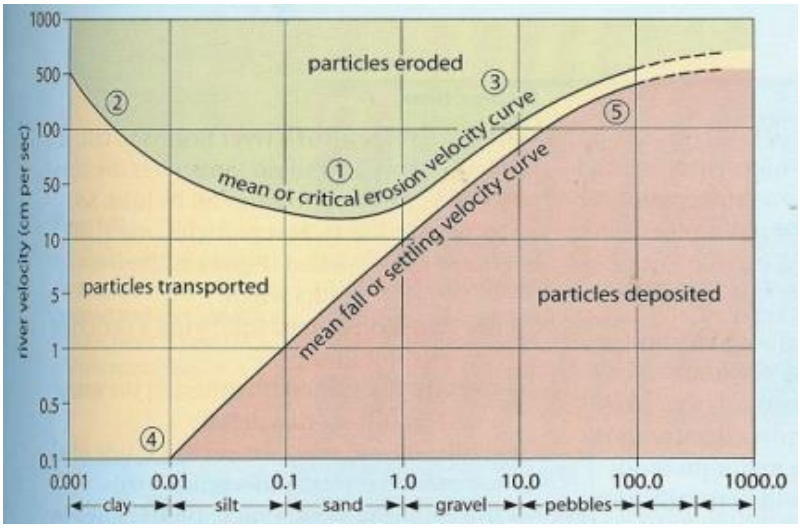

Figure 5) The Hjulström-diagram shows the relationship between the size of sediments and the velocity required to lift a particle of a certain size (GEOCACHING, 2011).

It is because of these three functions of running water (erosion, transportation, deposition) that one can find flood history saved in sediment cores.

A prerequisite for sediment transport and sediment deposition is of course that there are sediments available in the area. The sediments may be accessible close to the river channel and can then be eroded during flood. Sometimes there are less sediments available, thus they might have been washed out during a previous flood event. Other events, such as avalanches, former floods or human activity may have enriched and increased the amount of sediments in the river.

2.4 Flood frequency analysis (FFA) & paleohydrology

The flood estimation procedure currently used in Norway has several important strengths; (i) it is relatively easy to apply, (ii) it requires data that are either readily available or can be derived from Norwegian catchments from existing databases, (iii) it builds on a wealth of experience from previous applications, and (vi) it is supported by a good dam safety record with respect to the management of flood risks (Wilson et al., 2011). Various concepts due to this flood frequency analysis method must be considered, including data quality, the assumptions constraining the application of the methods, and the determination of final flood estimates (Wilson et al., 2011).

A statistical flood frequency analysis is based on observed flood data, either at the site of interest (at-site flood frequency analysis), or from one or several comparable gauged basins within the same region in the case of limited local data availability (regional flood frequency analysis). A short data record may also be extended by model simulation and a frequency analysis can then be performed (Wilson et al., 2011). The analysis is based on the assumption that all events in the observed flood series represent a process that can be described by one single flood frequency distribution. A mathematical function is used to describe the distribution of events, and this function is then extrapolated to give values corresponding to return periods beyond the length of the observed record. Extrapolation should be avoided if possible, because the estimation uncertainty increases with increasing return period. If it is necessary to extrapolate after all, this should be done only as far as necessary and preferably only up to twice the length of the record (Wilson et al., 2011).

The Norwegian Water Resources and Energy Directorate's (NVE) guidelines used in Norway recommend an at-site analysis for stations with at least 50 years of data. But it is nevertheless important to know that flood frequency analysis contains uncertainties. Reliable data are an important prerequisite for a reliable flood frequency analysis. Data quality can vary significantly between stations. All data in NVE's data base (data which are used in this thesis) are quality controlled by the hydrologists before it is stored. This includes an evaluation of the rating curve quality for high flows and a check of the values of extreme flood water levels for possible registration errors (Midttømme et al., 2011).

Because instrumental data is limited by short time records, ways to extend the flood history will be of importance. Additional to the flood frequency analysis method, there has been added another source of flood information desired to make flood estimation more reliable; the study of paleohydrologic data. Sediment cores can be useful, because sediments and deposition of this can, under the right conditions, preserve and store flood sediments.

An important prerequisite for the sediment cores to be used in the discovery of past floods is that transportation and deposition of flood sediments have been present (Jarrett, 2000). A lot of material can be transported and deposited in a lake during a flood. But also in periods without floods, material is deposited in the lake. Organic material locally produces (autochthon), or terrestrial organic material

produces in the lake's catchment (allochthones) and minerogenic material can be washed in during rainfall events. These sediments are being deposited and preserved in the bottom of the lake, and newer sediments are deposited over the older ones. Because of this, lake sediments can work as an archive with continuous data over a long time – which again can be used to investigate and reconstruct the past floods and flood frequency (Nesje, 1992; Thorndycraft et al., 1998; Nesje et al., 2001; Støren et al., 2010; Bøe et al., 2006; Støren et al., 2011; Wilhelm et al., 2013).

Paleohydrology techniques have several advantages, among them the extension of flood history. This data can be obtained without direct monitoring and the fact that evidence of past high-flow conditions are preserved in sediments. By studying this, flood history can be revealed. Nevertheless, the major disadvantages with this method are that special flood preserving conditions must be available, and even if this criterion is fulfilled, there is not a perfect resolution of the sediment core, and the age-depth-dating also contains uncertainties. Another important challenge is that the climate has changed through the last thousands of years, and this non-stationarity is challenging due to flood frequency analysis. Non-stationarity is challenging not only for paleodata, but also for newer data. The climate has changed the last 100 years as well as the last 10 000 years, and it is also expected to change in the future.

Sediment cores have proved to be good archives for Holocene flood variations, and some places even with very high resolutions. In Norway, and the rest of Scandinavia, sediment cores are among some of the most important archives over climatic changes in Holocene (Vasskog et al., 2011). Sediment cores have already been used to reconstruct the changes in flood frequency and possible relations to climatic changes in the history (Thorndycraft et al., 1998; Nesje et al., 2001; Bøe et al., 2006; Støren et al., 2010; Støren et al., 2011; Vasskog et al., 2011; Wilhelm et al., 2013). Similar studies have also proved Holocene flood frequency reconstructions for central Europe, and the Alps (Wilhelm et al., 2013; Wilhelm et al., 2015; Wirth, 2013).

Identification of flood layers

To identify flood layers, one or more proxies are used; (i) grain size: used to identify the grading from coarse to fine sediments in the layers (i.e. Støren et al., 2008); (ii) organic content (using loss on ignition-analyses): flood sediments often contain high amount of minerogenic material and low content of organic material. This is the opposite of the background-sedimentation that often has a high content of organic material, and lower content of minerogenic material. The contrast between the two types of sediment deposits is important to distinguish between them (i.e. Bøe et al., 2006; Nesje et al., 2001); (iii) magnetic susceptibility (MS): how magnetic the sediments are, depends on the geology of the catchment area. Flood sediment deposit is often rich in para- and ferromagnetic minerals, and thus has high magnetic susceptibility (i.e. Støren et al., 2010); (iii) X-ray fluorescence (XRF): XRF-scanning gives information on mineral content with very good resolution, which again gives good possibilities to detect even thinner layers, and XRF gives very good fluctuations on minerogenic layers in organic background material (i.e. Vannière et al., 2013; Vasskog et al., 2011); (vi) CT-scanning: CT-scan provides even more detailed information than XRF-analysis, and it can reveal even thinner layers. From a CT-scan, the density through the core can be obtained, which is an indication of flood layers – whom is usually denser than the background sedimentation (i.e Støren et al., 2010)

3 Study site and data

3.1 Glomma, Vingersjøen and Flyginnsjøen

The study site of this thesis is Glomma river upstream Kongsvinger (see map, Figure 6). Glomma is the longest river in Norway with its 621 km. Glomma starts in Aursunden northeast of Røros, where it lies 860 meters above sea level. The river affects four counties and 28 municipalities along its way down to Oslofjorden near Fredrikstad, where the river ends. Glomma's catchment area is approximately 41 000 km^2 and covers almost 13 % of Norway's total land area (Eikenæs et al., 2000). The river is regulated with several bigger magazines and two transfers, in addition to a lot of smaller power stations (Pettersson, 2001).

Figure 6) Study site, showing Glomma's catchment, 2.604 Elverum station and 2.2 Nor station at Kongsvinger (NVE, 2017).

Southeast of Kongsvinger lies lake Vingersjøen, which under normal conditions has a water level of 142 m asl. Vingersjøen is 2.6 km^2 and the catchment area is approximately 71.95 km^2 (NVE, 2017). This lake is 4.7 km long north-south, with Vesle Vingersjøen as its southernmost part, separated from the rest of the lake by a small headland. In the southern part, there is a small creek from the pond Tarven entering Vingersjøen. The tributary of Tarven is a small stream that flows under a road bridge, and about 500 m southeast of this bridge is the water divide over to Flyginnsjøen, at a farm named Gropa. The elevation difference between Glomma and Vingersjøen (the saddle point) is only a couple of meters, and the culmination water level was in 1967 measured to 145.56 m asl. This measurement was done by NVE's old height system, so 0.26 m should be added to be comparable to the present height system (Pettersson, 2001). High water levels (which occur during flood) will then cause some of Glomma's water to flow into Vingersjøen, and further to Flyginnsjøen and towards Sweden (Pettersson, 2001). Flyginnsjøen is approximately 0.1191 km^2, and is probably an old kettle hole.

The bedrock in Kongsvinger area belongs to the Kongsvinger-group, and consists mainly of gneiss, granite and some conglomerate. The bedrock in Glomma's catchment further north of Kongsvinger contains mainly sedimentary rocks. The soils in the area around Kongsvinger are mainly fluvial and glacifluvial deposited sand, silt and gravel, but in some parts of the area there exist moraine and aeolian sand (see map, Figure 7). The marine limit at Kongsvinger is approximately 200 m asl (Sollid & Kristiansen, 1982).

Flyginnsjøen is regulated as LNF-area (Kommunedelplan, 2014), and there has been made a swimming area at the lake's northeast side. The area around the lake is dominated by forest and cultivated land. Close to the lake, there is also a golf course and some industrial buildings. The catchment area upstream Flyginnsjøen is regulated with dams at Føskersjøen, Bæreia, Sigernessjøen and Lierfløyta. Flyginnsjøen was earlier used for log driving, sawmill, mill and power plants (Steffensen, 2014). According to Lilleengen et al. (2005), there was a significant sawmill in the river in 1791, but there are no such activities today (Steffensen, 2014).

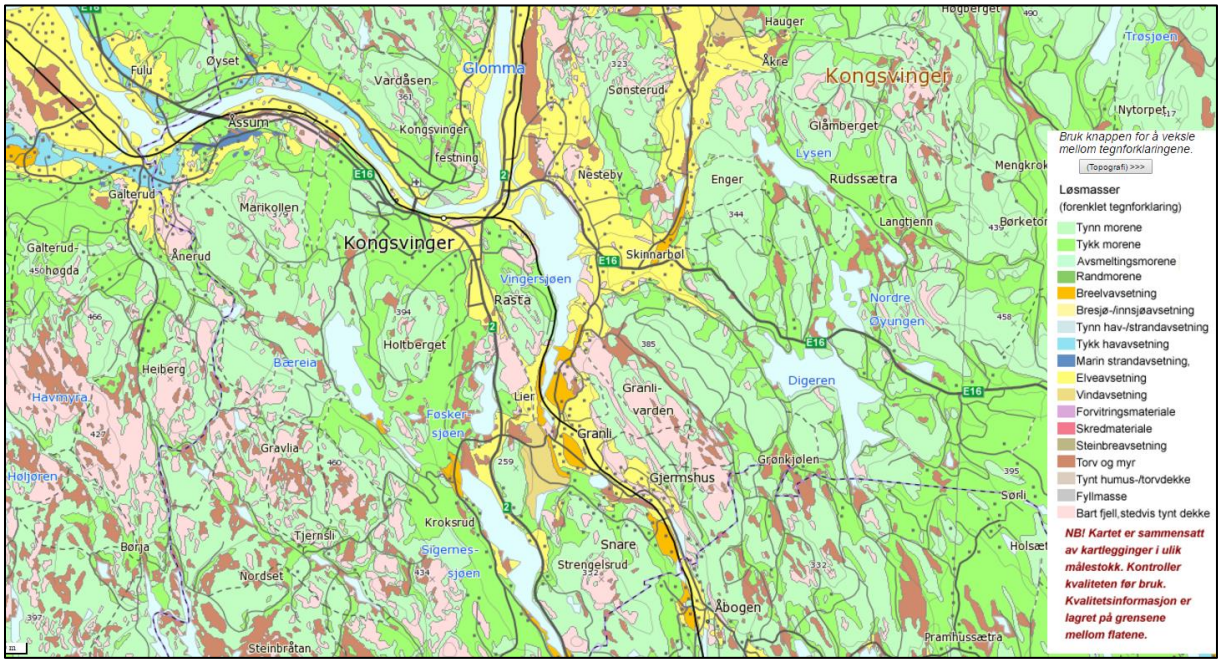

Figure 7) Map over soils in Kongsvinger area (NGU, 2017).

Bifurcation

During normal conditions, water flow from Vingersjøen into Glomma. But when Glomma is flooding, bifurcation, a natural forking of a river, occurs and 1-2 % of the water flows from Glomma and over to Vingersjøen (see map, Figure 8 and Figure 9). This water-loss contributes to reducing the flood sizes in Glomma downstream Kongsvinger (Hegge, 1968; Klæboe, 1946; Pettersson, 2001).

Bifurcation in Glomma at Kongsvinger occur if the water flow exceeds the threshold of approximately 1500 m^3/s. Whenever the floodwater overspills this threshold, this significantly changes the flow regime in the small stream Vingersjøen entering Flyginnsjøen. The dramatic increase in discharge remobilizes abundant glacifluvial material in the catchment of Flyginnsjøen, and causes deposition of fine-grained minerogenic material that contrasts the organic rich mud normally deposited in the lake.

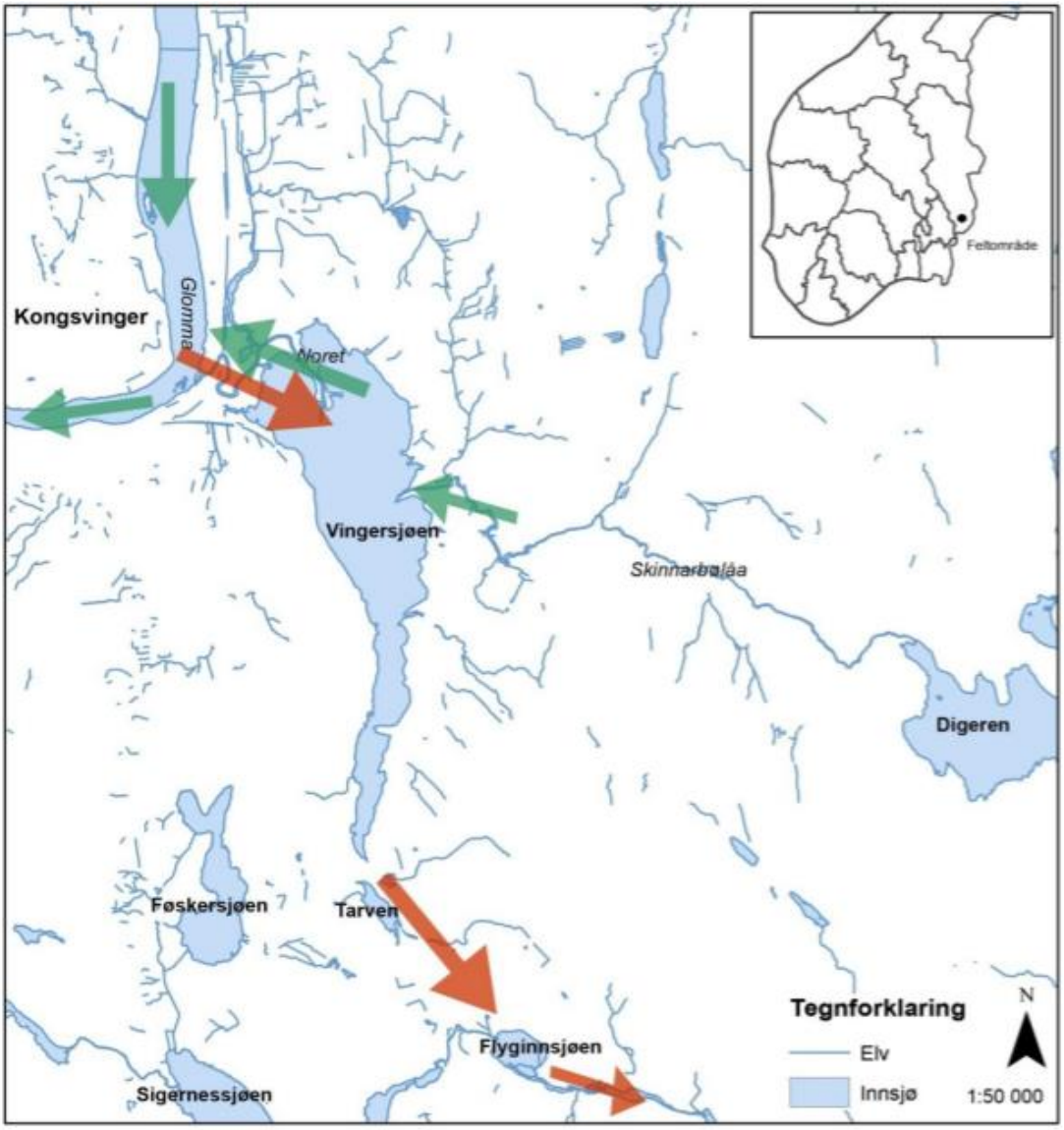

Figure 8) Map showing Kongsvinger-area. The green arrows illustrate Glomma's normal waterflow, while the red arrows illustrate Glomma's interaction with Vingersjøen and Flyginnsjøen during bifurcation (Steffensen, 2014).

Why Flyginnsjøen is suitable as Glomma's flood archive

Not every lake is suitable to be used as a flood archive – and there are certain criteria that should be fulfilled to have a lake with good flood conservation capacity. Gilli et al. (2013) made a list of criteria that should be fulfilled in order to have a lake with good flood preserving conditions. The selection of appropriate lakes is crucial for the approach of flood reconstruction. The understanding of the transport and depositional processes of flood-transported particles allows us to set criteria to select lakes holding promising flood records (Gilli et al., 2013).

The geomorphological conditions around the lake are of importance for their availability to preserve flood history. Most important is that the lake should have evident inflow, which ideally is only activated in the case of an extreme event (flood). That provides a certain threshold with an 'on/off signal' so that only the larger extreme events are recorded in the lacustrine archive (Gilli et al., 2013). Another prerequisite is that there must be a contrast between flood deposits and regular background sedimentation, so that flood events can be lithological and geochemically recognized (as explained in chapter 2; "Identification of flood layers"). Finally, coring ability to recover desired time interval should be present. Standard coring techniques with various piston-coring methods are capable of reaching approximately 20 m sub lake-floor depth, so sediments thicker than this can be hard to get. Therefore, the sedimentation rate should not be too large, so that it will not exceed this limit. Rather small lakes with little inflow are ideal, if a complete Holocene section is the target (Gilli et al., 2013).

These criteria are all present in Glomma and Flyginnsjøen; (i) the discharge threshold of 1500 m^3/s (which results in bifurcation, and let water from Glomma at Kongsvinger flow over to Vingersjøen and further southwards to Flyginnsjøen) works as an on/off-signal of floods, (ii) the flood sediments from Glomma are in contrast to the background sedimentation in Flyginnsjøen and (iii) the sedimentation rate in Flyginnsjøen is not too large, making coring possible. Since these criteria are fulfilled, Flyginnsjøen is believed to be suitable as a flood archive.

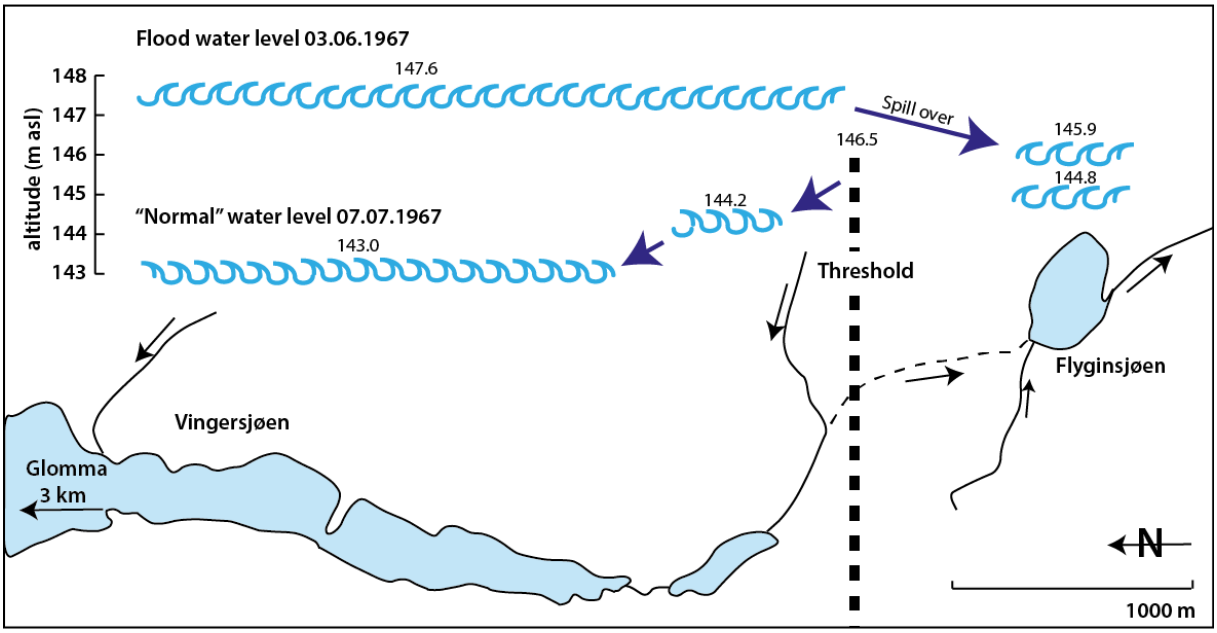

Figure 9) The map shows the saddle point (the lowest point) between Glomma and Vingersjøen. The "normal" water level (07.07.1967) shows the waterflow during normally conditions. The flood water level (03.06.1967) shows the waterflow during bifurcation, when water exceeds the threshold and flow over to Flyginnsjøen (Støren, 2017).

3.2 Flood data

3.2.1 Instrumental data

Instrumental data are physical measured information, such as water discharge (m^3/s) and water level (m). There are many measuring stations along Glomma, and in this study, systematic flood data obtained from gauging station at Elverum (2.604 Elverum) from 1871-1936 (unregulated period) and 1937-2015 (regulated period), and Kongsvinger (2.120 Nors Bru) from 1851-1936 are used. The period 1917-1937 was not completely unregulated, but the total effect of the regulations was not significant (Pettersson, 2001). Pettersson (2001) therefore assumes that the data after 1937 represent the regulated period. I have used the same assumption as Pettersson. Measuring stations 2.604 Elverum and 2.120 Nors Bru contain systematic water level- and discharge observations before the biggest regulations happened in Glomma, and therefore represent non-regulated streamflow values.

In 1851, an observation post was established close to 2.120 Nors Bru, Glomma, upstream Kongsvinger city center. Water level and water flow were measured until August 1935, but there were some gap years without observations; 1855-1860 and 1867-1868 (Pettersson, 2001).

Norsfoss is located approximately 20 km upstream of Kongsvinger. Here there are two measuring stations; 2.2 Nor and 2.393 Norsfoss, which started its operations in October 1936 and January 1975, respectively. Nor was shut down in 1998, but Norsfoss is still in use. Glomma's catchment at Norsfossen, nearly 19 000 km^2, is approximately 1 % smaller than the one at Kongsvinger (Pettersson, 2001).

Water level observation in Vingersjøen started in March 1911, and consisted of daily readings until 1924. This identification number of the station is 2.121. After 1924, it was decided that the readings should only be done in the months of May, June and July. The observer quit in 1926, and after this the readings ceased. The period without readings lasted until 1938, when they were restored. From then on, the readings were done in the three summer months and when the water level exceeded 5.00 meter on the water mark. These readings lasted until 1986, when again they ceased, as the station was shut down (Pettersson, 2001).

In Vrangselva there exists one single hydrologic measuring station for water level and water flow observations. It is close to Magnor. Here there have been done continuous observations since March 1911. The station has been relocated several times, but the difference between the different catchments has been minimal. The different station numbers are as followed: 313.3, 313.11, 313.9 and 313.10. The existing station today is 313.10, and it is located approximately 800 meters upstream Magnor Bru (Pettersson, 2001).

There are a lot of hydrological stations along Glomma river, and Table 1 shows the measuring stations in Kongsvinger area and the one in Elverum (Pettersson, 2000), with its names, observation periods (and the years without observations), if it is regulated or not and catchment areas. The catchment areas are from NVE (NVE, 2017).

Table 1) Hydrological stations in Kongsvinger area (Pettersson, 2001; NVE, 2017).

Station number	Name	Observation period	Regulations	Interruptions in observation period	Field area (km^2)
2.120	Nors bru	1851-1935	Unregulated until 1917	1855-1860 & 1867-1868	19245.93 km
2.121	Vingersjø	1911-1986	Unregulated	1926-1938	71.95 km
2.2	Nor	1936-1997	Regulated		18933.14 km
2.393	Norsfoss	1975 – present	Regulated		18933.56 km
2.444	Kongsvinger kraftverk	1979 – present	Regulated		19280.59 km
313.10	Magnor	1911 – present			357.86 km
2.604	Elverum	1871-present	Regulated		15449.93 km

The instrumental measurements have not been going on for too long, and the longest continuous time records we have contains 145 years of measured data (2.604 Elverum), but usually they contain less than 50 years of information. Despite that the instrumental data are accurate and objective, the limited time series is a challenge. Klæboe (1946) made a list of bifurcation events in Glomma at Kongsvinger in the period 1851-1945. Hegge (1968) complemented Klæboe's estimations in 1968 with data from 1946-1967. These estimates were extended to year 2000 by Pettersson (2001).

From 1851 to 2000, there have been 75 events of bifurcation, distributed on 73 years. Two of the years (1957 & 1987) had both spring- and autumn floods. Four of the bifurcation events happened during autumn, while the rest happened in spring time. There are two periods without any observations; 1855-1860 and 1867-1868 (Pettersson, 2001).

From 2000 to 2013, there have been four more years with bifurcation; 2008, 2010, 2011 and 2013. Table 2 shows the bifurcation events from 1950 to 2013. The 1st column shows the year of the bifurcation, the 2nd column shows the transferred water amount (million m^3), the 3rd column shows the duration of the flood (number of days where the discharge exceeded 1500 m^3/s), the 4th column shows the maximum discharge (m^3/s), and the 5th column shows the season of the flood (spring or autumn). From instrumental measurements, we know about 24 bifurcation events at Glomma, Kongsvinger between 1950 and 2013 (Pettersson, 2001; updated by Aano, 2017 (pers.comm. Engeland, 2017)).

Figure 10 shows maximal transferred water amount from the period that sediment core FLS113 covers; from approximately 1950 until 2013. This period has three years with dominating water discharges; 1966, 1967 and 1995, with respectively maximum discharge of 14.06, 29.01 and ca 19 m^3/s.

Table 2) Bifurcation events in Glomma at Kongsvinger from 1950 to 2013 (Pettersson, 2001; updated by Aano, 2017).

Bifurcations	Transferred water (mill m^3)	Duration (days)	Max discharge (m^3/s)	Season
2013	2.8	4	18.8	Spring
2011	0.3	3	2.6	Spring
2010	0.05	2	0.4	Spring
2008	1.8	11	7.1	Spring
2000	0.28	3	1.4	Spring
1995	Ca 19	10	Ca 55	Spring
1993	0.18	2	1.9	Spring
1988	0.93	7	3.9	Spring
1987	0.53	2	5.8	Autumn
1987	0.15	3	0.8	Spring
1986	3.33	7	8.7	Spring
1985	0.98	4	5.6	Spring
1983	0.13	1	1.5	Spring
1979	0.09	2	0.7	Spring
1978	0.38	3	3.1	Spring
1975	0.11	2	0.7	Spring
1973	0.22	2	1.6	Spring
1967	29.01	12	50.6	Spring
1966	14.06	10	52	Spring
1963	0.16	2	1.3	Spring
1959	1.33	5	8.6	Spring
1957	1.95	4	12.8	Autumn
1957	0.03	1	0.3	Spring
1952	0.43	2	4	Spring
1950	0.12	2	0.8	Spring

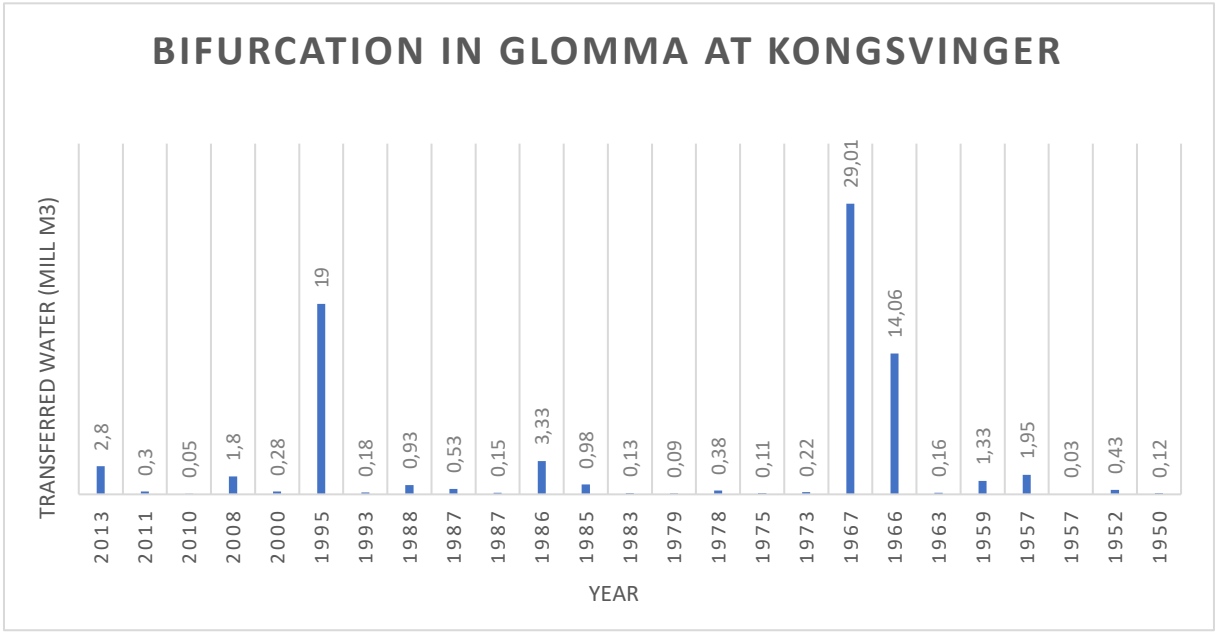

Figure 10) Bifurcation events in Glomma at Kongsvinger from 1950-2013 (Pettersson, 2001; updated by Aano, 2017). Years on x-axis and transferred water amount (mill m^3) is shown on the y-axis. For the years with both spring- and autumn floods (1957 & 1987), only the spring flood is represented.

Some years stand out with much more transferred water than others; especially the flood in 1967 caused a lot of transferred water, as well as the year before. Both 1966- and 1967-floods are believed to be 100-years floods. In the more recent years, it is the flood from 1995 that stands out as the biggest one. The 1995-flood's maximum discharge was larger than for the floods in 1966 and 1967, but the amount of water transfer is significantly lower. Pettersson (2001) claims that the transferred amount of water from 1995 is uncertain.

Flood frequency is generally based upon annual maxima series (AMS), most often what is called Block Maximum Series (BMS), with a block size of one year. With this method, the highest flow peak within a year is chosen to represent that year's flood (Wilson et al., 2011). Figure 11 shows the annual maximum values (AMS) obtained from Elverum station in the period 1871-1936 (before regulations), and Figure 12 shows the AMS-values in the period 1937-2015 (after regulations). From these plots, one can see that there is a significant difference in the values before and after the regulations. The AMS-values after the regulations are lower than before, due to the regulations. Nevertheless, the big floods are not stopped by the regulations, although they might have been even bigger without.

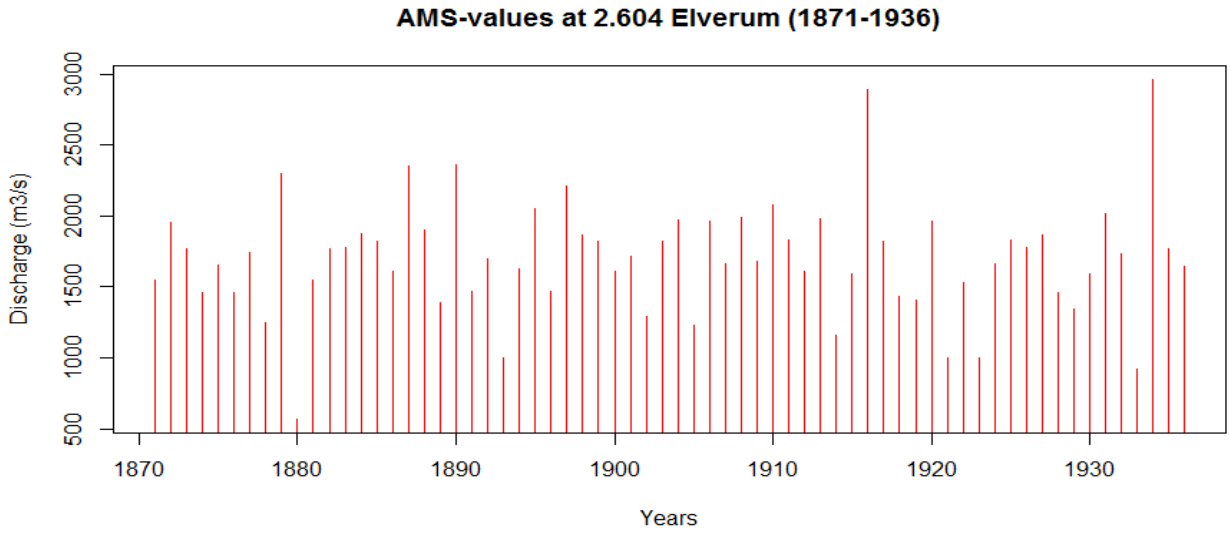

Figure 11) AMS-values from 2.604 Elverum (unregulated period, 1971-1936). Years on x-axis, discharge (m^3/s) on y-axis).

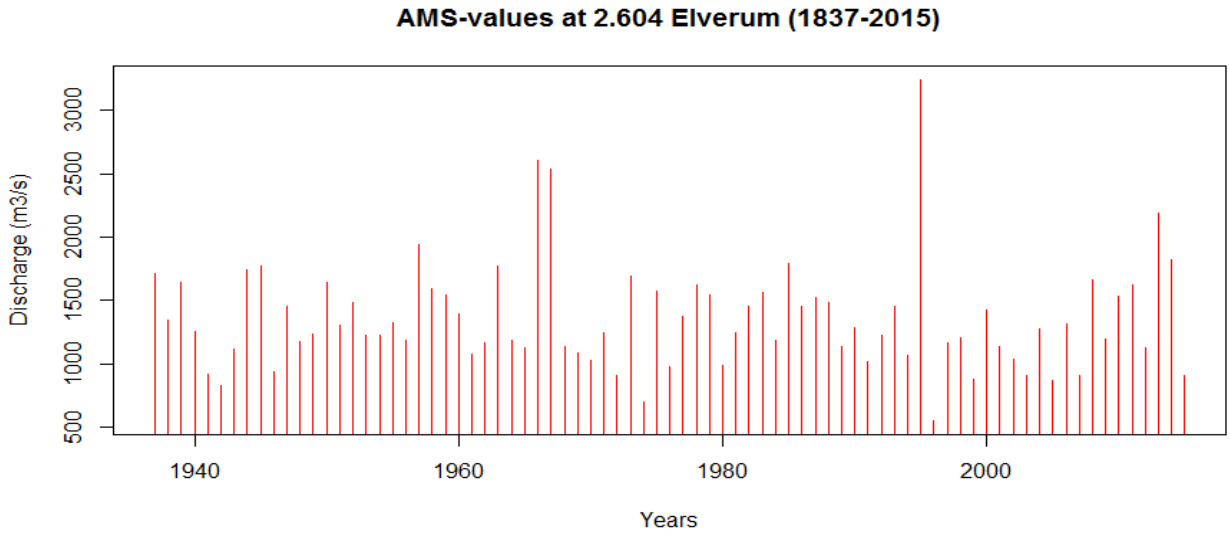

Figure 12) AMS-values from 2.604 Elverum (regulated period; 1937-2015). Years on x-axis, discharge (m^3/s) on y-axis).

3.2.2 Historical data

Historical flood information can come from flood marks on rocks, walls or buildings, paintings, newspapers, stories as well as official records like the one above (Roald, 2013; Otnes, 1982). Roald (2013) made an overview of floods from Glomma, which is mentioned in historical documents. The earliest flood in Glomma mentioned in historical sources occurred in the 1540s. In the official record (*Tingboka for Høsttinget*) in Solør-Odal in 1789, a huge flood approximately 250 years earlier is mentioned (Roald, 2013). This is probably the same flood that happened in Dalsälven in Sweden in 1544, described as the worst flood ever (Roald, 2013).

The largest floods in Glomma known from historical information happened in 1650, 1675, 1717, 1747, 1773, 1789, 1846, 1850, 1967, 1887, which all occurred in May or June. In the more recent years, the floods from 1916, 1934, 1966, 1967 and 1995, 2011 and 2013 are being highlighted as very big (Roald, 2013; Otnes, 1982).

Figure 13 A) Flood monument at Grindalen (Sælthun, 2016) and B) flood monument at Elverum Forest Museum (Wikipedia, 2017).

Despite the fact a lot of historical information often is subjective and only reveals the most destructive and extreme events, it is an important source of information to retain the flood history in Norway, before the systematic measurements started (Roald, 2013). Flood stones, like the monuments raised at Grindalen and Elverum museum (Figure 13), provide historical flood information. The flood stone at Elverum museum was raised after the floods in 1966 and 1967, which both were classified as 100-years floods (Roald, 2013). The marks on the stone correspond to the water level during the historical floods, all the way back to 1675. The largest historical flood, named Storofsen, happened in 1789 and has been estimated to a discharge of 3900 m^3/s (GLB, 1947). Flood heights before 1966 are transferred from the flood stone at Grindalen in Elverum, and to Elverum flood monument.

Figure 14 shows the flood marks from Elverum flood monument. On this stone, the 20 biggest floods registered through time are marked, and they occurred in Glomma at Elverum the following years (in decreasing size); AD 1789, 1995, 1675 & 1773, 1717 & 1724 & 1749, 1850 & 1934, 1916, 1827, 1966, 1846 & 1967, 1760, 1852, 1887, 1890, 1867 and 1897.

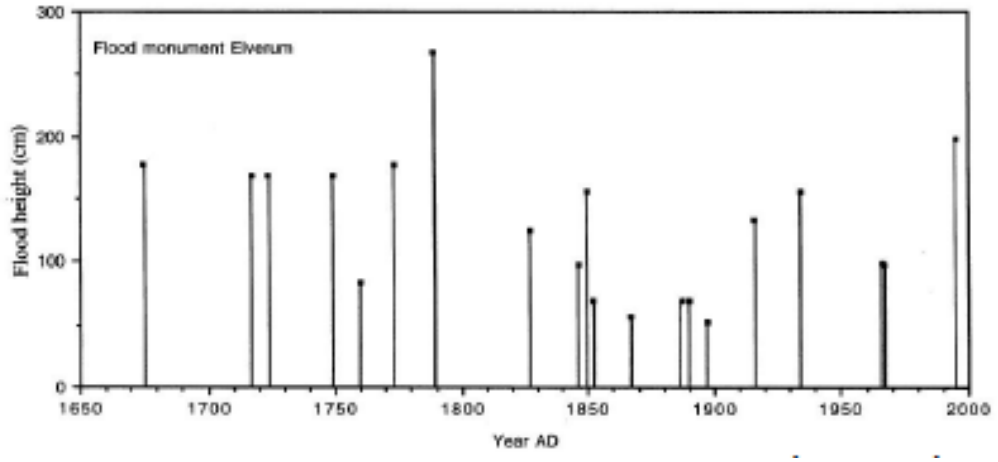

Figure 14) Age (x-axis) and flood heights (cm) (y-axis) of the historical floods from Elverum flood monument (Nesje et al., 2001).

In my thesis, I have chosen the flood from 1967 as a threshold flood. Its discharge (from instrumental data) is 2533 m^3/s. From the flood monument at Elverum, this flood is marked. Eight floods are marked higher than this threshold-flood and one is at the exact same height, therefore altogether nine floods from the historical period is added. The historical period in this case covers the period from approximately 1650 – 1850 (before the systematic measurements started). The floods exceeding 1967 is the floods from the following years: 1789, 1675, 1773, 1717, 1724, 1749, 1850, 1827, 1846.

Thus; the historical flood information used in this thesis is that nine floods exceed a chosen threshold (1967-flood) in the historical period covering approximately 200 years.

3.2.3 Paleohydrological data – sediment cores

Whenever the floodwater overspills the saddle point between Vingersjøen and Flyginnsjøen, this significantly changes the flow regime in the small stream Vrangselv entering Flyginnsjøen. The dramatic increase in discharge remobilizes abundant glacifluvial material in the catchment of Flyginnsjøen, and causes deposition of fine-grained minerogenic material that contrasts with the organic rich mud normally deposited in the lake.

The paleodata in this study comes from two sediment cores from Flyginnsjøen. FLS113 is the shortest core, 18 cm long, and represent the period approximately AD 1950-2013. FLP213 is 516 cm long, and represents the period approximately 175-10300 years before present (present = 1950). Both cores were taken from Flyginnsjøen in 2013, and have been studied before, related to other work on this area (Steffensen, 2014).

Figure 15 shows FLS113, and Figure 16 shows FLP213.

Figure 15) Picture of sediment core FLS113 (18.0 cm long), bottom side to the left, top to the right. The green on the top and bottom of the core is flower oasis.

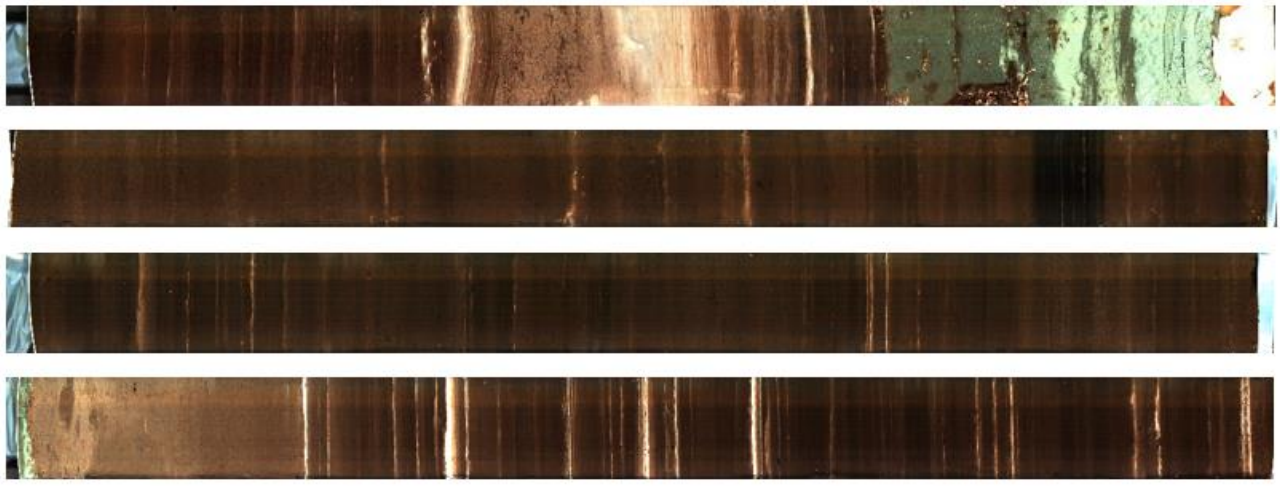

Figure 16 A-D) Picture of sediment core FLP213 (516.0 cm long).

Steffensen (2014) did the following analyses on the cores in her study; loss on ignition (LOI), magnetic susceptibility (MS), X-ray fluorescence (XRF), which all can be used as proxies for flood events. Figure 17 shows the sediment core FLS113 (18.0 cm long) and selected flood proxies (concentration of Potassium, Calcium, Titan, Iron, Rubidium and Strontium. Additionally, a black and white scale is shown, which is an indication of density (white is dense layers, black is low-density layers).

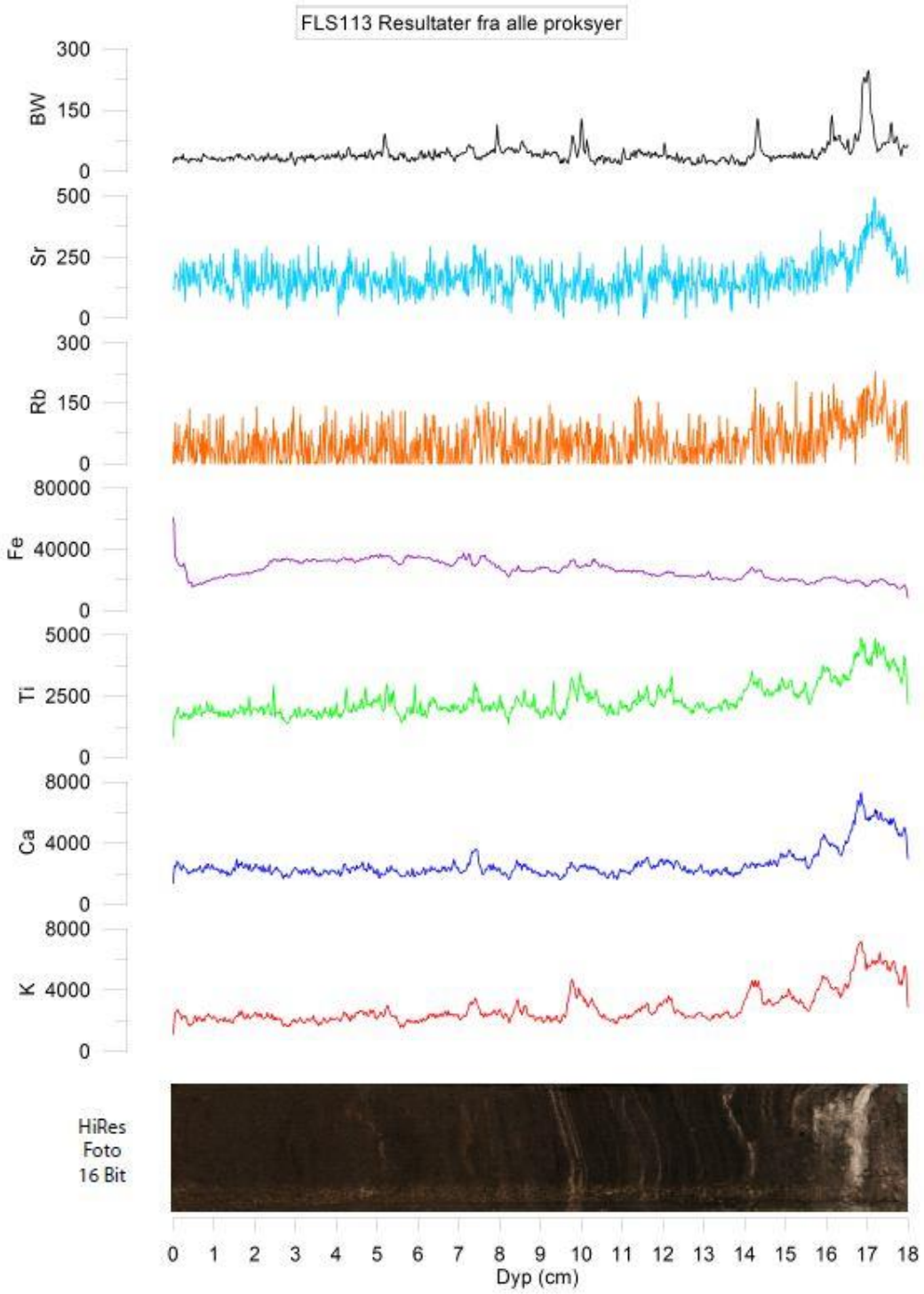

Figure 17) Sediment core FLS113 with selected proxies and a picture of the core (Steffensen, 2014). The x-axis shows the depth of the core (age increases with depth), and the y-axis shows the concentration of Potassium (K), Calcium (Ca), Titanium (Ti), Iron (Fe), Rubidium (Rb) and Strontium (Sr) (all with unit kcps), and BW (black-and-white-scale, from 0-225, where 0 is black and 225 is white).

Figure 18 shows the sediment core FLP213 (516 cm long, coordinates 33V 337421 6670329, taken at 16.4 m depth), and selected flood proxies (concentration of Potassium, Calcium, Titan, Iron, Rubidium and Strontium. Additionally, a black and white scale is shown, which is an indication of density (white is dense layers, black is low-density layers).

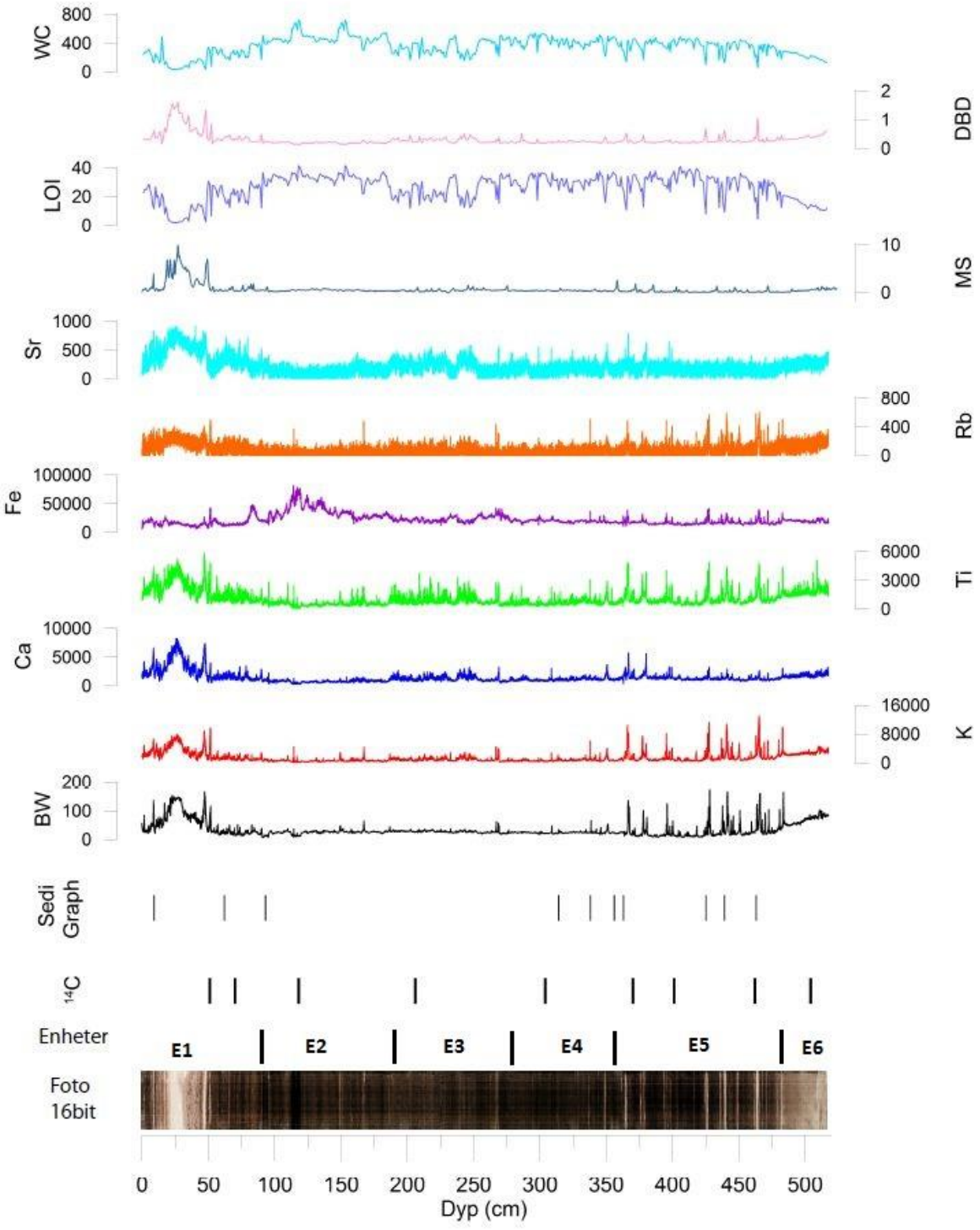

Figure 18) Results from measurements on sediment core FLP213 (Steffensen, 2014).. The graphs ^{14}C and SediGraph show where in the core the samples are taken. The BW-graph shows the black-and-white picture, from 0-225, where 0 is black. The y-axis of the XRF-data (K-Sr) have unit kcps. MS is in SI-unit, LOI is in % and DBD and WC is in unit gram per cm^3.

Common for both cores; there are several distinct peaks, occurring in certain faces. The cores are dominated by a dark brown mud, classified as background signal. This mud has high loss on ignition (LOI-values), low magnetic susceptibility (MS) and low Potassium (K) values. Periodically, lighter layers occur, containing more minerogenic materials. These layers are characterized by low LOI, high MS and high K-values (Steffensen, 2014).

The number of floods during Holocene (time period covering the last approximately 10 000 years) estimated from the long core (FLP213, 516 cm) from Steffensen (2014) are used in this thesis.

Figure 19 shows the flood count curves through Holocene. The flood counts are done for 30-year running windows, and by two different thresholds. The graph shows the flood counts using parameter Potassium (K) and Titanium (Ti). Steffensen (2014) found that K with a threshold P94 was best to reproduce the floods from FLS113. Using this threshold, 207 floods are counted the last approximately 10 000 years. Using the threshold P94 of Ti, 417 floods are counted through Holocene. There is clearly a relation between the two parameters K and Ti, even though threshold with Ti counts more than the double number of floods as threshold with K (417 compared to 207).

The flood rates seem to have natural fluctuations, and there have been periods with many floods separated by periods with fewer floods. The long trends seem nevertheless to reveal a drastic increase in flood frequency for last hundreds of years. Since almost 800 years ago, it seems like the flood frequency started to increase drastically, still with its characteristic fluctuations, but overall an increase in flood frequency. Never before (at least never before in the last 10 000 years), has the flood frequency been as high as it was approximately 200 years BP. But in recent decades, there seems to have been a decreasing trend, according to the plot.

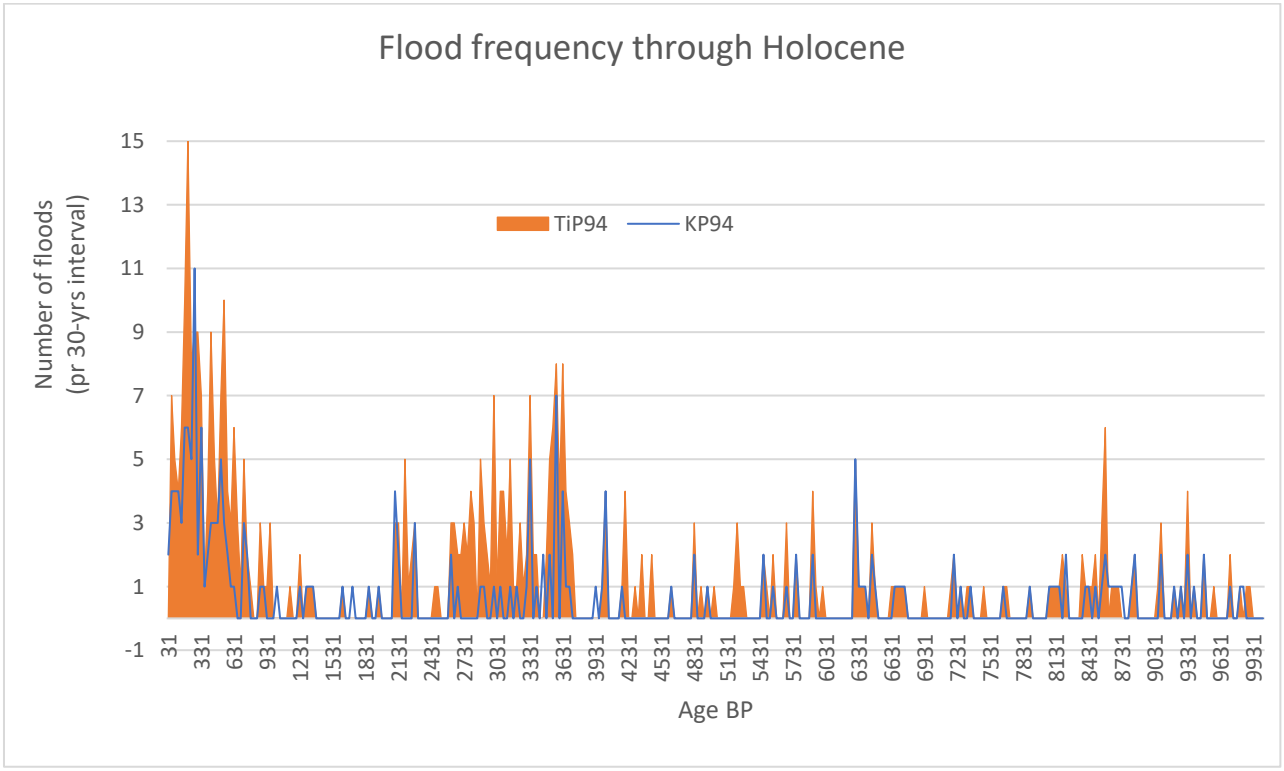

Figure 19) Number of floods through Holocene, with thresholds Potassium (K) P94 (blue) and Titanium (Ti) P94 (red).

4 Methods

To obtain the preferable results, I had to (i) update the list of bifurcation events in Glomma at Kongsvinger, (ii) investigate historical information about floods in Glomma between Elverum and Kongsvinger in the period before systematic measurements started, (iii) investigate if there is a relation between bifurcation events in Glomma and sediment layers in Flyginnsjøen, for the period that is covered by FLS113, and this way use paleohydrological information to receive flood history from the past, and finally (vi) use the historical- and paleohydrological flood information in addition to the instrumental information to improve flood frequency estimations.

4.1 Instrumental data & bifurcation events

Based on observed water levels in Vingersjøen, and the rating curve made based on the measurements from 1916, the transferred water amount from Glomma to Vingersjøen is estimated. This transfer occurs when the water flow in Glomma exceeds 1500 m3/s (Pettersson, 2001). Klæboe (1946) estimated the bifurcation events for the period 1851-1945. Water levels from 1851-1910 were taken from 2.120 Nors Bru. For the years before 1913, Klæboe used a correction of waterflow, because a dam was built in fall of 1912 to prevent the transfer of water. However, the dam was damaged the following year, but remains left in the lake resulting in somewhat reduced flow into Vingersjøen (Pettersson, 2001). Hegge (1968) complemented Klæboe's estimations with data from 1946-1967. These estimates were extended to year 2000 by Pettersson. For the period 1968-1986 there exist water level data from Vingersjøen, and the method used to estimate is the same as before 1968. After 1968, water level data must be estimated from observed water levels in Vingersjøen, during large floods, which are plotted together with observed discharges at Nor station the same day.

A rating curve representing the correlation between discharge in Glomma at Nor station and water level in Vingersjøen is used. Water levels in Vingersjøen at respectively 5.5, 6.0, 6.5, 7.0 m are achieved according to this curve at discharges of respectively 1720, 1985, 2250 and 2515 m^3/s at Nor (Pettersson, 2001). Based on discharge data at Nor, the water levels in Vingersjøen are then estimated. I have updated this list until 2013 (when the sediment cores were taken). I went through systematic data and found the times when water flow exceeded 1500 m^3/s (for full list see appendix), which is the threshold when bifurcation in Glomma at Kongsvinger occurs (Pettersson, 2001).

The 2.393 Norsfoss station contains daily measurements from 01.01.1975 (until present), with only few data missing. There was no water flow exceeding 1500 m^3/s and thus large enough to cross the saddle point between 2000 and 2008, but it happened four times afterwards; in May 2008, May 2010, June 2011 and May 2013. Then I estimated the water levels based on notes from Lars-Evan Pettersson (graphically; from water level- and discharge-plots). Further, I estimated transferred water (mill m^3).

Figure 20 and Figure 21 show the rating curves made by Pettersson that I used to estimate the discharge values for the bifurcation events between 2000 and 2013.

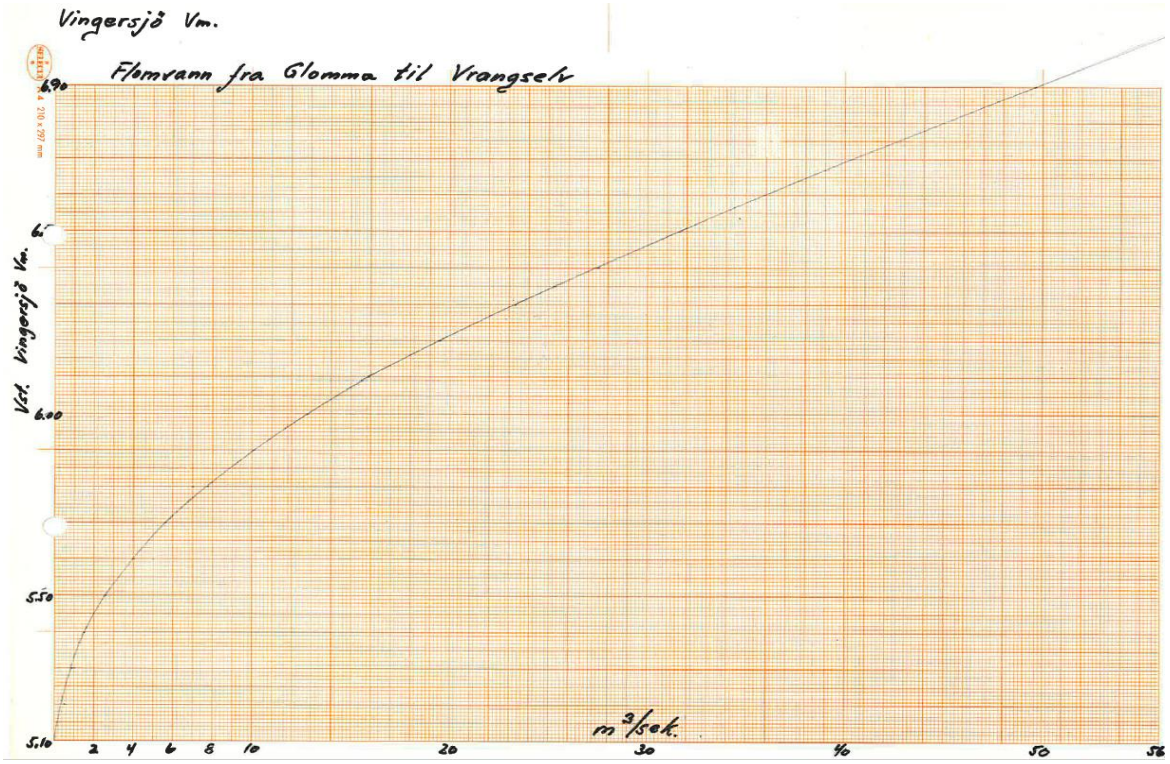

Figure 20) Rating curve between the discharge (m^3/s) in Glomma at Kongsvinger (x-axis) and the water level (m) in Vingersjø (y-axis) made by Pettersson.

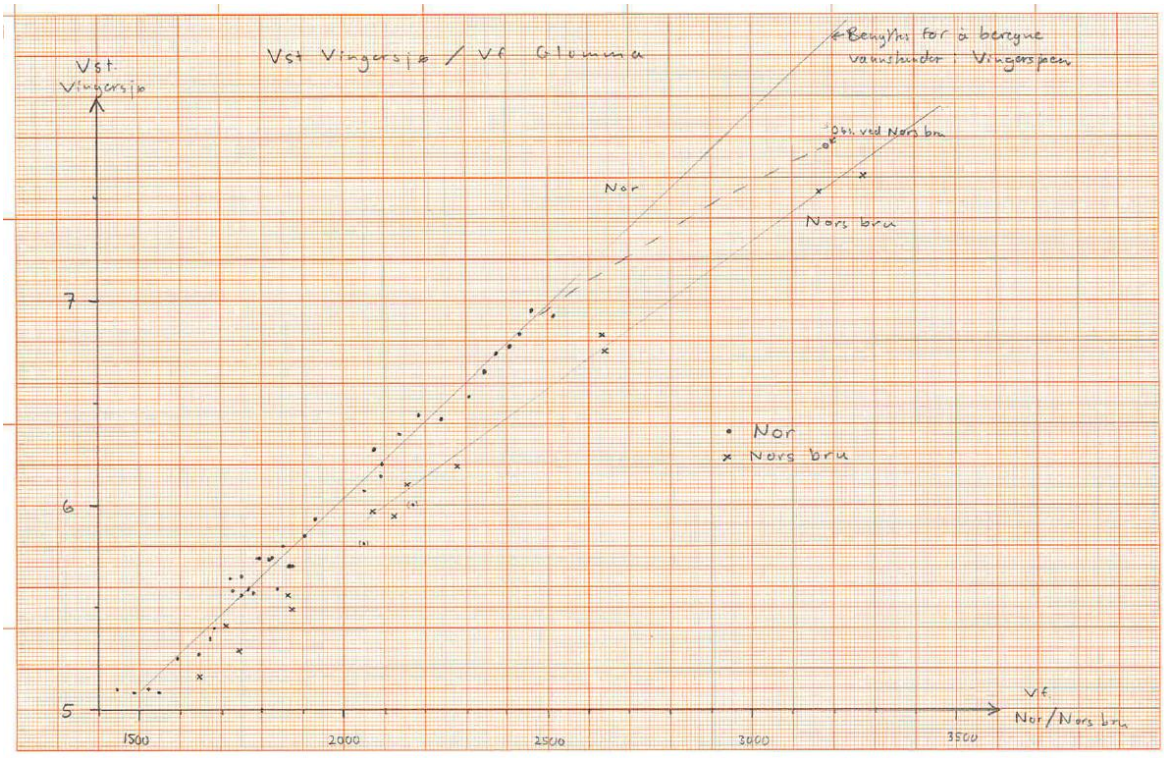

Figure 21) Curve showing relation between the discharge (m^3/s) at Nor/Nors Bru (x-axis) and the water level (m) in Vingersjøen (y-axis) made by Pettersson.

4.2 Historical data analysis

To identify and estimate sizes of floods from historical data, water levels from the flood monument at Elverum were used. The largest flood marked on the monument is Storofsen from 1789, and its estimated discharge is 3900 m^3/s (GLB, 1947). For the flood marks on the monument that overlapped with systematic data, flood values were extracted to establish a simple rating curve for the rest of the floods marked on the monument. These flood sizes were then extrapolated to Nor at Kongsvinger by linear regression, so that discharge of the same floods could also be obtained from there.

The heights of the floods are physically measured from the monument, and the estimated discharge is estimated at interpolation from some known discharges. The discharge from the following floods can be obtained from measurement stations; 1995, 1934, 1916, 1966 and 1967. Based on these numbers and the height-differences between the flood marks, spline interpolating was used to find the discharge values corresponding to the rest of the floods marked on the monument.

Plotting annual maximum series (AMS) values from station 2.604 Elverum and station 2.2 Nor show that there is a good correlation between the water discharge at the two stations. The correlation R was close to 1 (0.89), which means that there was a good relation between them; when there was a flood at Elverum, there was also a flood at Nor. From the graphical plot at Figure 22, we can see that the daily AMS-values are overall a little bit higher at Nor station than at Elverum station.

To estimate the flood discharge values for the floods marked on Elverum flood monument, a regression line between Elverum and Nor stations was made. This regression line between Elverum and Nor is: y = 1.0953x + 63.224 (Figure 23), where y is the estimated discharge in Nor, and x is the estimated discharge at Elverum.

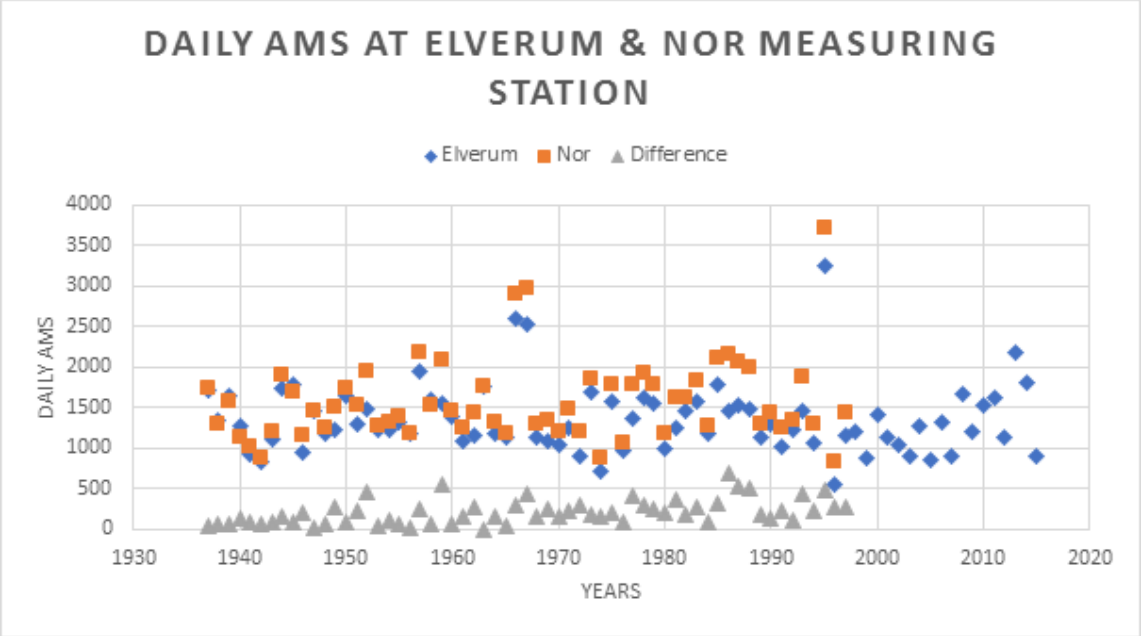

Figure 22) The graph shows the relationship between the AMS-values at Elverum station (blue) and Nor station (red), and the difference between them (grey).

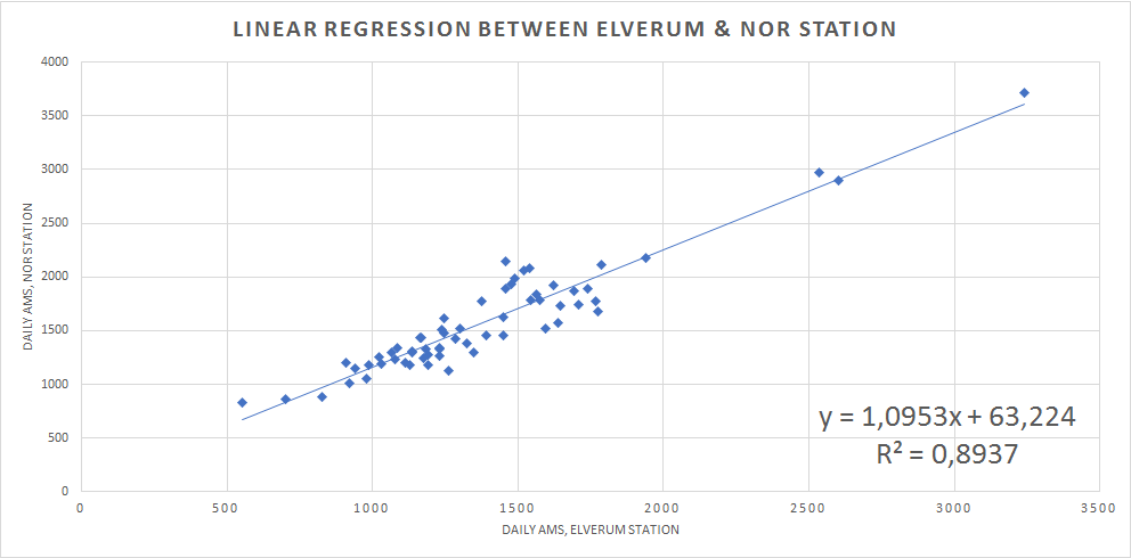

Figure 23) Regression line between the AMS-values at 2.604 Elverum (x-axis) and 2.2 Nor (y-axis).

4.3 Paleohydrology – sediment analysis

To test if there is a connection between the minerogenic layers deposited in lake Flyginnsjøen and bifurcation events in Glomma at Kongsvinger, sediment core FLS113 was analyzed at the highest possible resolution to enable a comparison with instrumental data. For this purpose, a Procon Alpha Core X-ray CT-scanner located at the EARTHLAB, Department of Earth Science, University of Bergen (UiB), was used to obtain 3-dimensional X-ray imagery of the sediment core FLS113. Computed tomography (CT) is an X-ray methodology yielding 3-dimensional results by placing an object on a rotational stage between an X-ray tube and X-ray detector. The object is rotating 360 degrees and capturing images at specific intervals.

Sediment core FLS113 was put inside the CT-scanner for analyzing. A CT-scan is the only way to get 3-dimensional views of the inside of a sediment core without destroying the object (Exact Metrology, 2017). The CT-scanner measures the attenuation of X-rays, and is thus an indication of density. There are also other factors than density which can influence the results, but with voltage exceeding 100 kV, these factors are usually ignored (e.g. Orsi & Anderson, 1999). The results are given as images with greyscale values, and not direct density values. The unit is therefore “greyscale values” or “greyscale”. It is 16-bit measurements, so there are 65.536 values on the greyscale. The resolution of the measurements for FLS113 is 80.1 micrometer, i.e. each voxel (volume pixel) has sides of 80.1 micron. To obtain 2-dimensional data from the core, a line through the core was chosen (cherry picking) where the sediment layers were best preserved, and 500 measurement points distributed along this 18.0 cm line were obtained.

Avizo 3D Software was used for analyzing the X-ray image; white represent dense layers, while black represent low-density layers. From this software, we could edit the 3D-picture of the core, using a variety of functions such as changing contrasts, edit colors, turn and tilt the core etc.

The longer sediment cores (FLP113 and FLP213) have not been scanned by CT-scanner (maybe an idea for another master thesis?), but other analyses have been carried out on these cores (see the data-chapter).

Rate of change

Rate of change (RoC) is calculated by dividing the change of the parameter y by the change of time. Rate of change is simply the time derivative of the variable y (measured parameter). Floods are fast events which potentially give distinct changes in the sedimentation environment in a lake. Therefore, the RoC-values in the measured parameters will be used as a tool to identify flood sediments in a lake. The flood sediments are characterized by a high and fast positive response in the various parameters, because these represent an increase in the amount of minerogenic materials. When the flood's intensity and sedimentation rate decrease, the rate of change will become negative. Because of this, every quick increase in RoC will be followed by a negative response. The RoC will therefore mark the start of a flooding, and not the peak of the flood (Figure 24).

A flood event with several pulses in the water discharge, and therefore several fast changes in the same layer, might give several impacts in RoC. On the other hand, a flood event with a gentler curve in RoC than the criterion will not be registered as a flood. The RoC is affected by the change in sedimentation rate. In periods with high sedimentation rate, the resolution will become higher, and therefore the sensitivity for RoC will also increase. Støren et al. (2010) still claim that this effect is small and negligible, and that the main reason for higher RoC is an increase in the runoff to a lake, which happen during a flood.

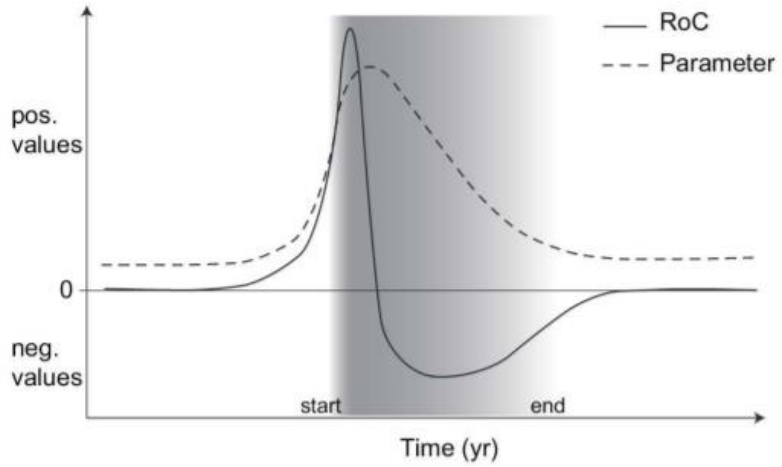

Figure 24) Model showing the relation between sediment layers, the change in the parameter and the rate of change over time (Støren et al., 2010).

Age-depth-model

To establish a chronology in the age of the lacustrine sediments, a core must be tested and analyzed. The specific age at every point through the core depends on the sedimentation rate between two points. In Steffensen's study (2014), two dating methods were used, both based on the decomposition of radioactive isotopes. Radioactive isotopes are unstable and will be decomposed to stable form. The time it takes for a quantity of radioactive atoms to be halved is constant and is called its half-life. This half-life happens in linear, known speeds for each isotope, and forms the basis for dating with radioactive isotopes (Walker, 2005).

The estimation of age with depth was done by lead dating (^{210}Pb, half-live: 22 days) in FLS213 (short core) and carbon dating (^{14}C, half-life: 5730 years) in FLP213 (long core). These datings were done

during another study (Steffensen, 2014), and samples from the cores were sent to laboratories in, respectively, England (Environmental Radioactive Research Center at the University of Liverpool) (Appleby and Piliposian, 2014) and Poland (Poznan Radiocarbon Laboratory) (Goslar, 2014) for this.

Flood layers deposited by quick events may potentially result in thick layers which have the same age. Since the age increases with depth, flood layers thicker than a specific value should be defined with the same age (e.g. Gilli et al., 2013). One example is the layer at 18–33.5 cm depth in sediment core FLP213. This layer of 15.5 cm thickness is extreme, compared to the others, which normally are only a few mm thick. This layer is probably caused by one single event – Storofsen, and those 15.5 cm of sediments in the core has therefore been given the same age (Steffensen, 2014). Anyway, Støren et al. (2010) show that if the flood layers' thickness is within the uncertainty of the age-depth-model, this will not affect the result in any significant way.

The CT-scan of sediment core FLS113 gave 500 measurements along a spline line (18.0 cm) through the core. The greyscale values were used, and the rate of change-values were calculated for these measurements. Further, several percentiles were tested for, desired to find the threshold giving exactly 24 values – because there happened 24 bifurcation events in Glomma at Kongsvinger during the time period FLS113 covers. Using the age-depth-model, these 24 density values were then checked against the years of bifurcation events to see if the dense layers could be explained by these bifurcations.

Choice of threshold in flood counts in the long core

The threshold found in sediment core FLS113 is not directly transferrable to the longer core FLP213, but if there is a correlation between the sediment layers in the core and the bifurcation events, I assume that the relation also is valid in the longer core.

In a previous study of these cores, the assumption that dense layers correspond to flood events (above a certain threshold) is used to count number of floods in the long core. Steffensen (2014) says in her thesis that "a PCA (principal component analysis) shows that variations in Potassium (K) best reflect variations in the sediments. RoC of K was therefore used to identify flood layers in Flyginnsjøen. Because there exists a continuous access to K in the environment, a threshold must be defined for what is flood and what is not". The threshold she found to best reproduce the number of floods measured in instrumental data in the period 1948-2013 (the 94th percentile of RoC of K), was used to count floods through Holocene. Additionally, she used a lower threshold (the 90th percentile of RoC of K) to increase the variability and test the sensitivity in the data. Values equal to, or larger than the threshold, were defined as flood events. Using this method, 438 and 792 floods were counted through Holocene, respectively by K P90 and Ti P90. These numbers might seem low (438 or 792 floods in a 10 000-years period) compared to today, but because of non-stationarity there might have been long periods through Holocene with significantly fewer floods than there is today.

The CT-scanner obtains data with such high resolution, allowing comparison between the sediment cores and the historical- and instrumental data. The data from the longer FLP-cores are good enough within the scope of this thesis. They can be used to test if the minerogenic layers in the sediment cores actually coincide with bifurcation events, and do not need to be reanalyzed.

4.4 Use of historical and paleohydrological data in flood frequency analysis

The R project for statistical computing is free software for statistical computing and graphics. In this study, R is used as a tool to analyze flood archives. Data and information from instrumental information, historical data and information from paleohydrologic data are collected and systemized. R is then used to identify non-stationaries in the flood series.

Similarity measures

Contingency tables (also called crosstabs or two-way tables) are used in statistics to summarize the relationship between several categorical variables. The table is a special type of frequency distribution table where two variables are shown simultaneously. In this case, the CT-table is used to compare two flood data series from (i) flood information from the bifurcation events (for when water discharge exceeded 1500 m^3/s) and (ii) information from flood sediments in the core (with a given threshold). These two series must have the same length.

The time period is from approximately 1950-2013. The CT-table does not take into account if there was more than one bifurcation event in a year; it only counts "bifurcation" or "no bifurcation" for each year. Twenty-two of these years had bifurcation events (24 events on 22 years; two years had both spring- and autumn flood), and the remaining 41 ± 7 (the uncertainty in dating) years did not have any bifurcation events. Then, it is compared from one year to the next, and the result of the test is presented in a CT-table (Table 3).

Table 3) Layout of CT-table.

	No bifurcations	Bifurcations
No sediment layer	Correct negative	Miss
Sediment layer	False alarm	Hit

where;
Hit = year with a bifurcation event and a flood layer in the sediment core.
Miss = year with a bifurcation event, but no flood layer in the core.
False alarm = no bifurcation event, but flood layer in core.
Correct negative = no bifurcation event and no flood layer in the core.

The hit-rate is the number of hits divided by number of hits + number of misses, and the false-alarm-rate is the number of false alarms divided by the number of correct negative + the number of false alarms. A high hit-rate and a low false alarm-rate is desirable.

To investigate if there is a relationship between the sediment layers in the core FLS113 and the bifurcation events in Glomma at Kongsvinger, two similarity measures have been calculated; correlation and critical success index (CSI, also called jaccard-index).

The correlation coefficient (R) of two variables in a data set equals their covariance divided by the product of their individual standard deviations. It is a normalized measurement of how the two are linearly related. If the correlation coefficient is close to 1, it would indicate that the variables are positively linearly related and the scatter plot falls almost along a straight line with positive slope. For -1, it indicates that the variables are negatively linearly related and the scatter plot almost falls along a

straight line with negative slope. And for zero, it would indicate no linear relationship between the variables.

The Jaccard-index is a statistic used for comparing the similarity and diversity of sample sets. Its coefficient measures similarity between finite sample sets, and is defined as the size of the intersection divided by the size of the union of the sample sets. Jaccardneedham is in this case the same as critical success index, CSI, which indicate the value of a warning.

The critical success index (CSI) is calculated using the values from the CT-table;

$$\text{CSI} = \frac{Hits}{false\ alarms + hits + misses} \tag{1}$$

This CT-table compares one year with another, and does not take into account the uncertainty in dating which increases with depth. Trying to compensate for this, running windows have been used. In R, this is implemented in the package "zoo". The running windows for a 3-year interval count number of bifurcation events in years number 1, 2 and 3. Then it compares it with the number of flood layers for years 1, 2 and 3. Next, it counts number of floods in year numbers 2, 3 and 4, and compares it with the number of flood layers for years 2, 3 and 4. So it goes, until all the years are covered. The 4-, 5-, and 10-year-intervals works the same way, only with longer time intervals. This way, one attempts to compensate or consider the uncertainty in dating and depth. The longer running window interval, the better hit is expected, because longer time periods are compared to one another. The correlation for the running window intervals is calculated, and indicates how well the two series fit.

4.4.1 Flood frequency analysis

In this study, a generalized extreme value (GEV) distribution is chosen, with three Markov chains, and a confidence interval of 90 % (from 5 % to 95 %). The GEV-distribution is shown to be a limiting distribution for block maxima (Fisher & Tippett, 1928; Gnedenko, 1943; Embrechts et al., 1997). The following equation is used;

$$F(x) = \begin{cases} exp\left\{-\left[1 - k\left(\frac{x-m}{\alpha}\right)\right]^{1/k}\right\} \\ exp\left\{-exp\left(-\frac{x-m}{\alpha}\right)\right\} \end{cases} \tag{2}$$

where m is the location parameter, α is the scale parameter and k is the shape parameter. For k = 0, the GEV distribution corresponding to the Gumbel distribution is used, k < 0, the GEV distribution corresponding to the Frechet distribution is used, and for k > 0, the GEV distribution corresponding to the Weibull distribution is used. A Bayesian approach, where the parameters are considered as random variables, is used to estimate the parameters and the return levels. Their posterior densities are calculating as;

$$\pi'(m,\alpha,k|\vec{x}) = \frac{l(\vec{\mathbf{x}}|m,\alpha,k)\pi(m,\alpha,k)}{\iiint\ l(\vec{\mathbf{x}}|m,\alpha,k)\pi(m,\alpha,k)dm\,d\alpha\,dk} \quad (3)$$

where π is the prior and $l(\vec{\mathbf{x}}|m,\alpha,k)$ is the likelihood of the observation vector $\vec{\mathbf{x}}$ given the parameters m,α,k. The denominator makes the integral under the probability density function (pdf) equals one.

Including historical flood information

The Bayesian approach was used for combining historical and systematic data in a flood frequency analysis. Depending on which data we have, the total likelihood is given as a product of the three major likelihood terms;

$$l_i = l_s \cdot l_b \cdot l_{ai} \quad (4)$$

where l_i is the total likelihood, l_s is the likelihood for the systematic data, l_b is the likelihood of the h-t number (h = period, t = number of floods exceeding a threshold) of floods not exceeding the threshold x_0 during the period h, and l_{ai} is the likelihood of (i) number of floods exceeding a threshold, (ii) number of floods within an interval defined by an upper and lower limit, or (iii) the exact size of all floods exceeding the threshold (Gaal et al., 2010; Engeland et al., 2017). Figure 25 shows an example of how to include historical flood information to lengthen the flood record.

The posterior distribution of the parameters was estimated using a MCMC-method implemented in the R package nsRFA (Viglione, 2012). For estimating the return levels, the posterior modal values of the parameters were used.

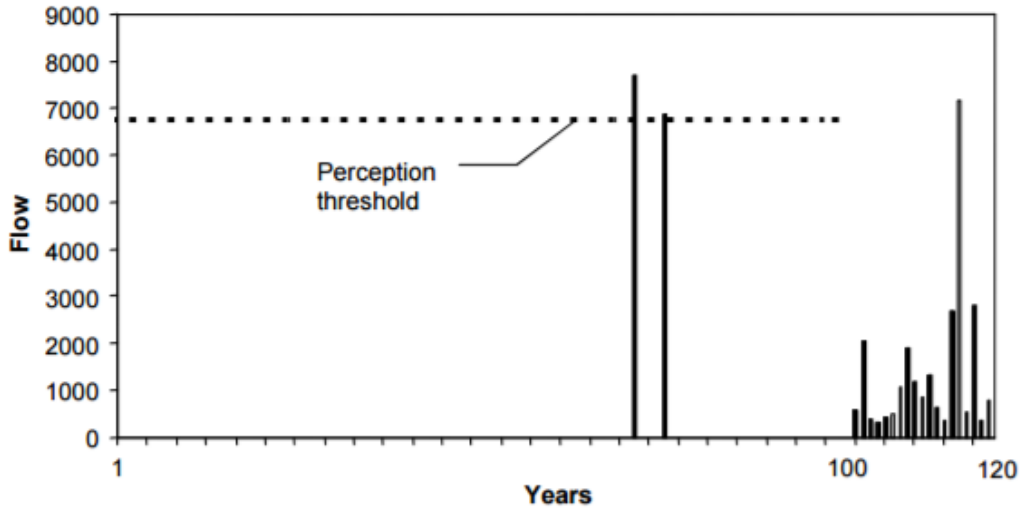

Figure 25) Illustration of how to include historical flood information in the Bayesian approach. The number of years in historical period (h) is in this example 100, the number of observation from systematic data (N) is 20 and the perception threshold (x_0) is 6842 m^3/s (Dirceu & Stedinger, 2005).

The particularity of this Bayesian MCMC-function is that it takes into account historical information (Payrastre et al., 2011). For the historical period, either the number of all floods exceeding a specific threshold for a specific period was specified, the number of floods within an interval, or the estimated sizes of these floods were used (Engeland et al., 2017).

For historical floods, I assume that all floods exceeding a certain threshold for a period are known. To include this information in the flood frequency analysis, two methods can be used; (i) in the simplest case, the number of floods exceeding the threshold is used; and (ii) in the better, and a bit more complicated case, the exact flood size of the flood events exceeding the threshold is used. In this study, the discharge values corresponding to the floods have been obtained from the height-differences at flood monuments.

Including paleohydrological flood information

The paleohydrological flood information is included in the flood frequency analysis to base the flood estimation on an even longer flood record. From flood counts in sediment core FLP213, there were 155 floods during an approximately 670 year-period (ca 1200-1870) (Steffensen, 2014). The period after 1200 is used, because it is assumed that this period was quite stationary when it comes to number of floods.

This information is added to the flood frequency estimation. A lower and an upper limit is defined, respectively 1300 m^3/s and 3900 m^3/s. The discharge threshold when bifurcation occur in Glomma at Kongsvinger is estimated to 1500 m^3/s (Pettersson, 2001) which corresponds to 1300 m^3/s at Elverum, therefore the lower threshold of 1300 m^3/s is used. The higher threshold of 3900 m^3/s is the estimated discharge value of Storofsen, which is believed to be the largest flood in history (Bøe et al., 2006). It is believed that all the floods in historical time occurred within this interval, and this is the reason for the choice of the upper and lower limit. Then, the Bayesian MCMC-package implemented in R is used to estimate the flood frequency.

Return level plots

To demonstrate the use of historical- and paleohydrological information, the fitted distributions with 90 % confidence interval were plotted together with their empirical distributions. The 90% confidence interval represent the estimation uncertainty caused by the limited sample size, and is estimated by the MCMC-approach by calculating a frequency curve for each of the posterior parameter sets and the extract the 90% confidence intervals from these frequency curves. In the plot, the models fitted to only systematic data, both systematic data & historical information, and systematic + historical + paleohydrological information are included. The Cunnane plotting position (Cunnane, 1978) is applied – where the exceedance probability of x_i with rank I from a dataset with m members sorted in decreasing order is given as;

$$\hat{p}_i = \frac{i-0.4}{n+0.2} \quad (5)$$

For introducing the historical floods, the plotting positions given by Hirsch and Stedinger (Hirsch & Stedinger, 1987) are used;

$$\begin{aligned} p_i &= \frac{i-0.4}{l+0.2} \cdot \frac{l}{n} && i = 1, \dots, l \\ p_i &= \frac{l}{n} + \frac{n-l}{n} \cdot \frac{i-l-0.4}{s-e+0.2} && i = k+1, \dots, t+s \end{aligned} \quad (6)$$

where i is the rank, l is the number of extraordinary floods, n is now the length of the period for which we have information about floods (note that $n = h + s$), s is the length of the systematic record, h is the length of the historic information and e is the number of extraordinary floods in the systematic record (note that the number of historical floods $t = l - e$) (Engeland et al., 2017).

Current methods for flood frequency analysis assume that the data sample consists of independent, identically distributed (iid) events. This criterion of independence implies that there are no autocorrelations, trends or shift in the sample, thus the magnitude of one event should not be dependent on the magnitude of the previous event, and there should not be systematic or abrupt changes over time. The assumption of identical distribution may be violated if the floods are caused by different generating processes, which can be the case in Norway where some floods are caused by extreme rainfall only, and others are caused by considerable amounts of snowmelt.

4.4.3 Return level graphs

To make the flood return level plots, I have used different kinds of flood information; systematic data, historical information, paleohydrological information, and combinations of these. Plotted in the same graph, these can be compared to each other, and return levels can be obtained for each of the information source.

1) Systematic data.
   AMS-values from the specific measuring station from the period of interest.
   a. From 2.604 Elverum (before regulations), 66 AMS-values are used (1871-1936),
   b. from 2.604 Elverum (after regulations), 79 AMS-values are used (1937-2015),
   c. from 2.604 Elverum (the whole period) 145 AMS-values are used (1871-2015)
   d. from 2.604 Elverum – the last 60 years (1956-2015)
   e. from 2.604 Elverum – the last 30 years (1986-2015)

2) Historical information.
   a. Number of floods exceeding the threshold. Nine floods in historical time (200 years before systematic measurement started; ca 1650-1850) were bigger than the threshold-flood (1967, 2533 m^3/s). The nine floods happened in the following years (with decreasing size); 1789, 1675, 1773, 1717, 1724, 1749, 1850, 1827, 1846. These floods are obtained from the flood monument in Elverum.
   b. Estimated discharge for the floods by using the relative height from the flood monument at Elverum, the known discharges (for six of the floods on the monument) and extracting them. Corresponding to the floods mentioned above (m^3/s); 3900, 3090, 3090, 3034, 3034, 3034, 2963, 2794, 2533.

3) Paleohydrological flood information.
   From flood counts; 155 floods happened in 670 years (ca 1200-1870) (Steffensen, 2014). The Holocene period (of approximately 10 000 years) has varying flood frequency, and is affected by climate changes and other factors making this period non-stationary. Therefore, I have chosen to use the flood counts from 1200 until present in my flood frequency analysis and uses the assumption that this represent a stable period.

4) Flood information from observations + historical information + paleodata. This information contains flood history from approximately 1200 to 2015. This is more than 800 years of flood information. Therefore, the flood frequency analysis will be based on much longer flood record, compared to previous flood frequency estimations based on systematic measurements which usually contain less than 100 years of information.

5 Results

The results in this thesis are obtained using the method explained in the previous chapter. First the results of the updated bifurcation list are presented, then the flood information obtained from historical sources, and at last the information obtained from paleohydrological sources – sediment cores and analyses of these.

5.1 Instrumental flood information

I have used information from 2.120 Nors Bru (1851-1936) which was the period before the big regulations in Glomma. These data consist of 77 years of data. I have also used information from 2.2 Nor (1937-1997) which was the period after the regulations, and consists of 62 years of data. Systematic information from 2.604 Elverum is also used. This station contains measured data from 1871-2015 (it is still in use, but this is the period I have used information from).

From Pettersson's article (Pettersson, 2001), bifurcation events in Glomma at Kongsvinger up to year 2000 are listed. Table 4 shows the updated bifurcation events, and its corresponding transferred amount of water, duration maximum discharge, dates and season for the bifurcation events from 2000-2013. Four years in this time period had water discharges exceeding 1500 m^3/s.

Table 4) Table showing year, transferred water amount, duration, maximum discharge and dates for the bifurcation events from 2000-2013.

Year	Transferred water (mill m^3)	Duration (days)	Max discharge (m^3/s)	Dates	Season
2008	1.8	10	7.1	03.-12.05.08	Spring
2010	0.05	2	0.4	22.-23.05.10	Spring
2011	0.30	3	2.6	11.-13.06.11	Spring
2013	2.80	4	18.8	23.-26.05.13	Spring

5.2 Historical data analyses

In addition to instrumental flood information, I have added 200 years of historical flood information, from approximately 1650-1850. Floods above 4.2 m on the water level gauge in this setting are considered as damage floods. This is equivalent to the size of the flood from 1967, so this flood is used as a threshold for historical large floods. From Elverum flood monument and other historical sources, we know that the following floods (with decreasing size) were bigger than 1967-flood; 1789, 1675, 1773, 1717, 1724, 1749, 1850, 1827, 1846. The latter have the same height as the 1967-flood (the threshold flood), but is nevertheless included. Thus, nine floods altogether exceeded the threshold-flood in this period. Estimated discharge values of these floods at Elverum are respectively (unit m^3/s); 3900, 3090, 3090, 3034, 3034, 3034, 2963, 2794 and 2533. Estimated discharge values of the same floods adjusted to Nor station are respectively (unit m^3/s); 4335, 3448, 3448, 3386, 3386, 3386, 3309, 3123 and 2838.

Figure 26 shows the rating curve for the floods marked on Elverum flood monument. The six red points represent the six floods with known discharge values (1789 (Storofsen – estimated before), and the floods overlapping with instrumental data (the floods in 1995, 1934, 1916, 1966 and 1967)). This

rating curve was used to estimate the discharge values for the rest of the floods on the monument (not overlapping with instrumental data).

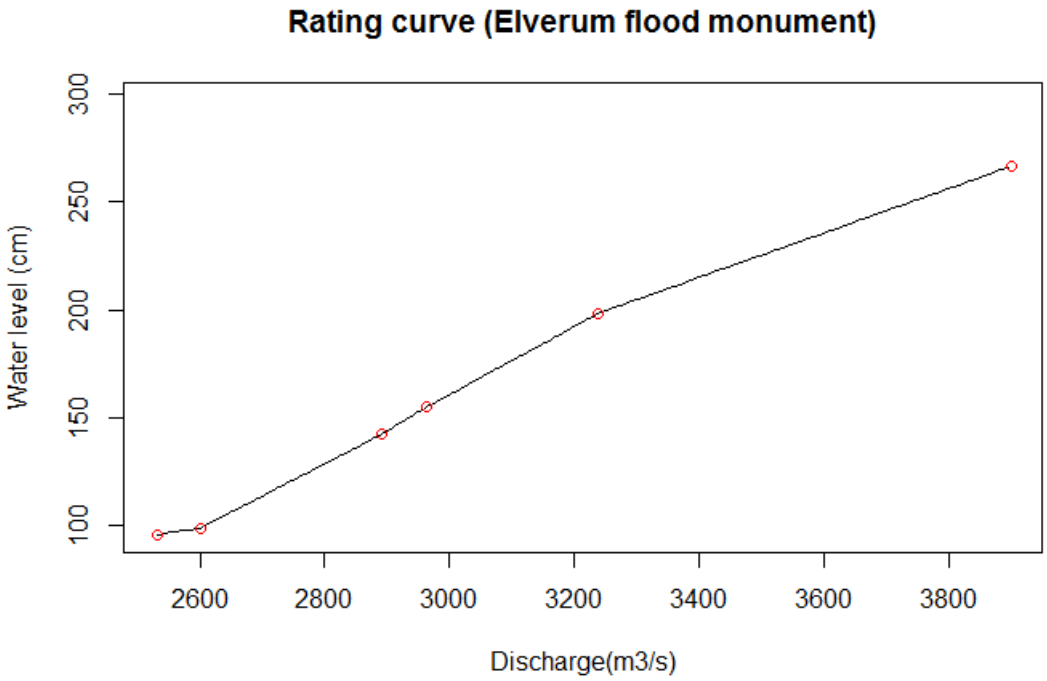

Figure 26) Rating curve from Elverum flood monument showing the relationship between discharge values (x-axis) and water levels (y-axis). The six red points refers to the known flood sizes (discharge values).

Table 5 shows the estimated discharges of the floods marked on the flood monument at Elverum. The 1st column shows the year of the flood events, the 2nd column shows the height on the flood mark, the 3rd column shows the estimated discharge value of the floods and the 4th column shows the estimated discharge values at 2.2 Nor, using the regression analysis (y = 1.0953x + 63.224).

Table 5) Table showing year, heights, and estimated discharge values at Elverum and Nor stations.

FLOOD YEAR	HEIGHT (CM) FLOOD MONUMENT	ESTIMATED DISCHARGE AT 2.604 ELVERUM (m^3/s)	ESTIMATED DISCHARGE AT 2.2 NOR (m^3/s)
1789	266.5	3900	= 4335
(1995)	198.5	3238	= 3610
1675, 1773	176	3090	= 3448
1717, 1724, 1749	167	3034	= 3386
1850, (1934)	155	2963	= 3309
(1916)	142.5	2892	= 3231
1827	125	2794	= 3123
(1966)	99	2600	= 2911
1846, (1967)	96	2533	= 2838

5.3 Paleohydrology – sediment cores

To add even more years of flood information, I used the information saved and preserved in sediment cores. Paleohydrological information potentially contain thousands of years of flood history, and the sediment cores from Flyginnsjøen (which I used) are believed to contain all floods (with higher discharge than 1500 m^3/s) that have happened in Glomma at Kongsvinger through Holocene. This threshold might have changed during Holocene, but this is nevertheless the best assumption I have, and it is therefore used to represent the threshold during Holocene as well.

To use paleohydrologic flood information from sediment cores, I must determine that there is a relationship between the sediment layers in the cores and the bifurcation events in Glomma at Kongsvinger. First, I will present and describe the sediment core FLS113, then introduce the age-depth model and afterwards identify the layers in FLS113 with high density and investigate if these can be explained by bifurcation events.

Sediment core FLS113

Sediment core FLS113 (figure 27) comes from the bottom of Flyginnsjøen, therefore the two first letters "FL". The "S" refers to the method used to bring this core up; a Swedish HTH gravity corer (developed in Umeå) that is sensitive and less destructive, and therefore often used to take up the upper sediments (Renberg & Hansson, 2008). The numbers in the name refer to the 1st taking ("1"), and this was done in 2013 ("13").

FLS113 is a cylinder; 18.0 cm long and 7.0 cm in diameter. It was sliced into to equal parts (from top till bottom), where one is being used to do analysis and tests, and the other one is kept untouched – as a reference core. With the naked eye, we can see that the core mainly contains a dark mud-like structure. Somewhere in between this mud, there are lighter layers. These layers are more or less horizontal, and some are more distinct than others. The green on the top and bottom of the sediment core is floral oasis, simply used to hold the sediments together.

The core can roughly be divided into three parts; the upper five centimeters of the core seems almost homogenous, with a dark grey/almost black material. There are some structures in this part, but no distinct white layers. The middle part (from 5 to approximately 14-15 cm depth) is a section consisting of white, almost-horizontal layers, separated by the dark mud. The last part is the 4 cm at the bottom of the core. This part is dominated by lighter sediments. Unlike the other white layers, this part is different in more than one way; this layer is much thicker than the other layers, and it is also folded. The reason for these, somewhat strange and unexpected characteristics, is believed to have happened during the core taking. The bottom part of the core was probably disturbed when the core was taken from Flyginnsjøen. Despite the fact that this part is affected by human touch, and therefore probably not perfectly representative, it does show that there is a great lighter layer, much thicker than any of the other layers in the core.

Figure 27) Picture of sediment core FLS113 with cm-scale.

Age-depth-model

The age-depth model (Figure 28) is made using ^{210}Pb dating (for table, see appendix). The age is measured at sediment core FLS213. To make age-dating on a core, the core must be cut into pieces, and in this case, they were sent to a laboratory in Liverpool, UK, to be examined. The core will be destroyed to date it, and therefore FLS113 cannot be used. FLS213 was taken right next to FLS113, so they should give the same results, and the age-depth relationship in this core should be representable for FLS113 as well. The age increases with the depth as younger sediments will always be deposited over older sediments. Sediments will become more and more compressed with overburden sediments. Because of this, the relation between depth and age is not linear. The uncertainty with the dating-method also has some limitations. The margin of error increases with increasing depth, starting with ± 1 year at the top and ends with ± 7 years at the bottom. This figure shows the relation between the age and depth and the uncertainty bars. Sediment core FLS113 covers the last approximately 65 years.

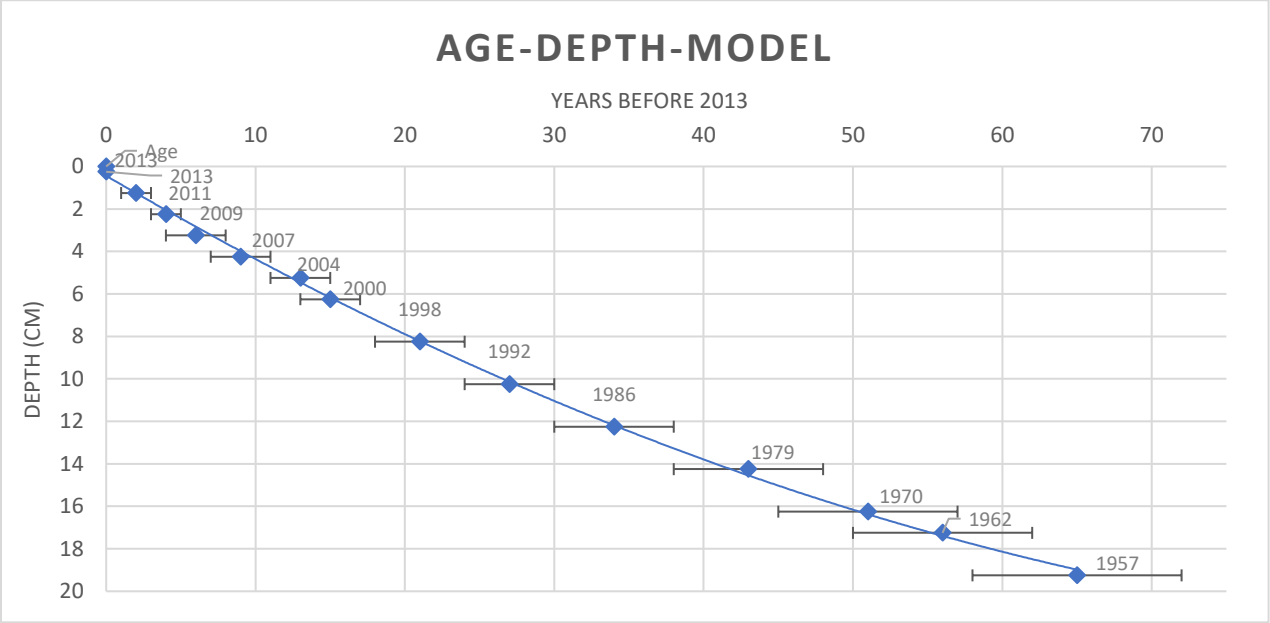

Figure 28) Age-depth model (based on FLS213) shows the relationship between the depth in the core and the age. Error bars show the uncertainties which increases with increasing depth.

Identification of flood layers

In this study, I work with the assumption that flooding results in dense layers in the sediment cores. The dark mud in the sediment cores is background sedimentation that happens in the river all the time. This happens under normal conditions, and is called sedimentation regime number 1. The almost black mud contains a lot of organic material. The XRF-analyses Steffensen (2014) did, show that this mud contains high values of LOI (loss on ignition) and low values of MS (magnetic susceptibility).

The lighter and denser layers are believed to be flood layers. When Glomma is flooded (if the water flow exceeds 1500 m^3/s), water from Glomma is transported to Flyginnsjøen via Vingersjøen. The water from Glomma contains different minerals in the sediments than the autochthon sediments that are in Flyginnsjøen (referring to "identification of flood layers" from chapter 2 (theoretical background)) and therefore, we can observe the layers resulting from flooding. The flood sediments are lighter in color due to the content of minerals. It is also shown that these layers have bigger

fractions than the mud. The mud has small particles (you can hardly tell the grains apart), but this minerogenic layer consists of silt fractions, which is coarser than the mud. Additionally, the flood layers have low values of LOI and higher values of MS. It has also higher density and lower water content. According to XRF-analysis, these layers have high count rate of Potassium (K), Calcium (Ca), Titanium (Ti), Silicon (Si) and low LOI (Steffensen, 2014). The higher rate of Si, K, Ca and Ti in the flood layers are due to the increased supply of minerogenic minerals that is washed into the lake during flooding in Glomma. This sedimentation type happens under what is called sedimentation regime number 2.

One assumes that floods results in dense layers, so to identify the flood layers in the cores, one must find the densest layers. The CT-scanning of the sediment core FLS113 reveals several layers in the core (Figure 29), and these are visualized using Avizo 3D software. From the spline line, 500 greyscale values were extracted. The rate of change values for these greyscale values were then calculated. Using Avizo 3D-software, useful and informational figures were obtained. The program allows us to change colors, making the different layers easier to detect. Figure 29 A shows black and white 2-dimensional slice through FLS113, and Figure 29 B shows a colored 3-dimensional volume rendering of FLS113. Green colors refer to dense layers, while blue refers to less dense layers. We clearly see that there are distinct layers that go through the whole core.

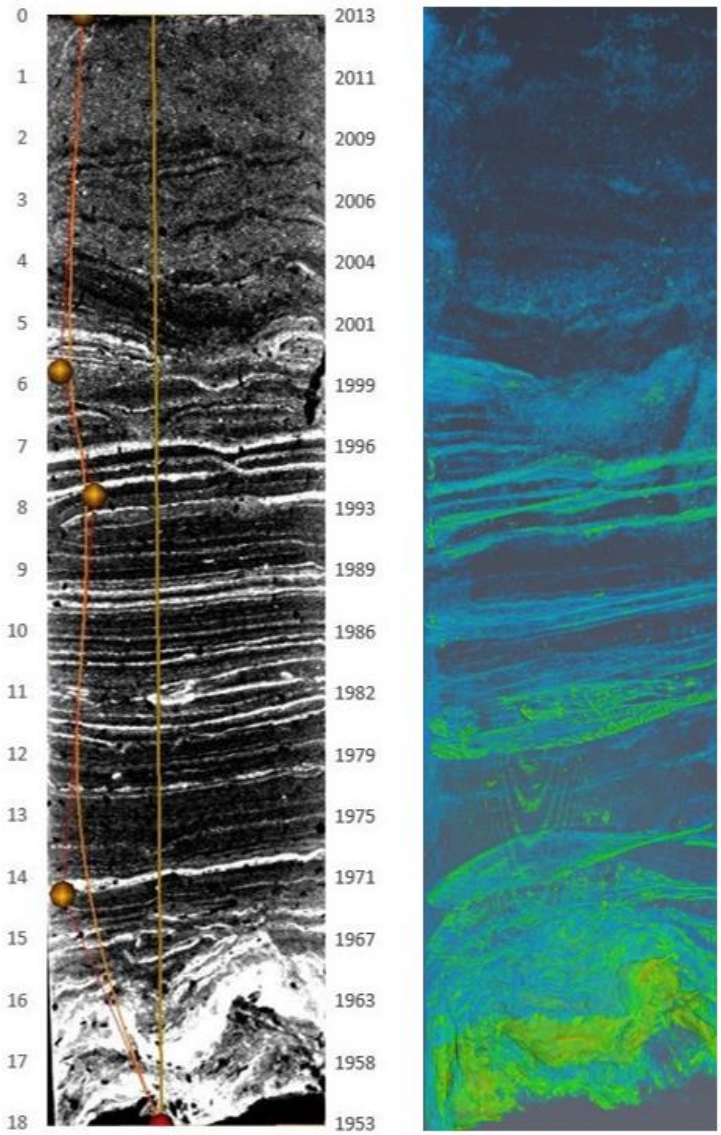

Figure 29 A) Sediment core FLS113 from Avizo 3D. White is dense layers, black is low-density layers. B) 3-dimensional CT-image of sediment core FLS113 showing near horizontal high-density layers (green/yellow) deposited in a low-density background matrix (blue).

From instrumental data, we know that bifurcation in Glomma at Kongsvinger has occurred 24 times in the period sediment core FLS113 covers. Therefore, I will try to find a threshold in sediment core FLS113 giving the 24 densest values. Assuming that bifurcation events result in dense sediment layers, the threshold can be used to reproduce the bifurcation events.

To find the correct threshold, I tested for five different thresholds; greyscale P94, greyscale P90, RoC of greyscale P94, RoC of greyscale P92 and RoC of greyscale P90. The threshold of RoC P92 gave exactly 24 dense layers.

Rate of change P92

Figure 30 shows the relationship between bifurcation events (blue) and density layers with a threshold of RoC P92 (red). The x-axis shows the age (age decreases with depth). The right y-axis shows the volume of water transferred from the bifurcation events, and the y-axis to the left shows the density of the density layers. Uncertainty in age-dating increases with depth, and error bars are therefore included for the density layers. From the graph, five of the bifurcation events cannot be explained by one of these sediment layers.

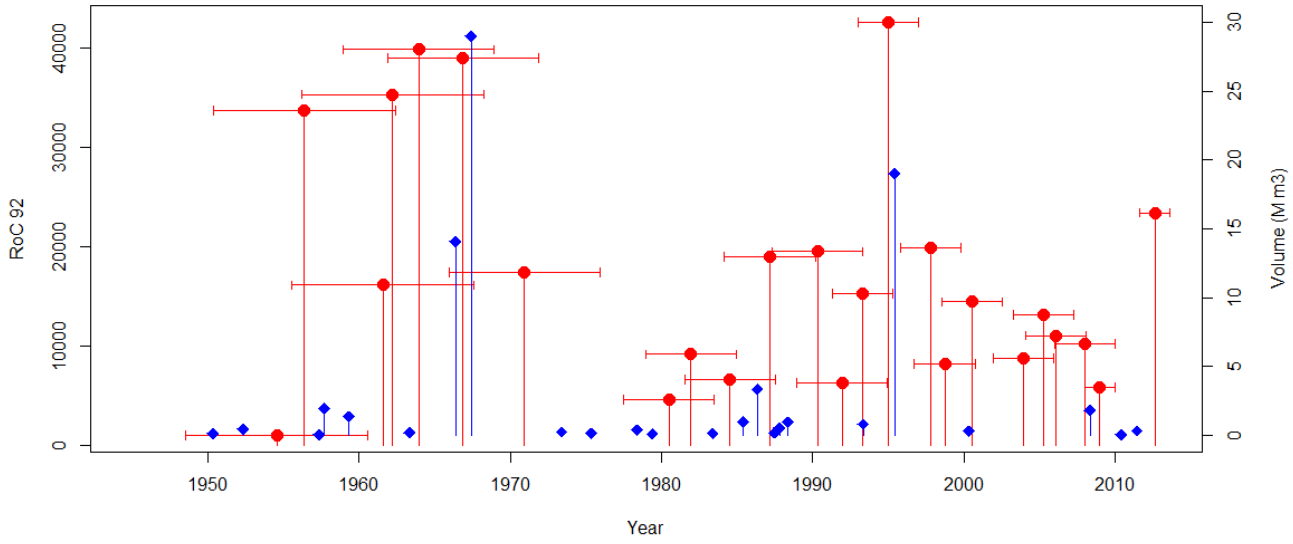

Figure 30) Relationship between bifurcation events (blue) and sediment layers with threshold RoC P92 (red). Error bars indicate age uncertainty on the sediment layers.

Greyscale along the spline line in sediment core FLS113

The previous plot (Figure 30) shows that there is a relation between bifurcation events and sediment layers in FLS113. The next figure (Figure 31) shows the same in another way; the relation between the greyscale values and the bifurcation events. The bifurcation events are marked with orange points, the x-axis shows the depth in the core, and the y-axis on the left side belongs to the bifurcation events, giving the amount of transferred water to each of the events.

The greyscale values mainly lie in the interval between 15000 and 23000 voxel values, but at approximately 16 cm depth, there is an outstanding peak, which reaches almost 33000. If we compare this to the picture of the scanned core, this peak corresponds to the thick, foliated layer in the bottom of the core. This layer is much more distinct than all the others, and this is also shown through the greyscale values. This plot confirms that there is a relationship between the bifurcation events and the grey scale values, which are indications of high-density layers.

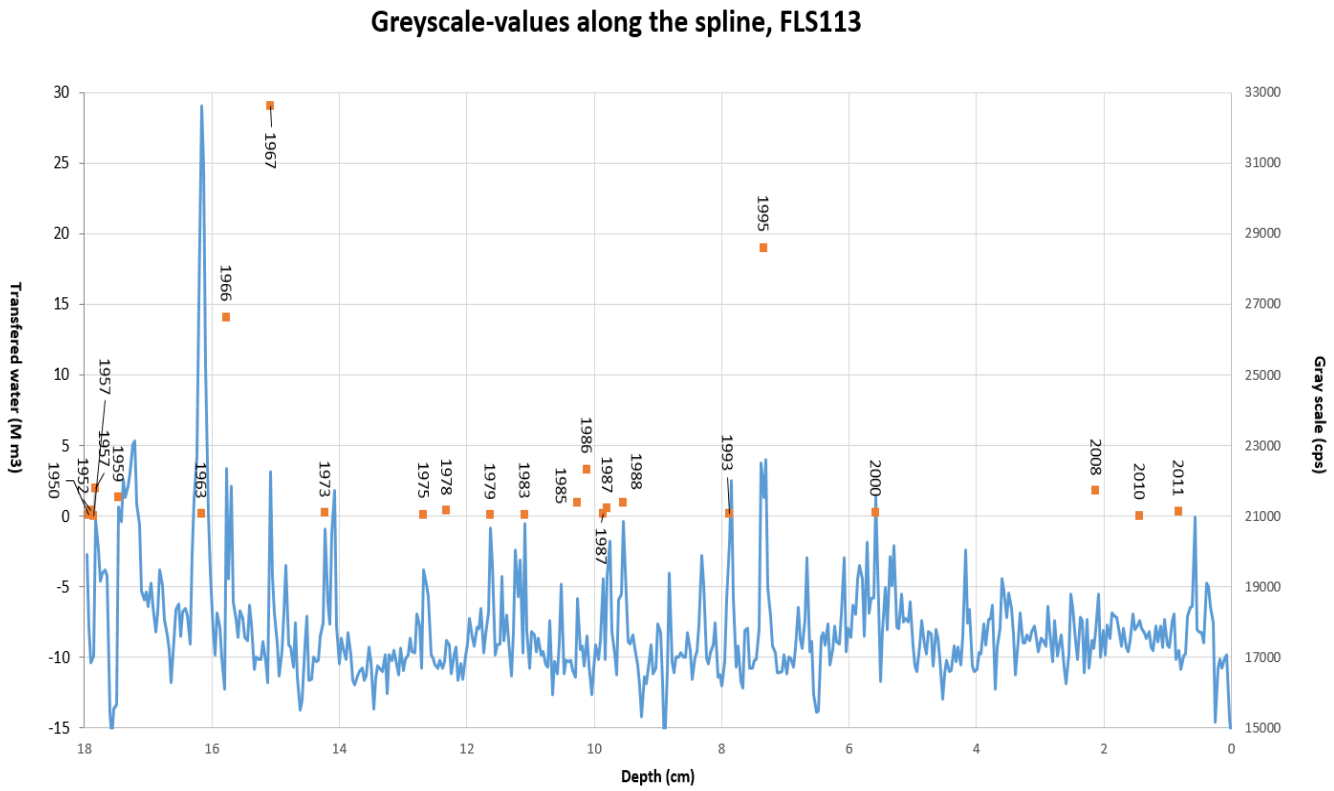

Figure 31) Greyscale values along the spline line in FLS113, and the bifurcation events plotted together. The x-axis shows the depth in the core, the right y-axis shows the greyscale values, and the left y-axis shows the transferred water amount of the bifurcation events.

Historical flood validation in sediment core

The CT-scan provides better and more detailed information of the sediment cores, and makes historical flood validations possible. In Figure 32 the colors are again changed; orange/yellow indicates dense layers while dark red refers to less dense layers. The threshold in Figure 32 A is higher than on Figure 32 B. These pictures are zoomed in sections of the core at approximately 9-10 cm depth, and there are reasons to believe that these layers might represent the floods and following bifurcations that happened in spring and autumn 1987 and spring 1988. The depth of these layers fits to these years, and we know from instrumental data that there were floods in 1987 and 1988. These layers also contain larger grains than the background sedimentation. Some of these grains were measured to have a diameter of 1635.22 micrometer (1.6 mm) and 1557.19 micrometer (1.6 mm). Larger grains indicate that there has been larger streamflow, which is used as a proxy for floods.

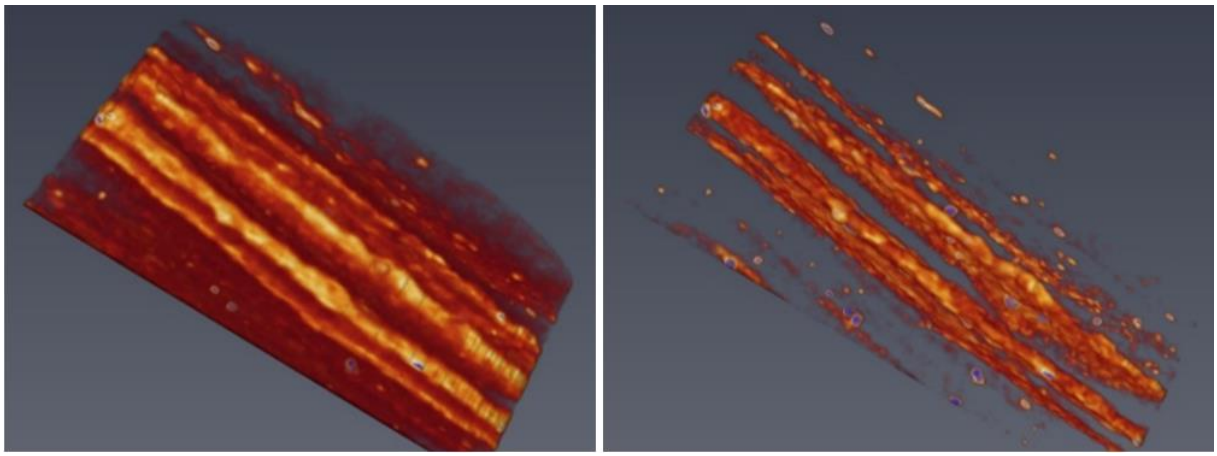

Figure 32) Close-up pictures of potential flood layers in sediment core FLS113, obtained by Avizo 3D. Yellow refers to the densest layers, while orange/dark red refers to less dense layers. The density threshold in picture B) is set higher than in picture A).

Figure 33 also shows the flood layers at 9-10 cm depth in sediment core FLS113. Blue refers to less density and red refers to high density. This figure shows some dense layers, which are probably made by flood events. There are some larger grains (with high density) and there are some gas pockets (low density) in this depth interval (Figure 33). This indicates that the layers with high density also have larger grain sizes than the background sedimentation. High waterflow (which occur during flood) can contain larger grain, so grain size is a proxy of flooding (see chapter 2, theoretical background, "transportation of sediments").

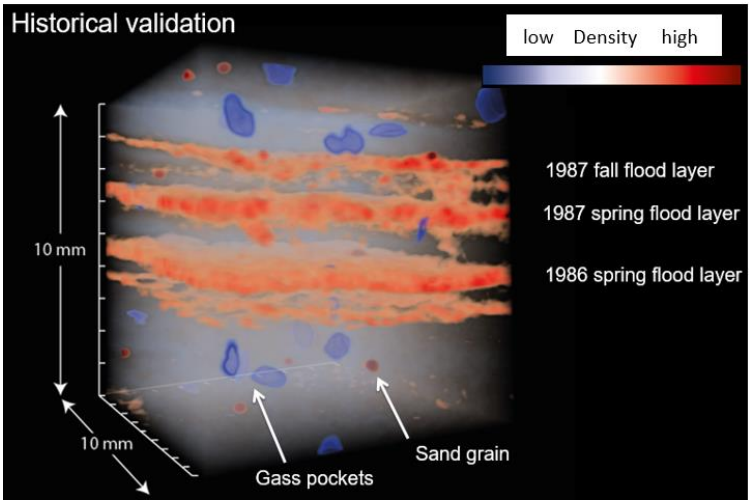

Figure 33) Close-up picture of sediment core FLS113 at approximately 9-10 cm depth, showing potential flood layers corresponding to the floods in spring 1987, and the floods in spring and autumn 1986 (Støren, 2017).

CT-table

Table 6 sums up the number of hits, misses, false alarms and correct negative for each of the thresholds tested for. Ideally, the number of hits should be as high as possible, and the number of misses and false alarms should be as low as possible. A perfect 1:1-relation between floods from sediment layers and floods from bifurcation events would have been 22 hits (not 24, because the CT-table counts only years with floods, and does not take into consideration if there is more than one flood per year, which is the case for two of the years; 1987 and 1957 had spring- and autumn flood), 47 correct negatives, 0 misses and 0 false alarms.

Table 6) CT-tables for the different thresholds (RoC P94, RoC P92, RoC P90, greyscale P94, greyscale P90), correlation between the different thresholds and the bifurcation events and the CSI-values.

ROC P94	NO BIFURCATION	BIFURCATION	CRITICAL SUCCESS INDEX, CSI
NO SEDIMENT LAYER	26	18	$\frac{4}{21+4+18} = 0.093$
SEDIMENT LAYER	21	4	

ROC P92	NO BIFURCATION	BIFURCATION	CRITICAL SUCCESS INDEX, CSI
NO SEDIMENT LAYER	27	17	$\frac{5}{20+5+17} = 0.119$
SEDIMENT LAYER	20	5	

ROC P90	NO BIFURCATION	BIFURCATION	CRITICAL SUCCESS INDEX, CSI
NO SEDIMENT LAYER	22	12	$\frac{10}{25+10+12} = 0.213$
SEDIMENT LAYER	25	10	

GREYSCALE P94	NO BIFURCATION	BIFURCATION	CRITICAL SUCCESS INDEX, CSI
NO SEDIMENT LAYER	37	19	$\frac{3}{10+3+19} = 0.094$
SEDIMENT LAYER	10	3	

GREYSCALE P90	NO BIFURCATION	BIFURCATION	CRITICAL SUCCESS INDEX, CSI
NO SEDIMENT LAYER	29	16	$\frac{6}{18+6+16} = 0.150$
SEDIMENT LAYER	18	6	

RoC P90 gives a hit of 10, and a CSI- value of 0.213, which indicate that 10 of the bifurcation events correspond to a sediment layer. This threshold gives the highest hit and the highest CSI-value of the five thresholds that have been tested. Greyscale P90 gives 6 hits (CSI-value 0.150), RoC P92 gives 5 hits (CSI-value 0.119), RoC P94 gives 4 hits (CSI-value 0.093), and Greyscale P94 gives 3 hits (CSI-value 0.094).

The number of hits are probably low, because they are only compared with a 1-1-relationship with the years. These estimations do not take account of the uncertainty in the age-depth. To try to compensate for this, estimation for the relation between bifurcation events and flood layers, using running windows, with intervals of 3-, 4-, 5-, and 10-years were done.

Table 7 contains a summary of the correlation for the different intervals for running windows, and the different thresholds. A correlation of 1 (-1) is a perfect positive (negative) correlation, and a correlation of 0 indicates no correlation at all. As high correlations as possible is desirable.

The p-value is estimated for the best correlation. This value tells how significantly different the correlation is from zero, and should ideally be as low as possible. In these calculations, it is corrected for the effective number of independent observations.

Table 7) Correlation (and corresponding p-value for the best correlation) for running windows (3-, 4-, 5- and 10-years running windows).

RUNNING WINDOWS	3 YEARS	4 YEARS	5 YEARS	10 YEARS
CORRELATION BETWEEN BIFURCATION EVENTS AND THRESHOLDS:				
RoC 94	-0.050	0.016	0.080	0.063
RoC 92	0.199	0.282	0.338	0.370
RoC 90	0.245	0.340	0.414	0.443
Grey scale 94	0.189	0.219	0.218	-0.001
Grey scale 90	0.179	0.214	0.204	-0.017
BEST CORRELATION:	RoC 90: 0.245	RoC 90: 0.340	RoC 90: 0.414	RoC 90: 0.443
CORRESPONDING P-VALUE:	0.134	0.095	0.080	0.189

The longer the window interval is, the better the correlation is. This is expected, because more and more years are compared with flood events. From correlation of the running window intervals, a threshold of RoC P90 is best. In all four running window intervals (3-, 4-, 5-, and 10-years), it is RoC P90 that gives the best correlation, respectively 0.245, 0.340, 0.414 and 0.443. The running windows is nevertheless not optimal, because the uncertainty in age-depth-dating is not even throughout the core. The uncertainty starts with ± 1 at the top and ends with ±7 at the bottom.

Therefore, another CT-table was made manually – this way one could take the correct age-depth-uncertainties into account, when comparing the years of the bifurcation events and the age (depth) of the sediment layers in the core FLS113.

Threshold giving 24 potential flood layers

A threshold of RoC P92 reproduces exactly 24 dense layers. Therefore, this threshold is used, and the depths of these 24 layers, and their corresponding ages (based on the age-depth model) is obtained. Table 8 shows the greyscale values and corresponding ages of the 24 densest layers in sediment core FLS113.

Table 8) Sediment layers detected using RoC P92 of greyscale as the threshold. Column 1 shows the number of dense layers, column 2 shows the greyscale values and column 3 shows the age (from age-depth-model) of these layers.

NO OF DENSE LAYERS	GREYSCALE VALUES	CORRESPONDING AGE (FROM AGE-DEPTH-MODEL)
1	17029.2	1954.560
2	21268.9	1956.393
3	19967.9	1961.590
4	32616.3	1962.225
5	22340.7	1963.956
6	22238.5	1966.889
7	20521.8	1970.935
8	18288.0	1980.483
9	17686.5	1981.942
10	17405.1	1984.532
11	19294.7	1984.532
12	16610.5	1990.308
13	17991.8	1991.944
14	18623.1	1993.315
15	22515.7	1994.989
16	17561.9	1997.785
17	18226.3	1998.721
18	17772.2	2000.547
19	17598.3	2003.912
20	17283.2	2005.280
21	17479.5	2006.079
22	17117.6	2007.966
23	17749.8	2008.954
24	19094.5	2012.623

From the CT-table (Table 6), five of the bifurcation events corresponded to a sediment layer in FLS113. Using the age-depth model these layers got corresponding ages. The ages of the bifurcation events are known, so by moving the floods within the limit of uncertainty in age-depth-dating, the number of hits can increase.

Table 9 shows this tuned alternative. Column one shows the depth in cm of the 24 layers that is detected with threshold RoC P92 of greyscale; column two the corresponding age (from the age-depth-model); column three; years of the bifurcation events; and column four is a tuned alternative. Some of the floods here are moved within the limits of uncertainty in age-dating, which increases with the depth, so that years of bifurcation events correspond to years of flood layers. Making the tuned alternative manually (and not using a statistical program), allows the years with both spring- and autumn flood to be taken into consideration (unlike the CT-table made in R, which only considered 22 bifurcation events).

Table 9) Table showing the tuned alternative, based on threshold RoC P92 of greyscale vales.

DEPTH (CM)	CORRESPONDING AGE	INSTRUMENTAL FLOODS (BIFURCATIONS)	TUNED ALTERNATIVE (HIT, MISS, FALSE ALARM)
0.40	2012.6 ± 1	2011	Hit
2.12	2008.9 ± 1 or 2	2010	Hit
2.56	2007.9 ± 2	2008	Hit
3.35	2006.1 ± 2	-	False alarm
3.67	2005.3 ± 2	-	False alarm
4.21	2003.9 ± 2	-	False alarm
5.47	2000.5 ± 2	2000	Hit
6.12	1998.7 ± 2	-	False alarm
6.44	1997.8 ± 2	-	False alarm
7.38	1994.9 ± 2 or 3	1995	Hit
7.92	1993.3 ± 3	1993	Hit
8.35	1991.9 ± 3	1988	Hit
8.86	1990.3 ± 3	1987	Hit
-	-	1987	Miss
9.79	1987.2 ± 3	1986	Hit
10.55	1984.5 ± 3 or 4	1985	Hit
11.27	1981.9 ± 3 or 4	1983	Hit
-	-	1979	Miss
11.67	1980.5 ± 4	1978	Hit
-	-	1975	Miss
-	-	1973	Miss
14.11	1970.9 ± 5	1967	Hit
-	-	1966	Hit
15.09	1966.9 ± 5 or 6	1963	Hit
15.77	1963.9 ± 5 or 6	1959	Hit
16.17	1962.2 ± 6	1957	Hit
16.31	1961.6 ± 6	1957	Miss
17.46	1956.4 ± 6	1952	Hit
17.86	1954.6 ± 6	1950	Hit

Hits = 19. Moving some of the floods (within the limits of uncertainties) makes 19 of the bifurcation events correspond to one of the flood layers from threshold RoC P92. With this tuned alternative, the 19 hit-floods are as the ones in the following years; 2011, 2010, 2008, 2000, 1995, 1993, 1988, 1987 (autumn), 1986, 1985, 1983, 1978, 1967, 1966, 1963, 1959, 1957, 1952, 1950.

Misses = 5. Not all the bifurcation events correspond to any flood layer, and five of them do not. These bifurcation events do not have a flood layer that they correspond to. This tuned alternative cannot explain the bifurcation with flood layers in the following years; 1987 (spring), 1979, 1975, 1973, 1957.

False alarms = 5. There are five flood layers (detected with threshold RoC P92) that do not have any corresponding bifurcation events. We believe from the layers/threshold that there should have been a bifurcation event at this particularly year, but this is not the case. This tuned alternative can detect flood layers at the following depth, that does not correspond to a bifurcation events; 3.35 cm depth (2006.1), 3.67 cm depth (2005.3), 4.21 cm depth (2003.9), 6.12 cm depth (1998.7), 6.44 cm depth (1997.8).

Table 10 shows the CT-table and the CSI for the tuned alternative based on a threshold of RoC P92.

Table 10) CT-table and CSI-value for tuned alternative.

	No bifurcations	Bifurcations	Critical success index, CSI
No sediment layer	42	5	$\frac{19}{5+19+5} = 0.655$
Sediment layer	5	19	

19 of the 24 sediment layers fit to a bifurcation event, using the tuned alternative. Then, only five years of bifurcation events do not correspond to a sediment layer, and five sediment layers cannot be explained by a flood event. This tuned alternative with threshold RoC P92 gave a critical success index of 0.66. This gives a good indication that there are relations between bifurcation events and sediment layers (potential flood layers).

5.4 Flood frequency analysis – return levels

The main objective of this study is to see if the flood frequency analyses can be improved by using additional flood information beyond the information from systematic data. The previous results presented have shown that historical- and paleohydrological flood information can be obtained and contains relevant data for an extended period of time.

Return level graphs including the different type of flood information and different length of the systematic period will be presented. There are several flood information sources and countless ways to select length of systematic data, which all give varying results. Therefore, several return level-graphs are presented in this final result-part.

The crosses on the plots (Figures 37-43) represent each of the AMS-measurements from systematic data. The black solid line corresponds to these values, and shows the estimated flood sizes of different return periods, based on this information only. The two dashed black lines represent its 90 % confidence interval. The nine black points on the graph represent the nine historical floods with estimated sizes. The green lines represent the historical information (that nine floods exceeded the threshold), and the two dashed green lines represent its 90 % confidence interval. The red line represents the estimated discharge for these historical floods, and the two red dashed lines represent its 90 % confidence interval. The blue line represents the return level period based on paleodata – 155 floods during approximately 670 years, and the two blue dashed lines represent the 90 % confidence intervals. The turquois line is made based on flood information collected from all sources; systematic data, historical- and paleo flood information, and the two dashed turquois lines represent its 90 % confidence intervals.

In the return level tables (Tables 11-15), discharge values based on each of these five information sources are listed; (i) systematic data, (ii) historical floods exceeding a threshold, (iii) estimated discharge for the floods exceeding this threshold, (iv) paleohydrological flood information and (v) combination of systematic data, historical information and paleohydrological information. Discharge values for the following design floods are present; Q20, Q200, and Q1000. These design levels have been chosen because these design levels are explicitly mentioned in TEK 10 (2016). For an easier visualization, the lowest values are marked yellow, and the highest values are marked green.

Elverum (1871-1936) – Before regulations

Figure 34 shows the return levels for design floods using the systematic data from 2.604 Elverum stations before the significant regulations and the two methods using historical information; (i) number of floods exceeding a threshold and (ii) the estimated discharge values of these floods.

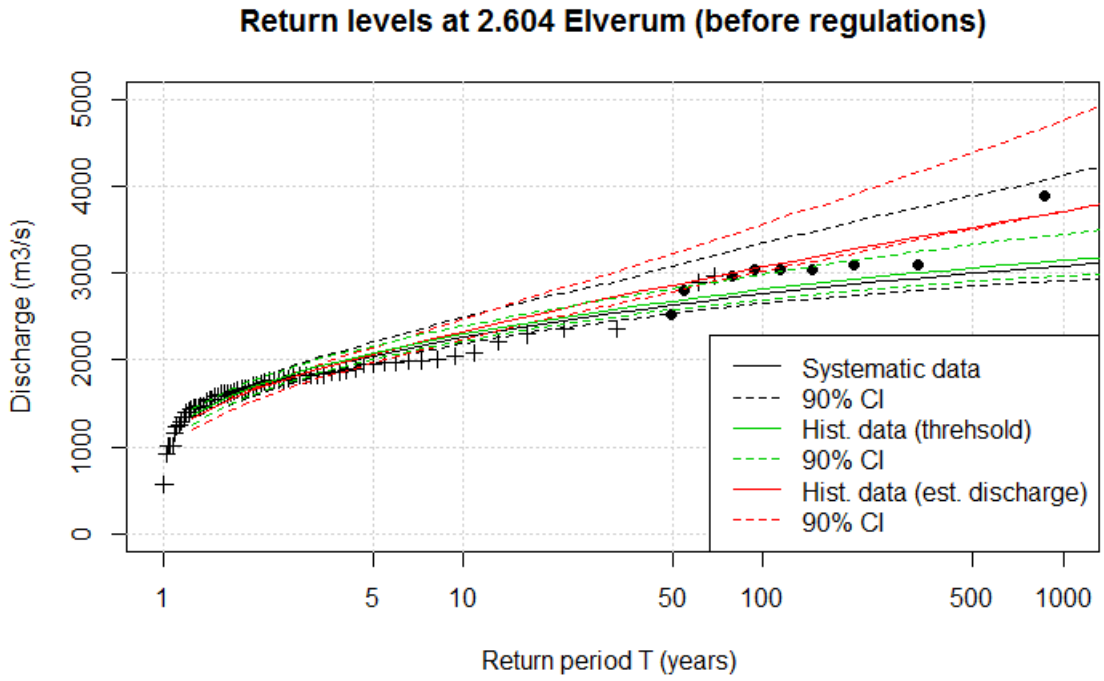

Figure 34) Graph showing the return levels using systematic data from 2.604 Elverum (black) from 1871-1936 and historical flood information (green and red).

Figure 35 shows the return levels for design floods using the systematic data from 2.604 Elverum stations before the significant regulations, the paleohydrological flood information and the combined flood information.

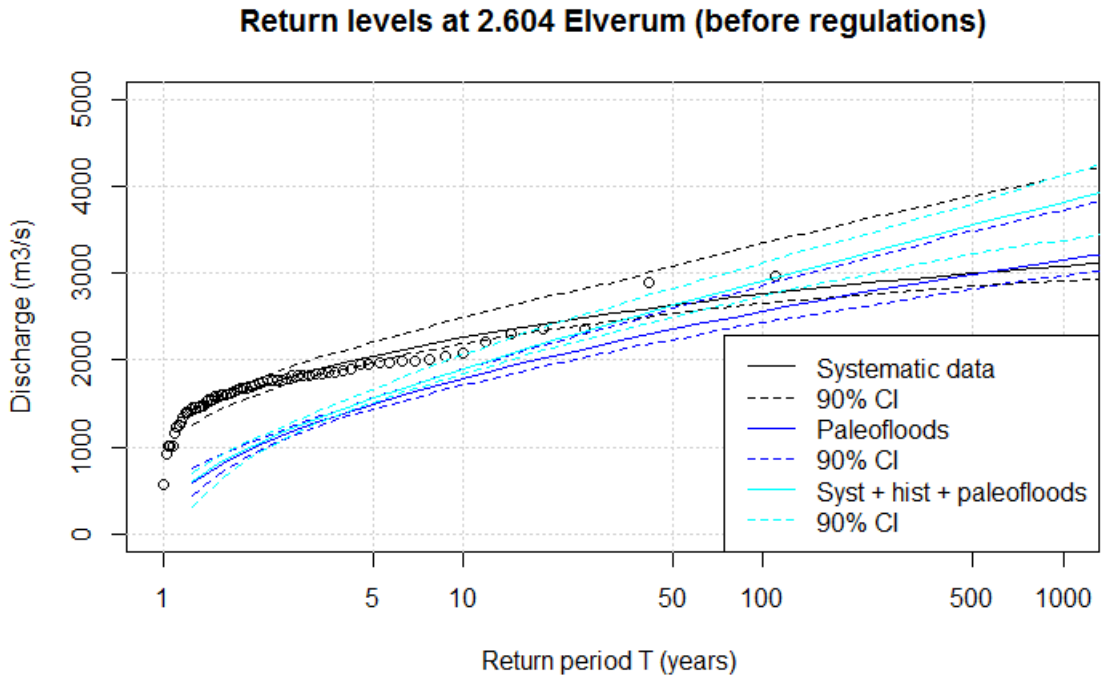

Figure 35) Graph showing return levels using systematic data from 2.604 Elverum from 1871-1936 (black), paleohydrological flood information (blue) and combined flood information (turquois).

Figure 36 shows the return levels for design floods using the systematic data from 2.604 Elverum stations before the significant regulations, together with historical-, paleohydrological- and combined flood information.

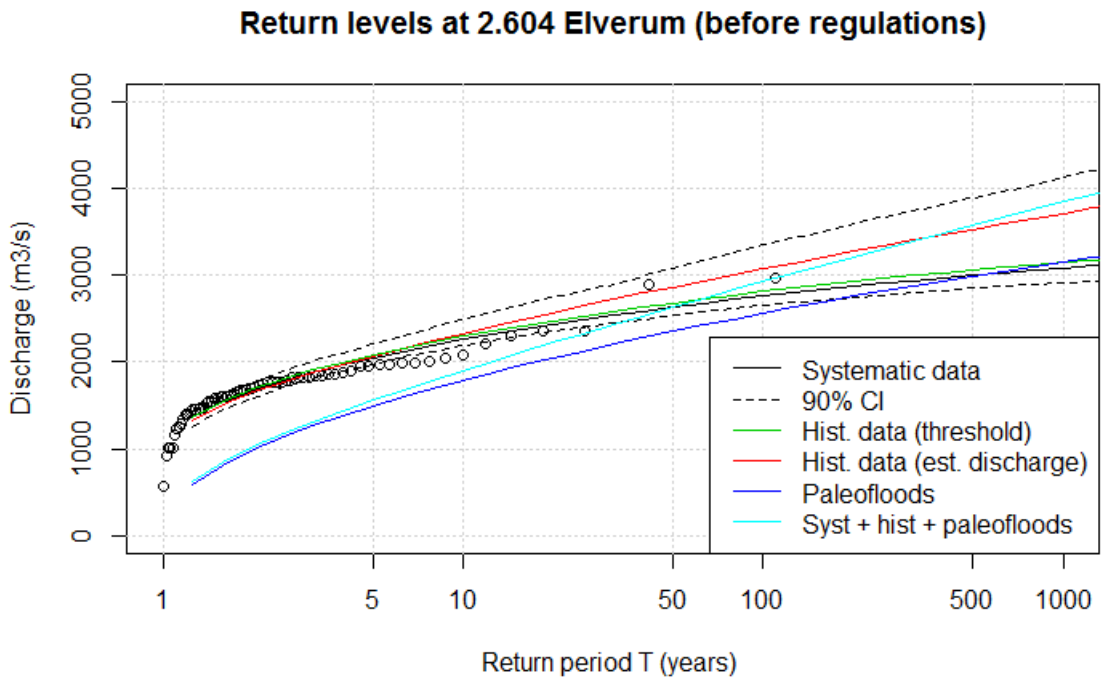

Figure 36) Return level graph will all flood information sources; systematic data (black), historical data (green and red), paleohydrological flood information (blue) and combined flood information (turquois).

Table 11 shows the return levels for different design flood sizes (Q20, Q200 and Q100), using different flood information sources.

*Table 11) Design floods with corresponding discharge values, using different types of flood information. Units: m3/s. Highest values are marked with **bold** text and lowest values are marked with italic text.*

2.604 Elverum (1871-1936)	Systematic data	Hist. data (threshold)	Hist. data (est. discharge)	Paleo-floods	Syst + hist + paleo
Q20	2437	2477	**2569**	*2046*	2228
Q200	2872	2930	**3277**	*2758*	3213
Q1000	*3083*	3135	3713	3152	**3849**

Elverum (1937-2015) – After regulations

Figure 37 shows the return levels for design floods using the systematic data from 2.604 Elverum stations after the significant regulations, together with historical-, paleohydrological- and combined flood information.

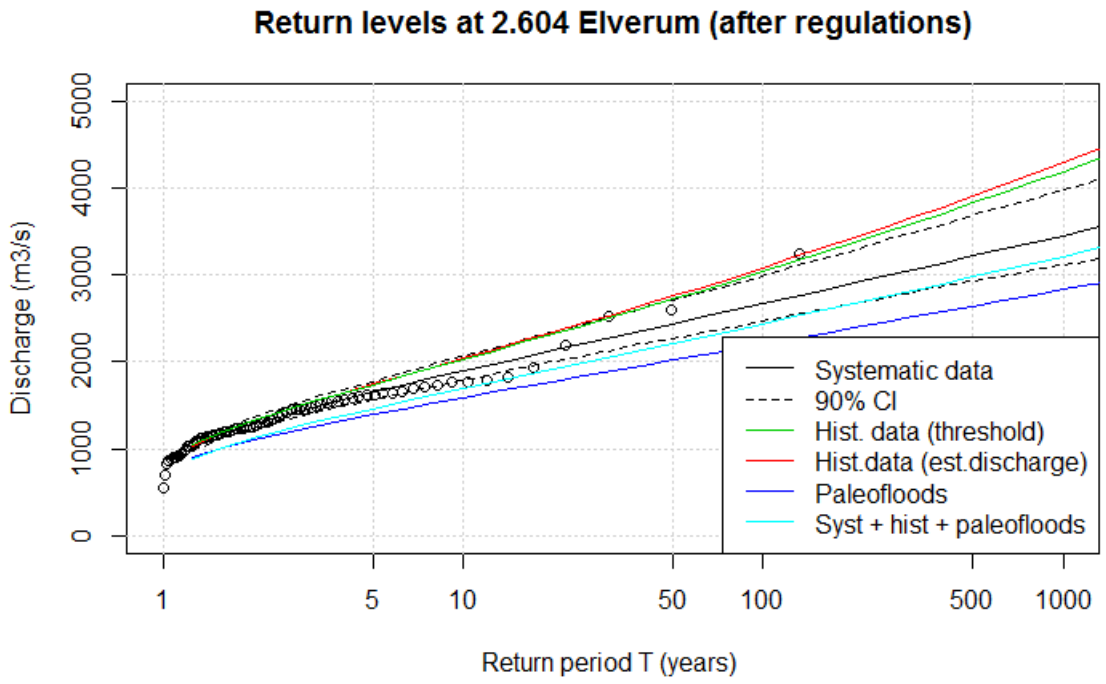

Figure 37) Return level plot, using AMS-values from 2.604 Elverum for the period after the regulations. Systematic data (black), historical information (green and red), paleohydrological flood information (blue) and combined flood information (turquois).

Table 12 shows the return levels for different design flood sizes (Q20, Q200 and Q100), using different flood information sources.

*Table 12) Design floods with corresponding discharge values, using different types of flood information. Units: m3/s. Highest values are marked with **bold** text and lowest values are marked with italic text.*

2.604 Elverum (1937-2015)	Systematic data	Hist. data (threshold)	Hist. data (est. discharge)	Paleo-floods	Syst + hist + paleo
Q20	2130	2322	**2342**	*1775*	1916
Q200	2906	3369	**3430**	*2393*	2670
Q1000	3458	4194	**4298**	*2831*	3217

Elverum (1871-2015) – whole period

Figure 38 shows the return levels for design floods using the systematic data from Elverum station using the whole period of data, historical-, paleohydrological- and combined flood information.

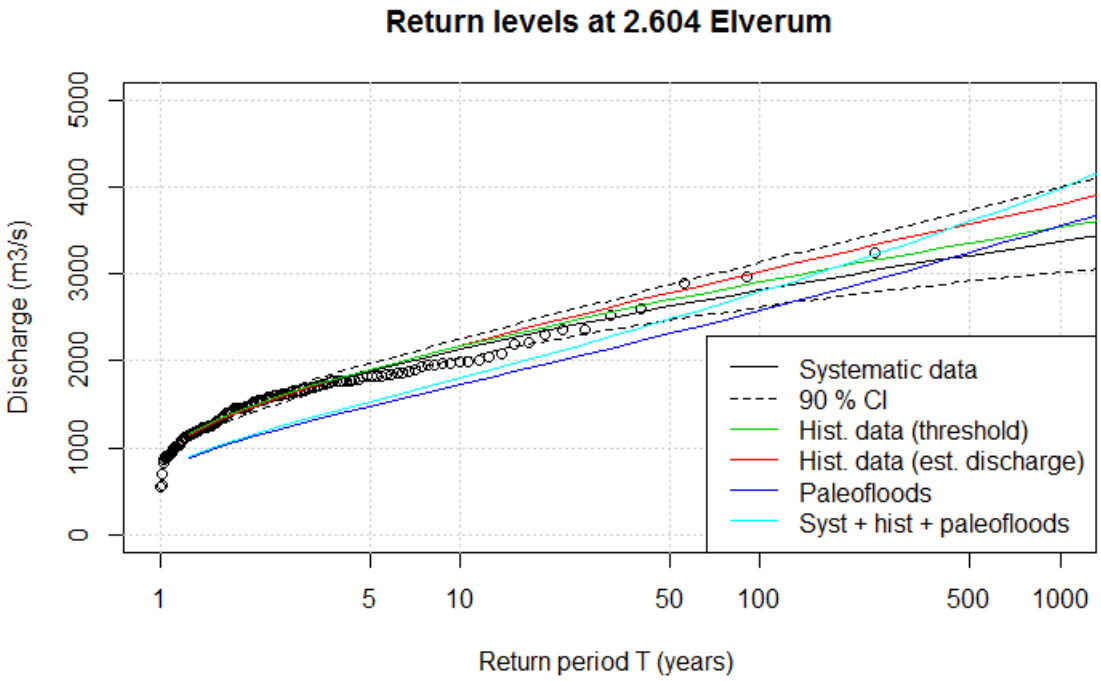

Figure 38) Return level plot, using AMS-values from 2.604 Elverum for the whole period. Systematic data (black), historical information (green and red), paleohydrological flood information (blue) and combined flood information (turquois).

Table 13 shows the return levels for different design flood sizes (Q20, Q200 and Q1000), using different flood information sources.

*Table 13) Design floods with corresponding discharge values, using different types of flood information. Units: m3/s. Highest values are marked with **bold** text and lowest values are marked with italic text.*

2.604 Elverum (1871-2015)	Systematic data	Hist. data (threshold)	Hist. data (est. discharge)	Paleo-floods	Syst + hist + paleo
Q20	2353	2405	**2447**	*1975*	2098
Q200	2995	3109	**3269**	*2861*	3150
Q1000	*3372*	3538	3808	3553	**4020**

Elverum (1956-2015) – the last 60 years

Figure 39 shows the return levels for design floods using the systematic data from 2.604 Elverum from the last 60 years, historical-, paleohydrological- and combined flood information.

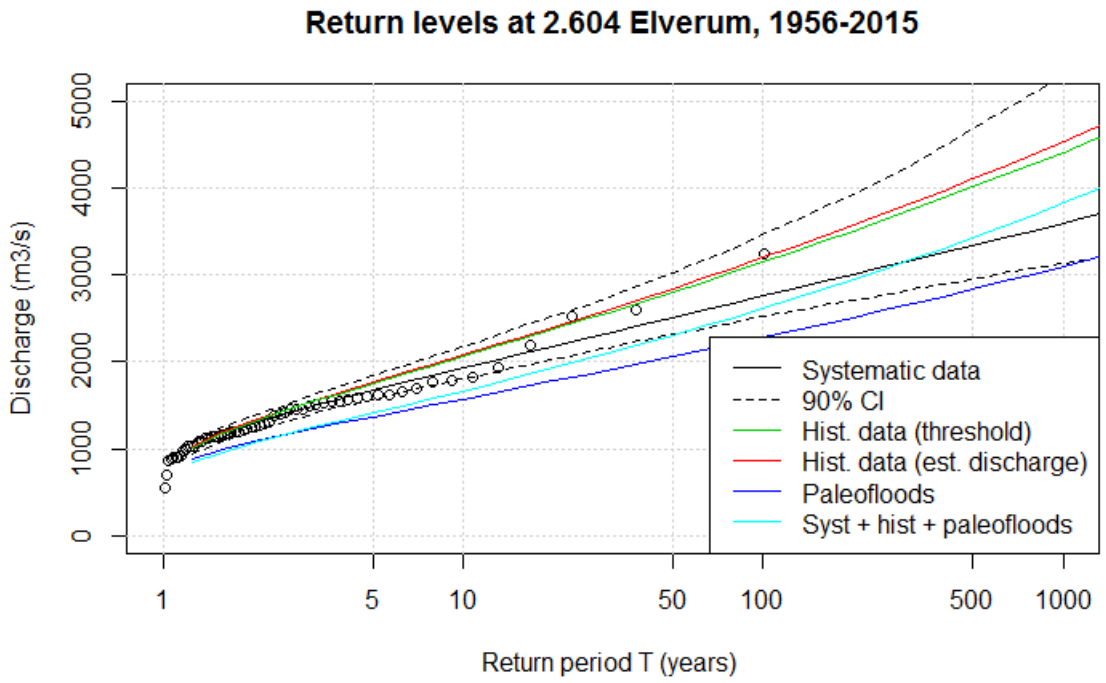

Figure 39) Return levels using systematic data from 2.604 Elverum from the last 60 years (black) and historical data (green and red) and flood information from paleohydrological data (blue) and combined flood information (turquois).

Table 14 shows the return levels for different design flood sizes (Q20, Q200 and Q1000), using different flood information sources.

*Table 14) Design floods with corresponding discharge values, using different types of flood information. Units: m3/s. Highest values are marked with **bold** text and lowest values are marked with italic text.*

2.604 Elverum (1956-2015)	Systematic data	Hist. data (threshold)	Hist. data (est. discharge)	Paleo-floods	Syst + hist + paleo
Q20	2180	2375	**2401**	*1777*	1928
Q200	3006	3510	**3577**	*2513*	2949
Q1000	3596	4417	**4533**	*3096*	3834

Elverum (1986-2015) – the last 30 years

Figure 40 shows the return levels for design floods using the systematic data from Elverum station from the last 30 years, historical-, paleohydrological- and combined flood information.

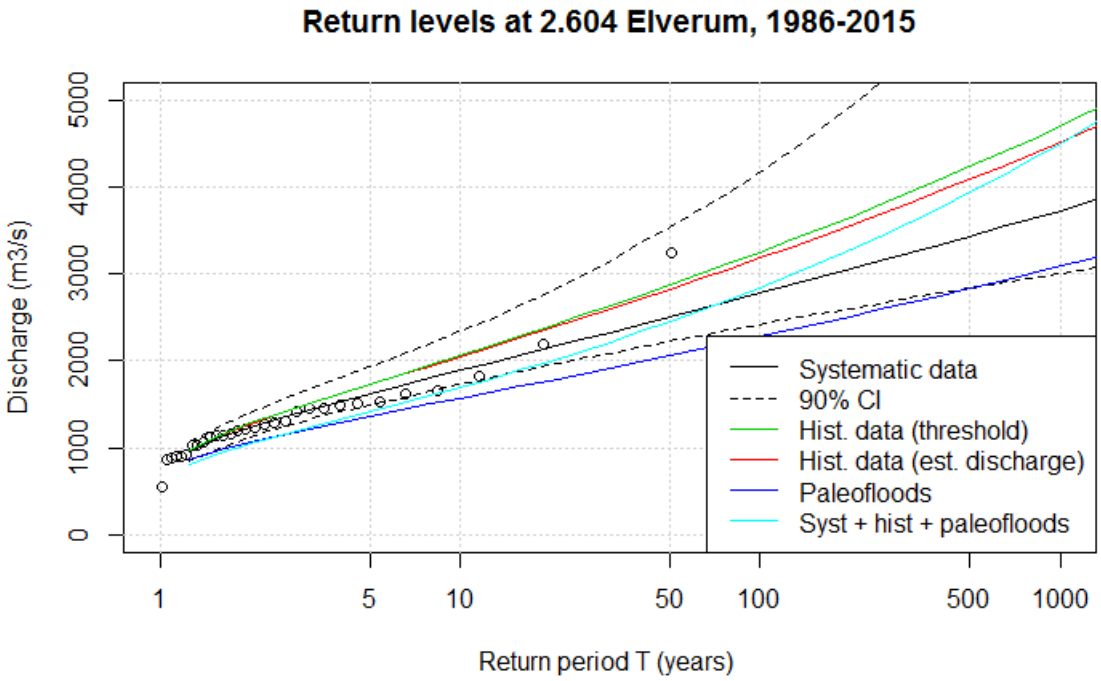

Figure 40) Return level plot, using systematic data from 2.604 Elverum for the last 30 years (black), historical data (green and red), flood information from paleohydrological data (blue) and combination of these sources (turquois).

Table 15 shows the return levels for different design flood sizes (Q20, Q200 and Q1000), using different flood information sources.

*Table 15) Design floods with corresponding discharge values, using different types of flood information. Units: m3/s. Highest values are marked with **bold** text and lowest values are marked with italic text.*

2.604 Elverum (1986-2015)	Systematic data	Hist. data (threshold)	Hist. data (est. discharge)	Paleo-floods	Syst + hist + paleo
Q20	2153	**2401**	**2375**	*1776*	1996
Q200	3057	**3659**	**3561**	*2513*	3277
Q1000	3735	**4706**	**4518**	*3093*	4507

Return levels using systematic data from Elverum (before regulations)

Figure 41 shows the return levels for design floods (Q20, Q200 and Q1000) using systematic information from 2.604 Elverum before the regulations, historical-, paleohydrological- and combined information sources. Pettersson's estimates for Glomma at Kongsvinger (Pettersson, 2000) are also presented on the same graph.

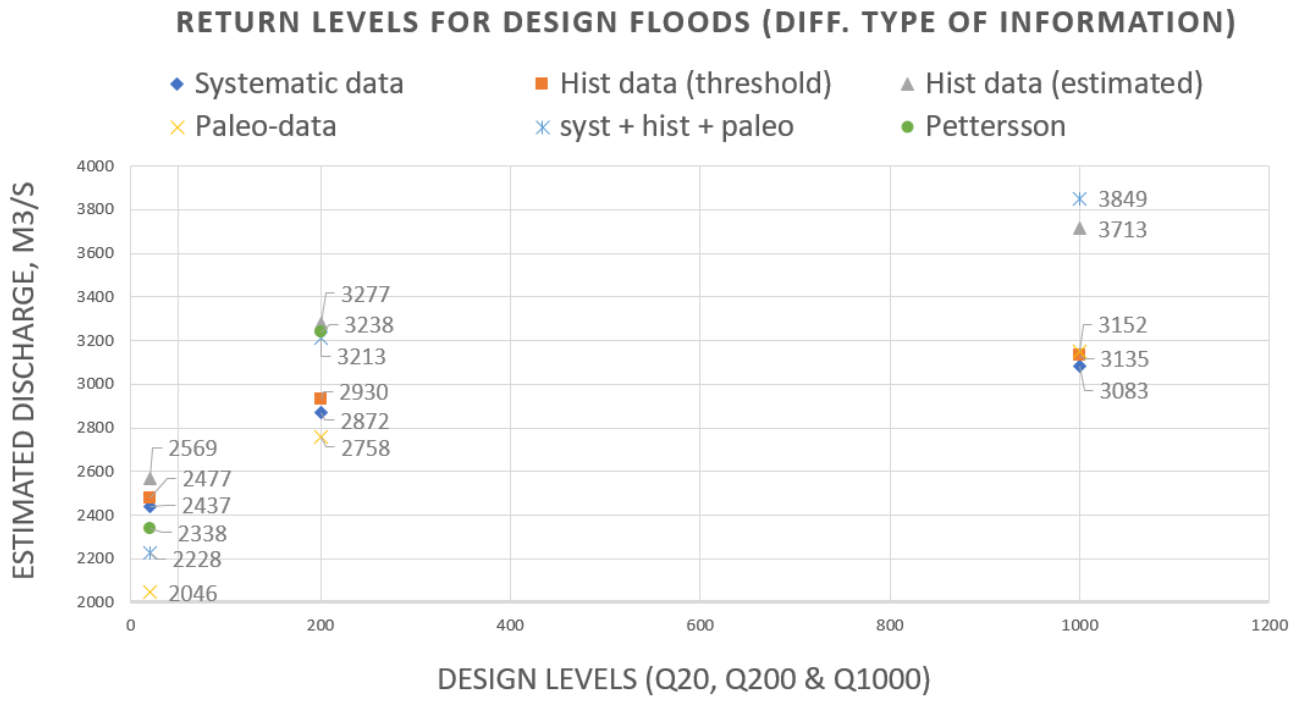

Figure 41) This figure shows return levels of design flood Q20, Q200 and Q100 using unregulated systematic data from 2.604 Elverum, and additional flood information sources, as well as estimations made by Pettersson (2000).

For the 20-year flood, it is the use of paleohydrological flood data in the flood frequency analysis that gives the lowest return level, while the use of estimated historical floods gives the highest return level. For the 200-year flood as well, the use of paleohydrological flood data that gives the lowest return level, and the use of estimated historical floods gives the highest return levels. For the 1000-year flood, it is the use of systematic data that gives the lowest return level, while the use of combined flood information gives the highest return level.

6 Discussion

6.1 Paleohydrological flood information; bifurcation events & flood layers

Bifurcation events & sediment layers

One of the objectives of this study was to see if paleohydrological information could be used to lengthen the flood record, and further be used to improve flood frequency analysis. If the sediment cores contain flood information, this can add valuable information from paleo-science to extend the flood record which might improve flood frequency analysis. Therefore, it must be confirmed that there is a relationship between bifurcation events in Glomma at Kongsvinger and the flood layers in sediment core FLS113 which overlap with instrumental data. The threshold for when bifurcation occurs in Glomma at Kongsvinger is today 1500 m^3/s (Pettersson, 2001). If the conditions at Vingersjøen's south end have changed, the rating curve used to estimate transferred water will be incorrect. More vegetation has grown in the area in recent years, so that the transmission capacity, especially at high water levels in Vingersjøen, might have been reduced. The rating curve may also have changed due to erosion or sedimentation during large floods (Pettersson, 2001). The threshold of 1500 m^3/s has probably changed during Holocene as well. It might have been lower at some times and higher other times, but it is not possible to know how high or low it has been, or when. Anyway, in this study, the value of 1500 m^3/s has been used as a threshold. It is used as an assumption and one must keep in mind the sources of uncertainty regarding the bifurcation events.

From the results, one sees that there is clearly a relation between the bifurcation events in Glomma and layers in the sediment cores, but this relation is not perfectly 1:1. 24 bifurcation events happened in the period covered by sediment core FLS113 and the assumption that flood events result in dense layers is used. Therefore, the aim was to find the threshold giving the 24 densest layers which the threshold of RoC P92 did. From the CT-table (Table 6) one sees that five of these 24 bifurcation events could be linked to sediment layers. Nevertheless, the way this method was used did not take into account the uncertainty in the age depth-model. The uncertainty increases with depth; therefore, a tuned alternative was made, allowing the age of the sedimentary deposit to be shifted within the age uncertainty at its specific depth in core. Using the tuned alternative based on threshold RoC P92 made 19 of 24 bifurcation events correlate to a sediment layer with a CSI-value of 0.66. This indicates that there is a good relationship between bifurcation events and sediment layers, although it is not perfect.

The remaining five bifurcation events do not correspond to a sediment layer (number of misses in the tuned alternative) (Table 9). According to the tuned alternative the floods in 1957, 1973, 1975, 1979 and 1987 cannot be explained by bifurcation events. Maybe the waterflow was not large enough to transport enough sediments to Flyginnsjøen which would result in a sediment layer. The bifurcation event in spring 1957 lasted only 1 day (with discharge exceeding 1500 m^3/s) and transferred 0.03 mill m^3 water – which is the lowest number on the bifurcation events-list. The bifurcation event in 1973 lasted two days and transferred 0.22 mill m^3 water. The bifurcation event in 1975 lasted also two days and transferred 0.11 mill m^3 water. The bifurcation event in 1979 lasted two days and transferred 0.09 mill m^3 water, and the bifurcation event in spring 1987 lasted three days and transferred 0.15 mill m^3 water. These five bifurcation events lasted less than four days and none of them transferred very high amount of water (to comparison; the average transferred amount of water is 3.26 mill m^3). Therefore, this might be a possible explanation why these events do not have a corresponding sediment layer. There are, however, other bifurcation events with small transferred amounts of water that could be

linked to a sediment layer. From chapter 2 – theoretical background – we know that the amount of available sediments at the time of the flood is important for erosion, transportation and deposition. Therefore, another possibility is that there might not have been enough sediments available during the bifurcation events in these years.

There were also five sediment layers that did not correspond to a bifurcation event (number of false alarms in the tuned alternative) (Table 9). The CT-scan of sediment core FLS113 (Figure 42) shows that there are more than 24 dense layers in the core. Therefore, there must be other processes that can create distinct, denser layers other than flooding events in Glomma. The most likely explanation is that local flood events in Vrangselv, or high surface runoff during heavy precipitation events, may cause the deposition of these layers without influence of floodwater from Glomma. Other possible reasons for this might be due to for example human activity. Farmers or others might have dumped sediments into the lake, which potentially can explain some of the dense layers. Avalanches could also add a lot of sediments to a lake, but the area around Flyginnsjøen is not very steep, so avalanches are not believed to have been triggered here. Natural variations in the background sedimentation, such as seasonal variability, are always present and some (maybe the thinnest) layers might be caused by these.

The tuned alternative (Table 9) and the plots showing relationship between threshold and bifurcation events (Figure 30) show that there is a relationship between bifurcation events and sediment layers. From Figure 31 most of the bifurcation events correspond to a peak on the greyscale plot. Because the uncertainty in dating increases with depth, the bifurcation events can be slightly moved. The bifurcation event from 2011 seems to fit to a peak, but this is not the case for the bifurcation events from 2010 and 2008. The bifurcation events from 2000 and 1995 correspond to each peak. Anyway, the 1995-flood was extreme, and had the largest amount of transferred water (after the flood in 1967). The peak corresponding to the flood from 1995 is nevertheless not as high as one could expect. This indicates that there is not always a strong relation between the amount of transferred water and the density of the flood layers. The bifurcation event from 1993 also corresponds to a peak from the greyscale-plot (Figure 31). There were several bifurcation events in the 1980s (1983, 1985, 1986, both spring and autumn 1987 and 1988). There are at least three peaks in the depth corresponding to these years – but since they happened in such short interval, it may not be possible to detect one peak for each of these events. The bifurcation event in 1979 corresponds to a peak, but the event on 1978 does not have a clear corresponding peak. The bifurcation events in 1975 and 1973 each correspond to a peak. When the depth increases, so does the uncertainty, and nevertheless the bottom on the core was disturbed during core taking, so there is a lot of uncertainty in the bottom of the core. The highest peak in greyscale (Figure 31) of all occurs at approximately 16 cm depth, and causes of this can be multiple. One possible explanation is that this peak comes from the flood in 1967, which had the largest amount of transported water in this period. Another possibility is that this peak is a result of both 1966- and 1967-flood, since they happened in two subsequent years, and both of them were large. A third possibility is that

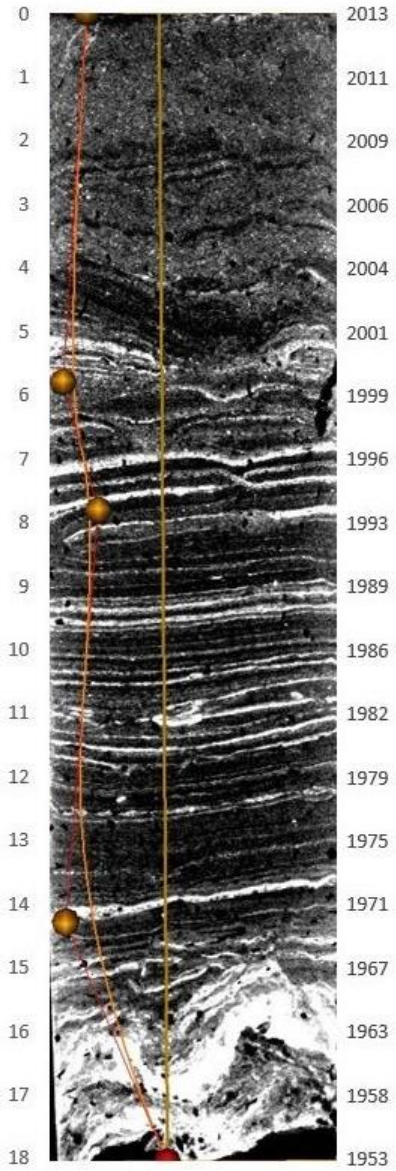

Figure 42) CT-scan of sediment core FLS113. On the left side, the depth in cm, and on the right side, the corresponding ages.

this peak comes from the flood from 1963. There might have been a lot of available sediments back then, which resulted in large depositions during a flood event. The broadest peak, at approximately 17 cm depth, might have been caused by the spring- and autumn flood that happened in 1957, or, according to the uncertainty in dating, this peak can also be linked to the floods from 1966 and 1967. It is impossible to know exactly which bifurcation resulted in the different flood layer, but there is good reason to believe that the link is present, and as shown 19 of the bifurcation events can be linked to sediment layers in the core.

Is there any relation between discharge in Glomma and sediment thickness in Flyginnsjøen?

It would be reasonable to think that bigger floods with higher water flow would erode and transport more sediment and therefore result in thicker flood layers. It might be correct in some cases. Steffensen (2014) found a thick layer in the long sediment cores FLP113 and FLP213 of respectively 15.0 and 15.5 cm thickness. This thickness of one single sediment layer surpasses all the other layers which have an average thickness of 0.3 cm. This thick layer is believed to be caused by Storofsen (e. g. Bøe et al., 2006; Steffensen, 2014). The availability of sediments was huge at the time of Storofsen, partly because of several earthflows and avalanches in the valleys during the extreme rainfall the days ahead of Storofsen (Roald, 2013). This flood had such an enormous impact because of the somewhat special conditions; deep frost in the ground from the year before prevented drainage and infiltration of rainfall and snowmelt. The relatively late spring that year contained a sudden increase in temperature in June-July, leading to a huge amount of snowmelt – first in the lower parts of the catchment and later in the higher mountains. In addition, there was heavy rainfall the days before the flood because of a very special weather system over Europe (Roald, 2013).

Even if it is reasonable to expect a relation between amount of transferred water and thickness of sediment layers, the analyses in this study show something else. According to the study of the flood layers in core FLS113 and the amount of water transfer from Glomma to Flyginnsjøen (Pettersson, 2001), there is no clear relation between these two. One specific example is the big flood that happened in 1995 – Vesleofsen, which was extreme and one of the biggest floods in Norwegian history. This flood should – if there is a relationship between transferred amount of water and thickness of the sediment layer – result in a thicker layer than the smaller floods. But this is not the case; the 1995-flood layer that is found in the sediment core (based on the depth-age-model) is not significantly thicker than other flood layers, from smaller flood events. Also, the peak corresponding to this flood event from greyscale values (Figure 31) is not outstanding compared to the other peaks. The 1995-flood was extreme compared to the other floods from instrumental data. According to Lundquist and Repp (1997) this flood would probably have been the same size as Storofsen without the regulations. One of the thresholds Steffensen (2014) used (the 2000-flood) did not even detect a flood layer representing the 1995-flood (Steffensen, 2014). On the other hand, the flood from 1959 has a relatively thick layer, despite that the discharge and transfer of water was not extreme. The flood layers in the later years were not that big, and this might be because of lack of sediments. Much of the sediments might have already been washed away by previous flood events.

Therefore, it is assumed that there is no evident relationship between the thickness of the flood layer and the actual size of the flood. The amount of deposited sediments and thickness of layers depend on both the size of the flooding event and the available amount of sediments at the time the floods occur.

Paleohydrological flood information

That paleohydrology can be used to extend the flood record further has been confirmed in this study. There is good relation between bifurcation events and the dense sediment layers in the sediment cores for the period that can be validated by systematic measurements. Therefore, I assume that this relation also can be used further back in time – using the longer cores, covering longer time period.

Nevertheless, regarding the paleohydrological flood information, there are also some uncertainties; especially due to the threshold chosen to represent flood events. This threshold is based on XRF-analyses of varies elements where high occurrences of for example Potassium and Titanium were used to count number of floods (Steffensen, 2014). The selection of this threshold is important, and using another threshold (either higher or lower, or the use of another element) would change the flood counts. It is difficult to know the threshold, and the threshold might also have changes through times. Nevertheless, in my study I used the threshold from Steffensen (2014), which she justified in her thesis.

Climatic variations during Holocene is present, which Figure 22 clearly shows. The flood rates have changed throughout this period. Holocene is the period covering approximately the last 10 000 years and in this period, there have been times with high flood frequency and other times with low flood frequency. So, the length of paleohydrological information used in flood frequency will influence the results. I have used the time after year 1200 until present as the paleohydrological flood period and done analyses based on the assumption that this is a stable period. Nevertheless, this is probably an unrealistic assumption. Climate change and non-stationarity have been present in this period and make flood frequency based on stationarity challenging. One cannot know for sure how the climate has changed and even though there exist a lot of future climate scenarios – one cannot know if they are correct. Another source of uncertainty is that flood sizes might have changes through time. A 200-year flood today may have been larger (or smaller) if we go many years back in time. The size of a 200-year flood in the future might also be different than the size of a 200-year flood today. No one knows the future – and that is also what makes the future challenging and also exciting …

Using the paleohydrological flood information in the flood frequency analysis influences the return levels. The size of the estimated design floods (Q20, Q200 and Q1000) is reduced in all cases, using paleohydrological flood information (see Figures 36-40) except the 1000-year flood based on the period before regulations (Figure 36) and the 1000-year flood using the whole period (Figure 38) from Elverum. In these two cases, it is the flood frequency analysis based on systematic data alone that gives the lowest return levels. Overall, the use of paleohydrological flood information reduces the discharge values of the design floods. A possible explanation might be that there have been fewer floods in this period (ca 1200 – present) than in later years covered by instrumental data. The flood frequency in this period might have been lower and therefore the return levels of future floods is expected to be lower when using this information in flood frequency analysis.

According to building regulations (TEK 10, 2016), buildings and infrastructure should resist or be protected from floods with 20-, 200- or 1000-years return periods, depending on the consequences of flooding. Since the use of paleohydrological information in frequency analysis makes almost all of the design flood sizes smaller than using systematic data or historical data, I personally would have been careful using the estimates based on paleohydrology. The difference between the lowest and highest expected discharge values for the 1000-year flood is large. For the period after regulations in Glomma (Figure 37) the use of paleohydrological data gives the lowest return level (2831 m^3/s), while the use of estimated historical flood sizes gives the highest return level (4298 m^3/s). This difference is significant and to be on the safe side, I would, in this case, rather use the flood frequency analysis based on historical information.

Also, there has been done little investigation on the use of paleohydrological information in flood frequency analysis. Therefore, it would be unreasonable to base the building regulations upon one single study. The study of sediment cores as a possible flood information source is relatively new, and there are not many studies that have used paleohydrology in flood frequency analysis. This is, nevertheless, an interesting investigation and I would highly recommend more research on this area.

6.2 Historical flood information

Another objective of this study was to see if historical flood information could be used to lengthen the flood records and eventually be used to improve flood frequency analysis. The investigation of historical floods during this study made nine floods in a 200-years period be added to the flood record, but there are also challenges present when using this type of information. The historical sources might be inaccurate and maybe some of the large floods were not preserved for the posterity. The historical flood information used in this thesis is based on the flood marks on flood monuments and discharge values of these height have later been estimated. This also present possible uncertainties; the heights might be incorrect which would make the estimation of discharge values also incorrect.

The use of historical information in the flood frequency analysis influences the return levels of the design floods. Two methods were used to include historical flood information to the analysis; (i) either the number of floods exceeding the specific threshold (in this case the 1967-flood) or (ii) the estimated magnitudes of these floods was used. These two information sources give somewhat different results in the estimated return levels for the design floods.

The use of estimated discharge values of the historical floods gave higher return levels than the use of the number of floods exceeding the specific threshold for all design floods (Q20, Q200 and Q1000) for all the periods (Figures 36-40). The use of historical flood information, both (i) and (ii), gave higher return levels for the design floods (Q20, Q200 and Q1000) for all the periods (Figures 36-40) than using systematic data alone.

Overall, the use of historical data in flood frequency analysis make the expected design foods larger than using systematic data or paleohydrological data. A possible explanation is that the period containing historical data might have been a period with larger floods compared to later (systematic time) or previous years (paleohydrological time). Since using historical data makes the return levels larger, the sizes of the historical floods must probably have been larger. One possibility is that these historical floods might have been influenced by the Little Ice Age (LIA). This was an especially cold and snow rich period (generally defined from the middle of the 1500s to the middle of the 1800s). The amount of snow available plays an important role in flood generating processes (Chapter 2, “Theoretical background”). Therefore, this period might have been a period with larger floods than before the LIA.

Another possible explanation might be that one large flood – Storofsen – influences the results a lot. Storofsen is believed to be an extreme event in historical times as well as from paleohydrological data. No flood layer from the long sediment core FLP213 (516 cm long, representing approximately the last 10 000 years) has a distinct layer as the one corresponding to Storofsen. This layer is 15.0 cm thick, while the other flood layers have a mean average thickness of 0.3 cm. There were probably a lot of sediments available when Storofsen occurred and this extreme flood also led to several avalanches, causing a lot of sediments to be deposited in the lake. Anyway, this indicates that Storofsen was not only extreme in historical times (in my study: 1650-1850), but also in Holocene. Storofsen has been estimated to a discharge of 3900 m^3/s (GLB, 1947) at Elverum and it was characterized as a 1000-year

flood. Since Storofsen was a special case for Holocene, maybe it was not a 1000-year flood, but really a 10 000-year flood. Storofsen was anyway an outlier and to test how significant this flood is for the return levels and the sensitivity of these, I estimated several return levels where Storofsen is given different magnitudes.

In Figure 43 Storofsen has been given the following sizes; (i) a 100-year flood, (ii) a 1000-year flood, (iii) a 5000-year flood, (iv) a 10 0000-year flood and (v) in the last example Storofsen is excluded. The AMS-values (black crosses) are from Elverum station (before regulations), and the nine historical floods exceeding the 1967-flood are marked on the graph (black dots). Figure 43 shows the sensitivity test of Storofsen – how much Storofsen influences the return levels of design floods due to its given size.

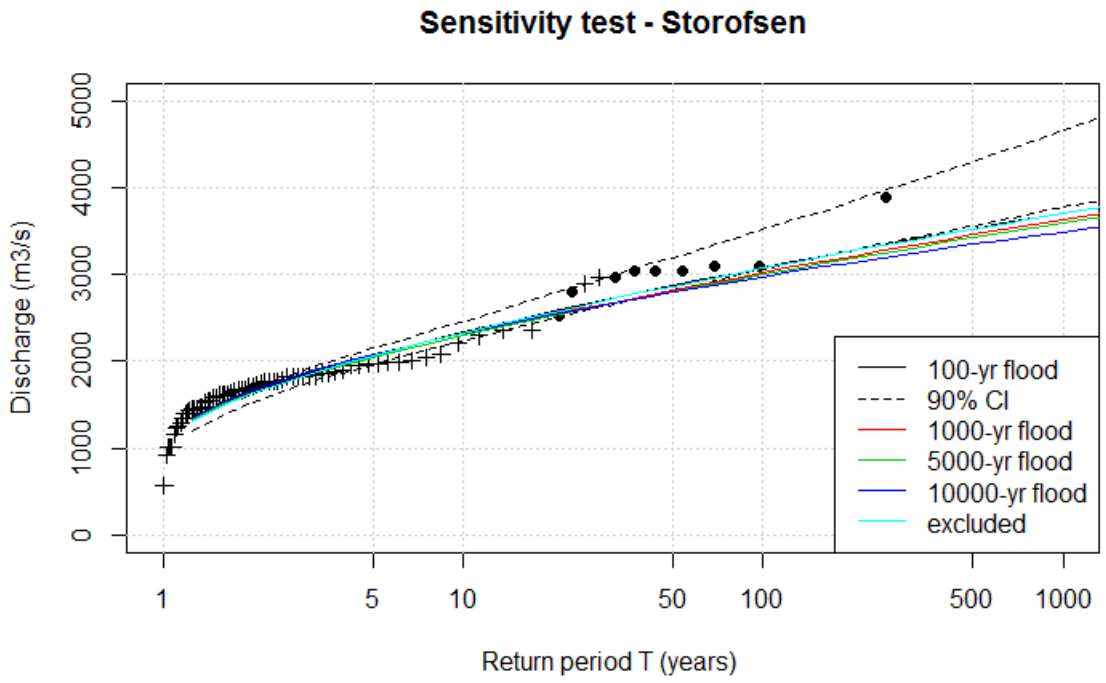

Figure 43) Return levels where Storofsen have been given different sizes, to see how/if this (extreme) flood influence the return levels significantly. Storofsen as a 100-year flood (black), as a 1000-year flood (red), as a 5000-year flood (green), as a 10 000-year flood (blue) and excluded (turquoise).

The line representing Storofsen as a 100-year flood is not visible, because the line excluding Storofsen from the estimations lies above it.

Table 16 shows the return levels of the design floods, where Storofsen is given different sizes and where the flood is excluded.

*Table 16) Design levels based on Storofsen with different sizes and where Storofsen is excluded from the flood frequency estimations. The highest numbers are written in **bold** text, and the lowest numbers are written in italic.*

	Storofsen = 100-yr flood	Storofsen = 1000-yr flood	Storofsen = 5000-yr flood	Storofsen = 10000-yr flood	Storofsen excluded
Q200	3279	3217	3189	*3144*	3274
Q1000	3709	3630	3589	*3488*	3701
Q10000	4250	4146	4087	*3891*	4235

When Storofsen is given the size of a 10 000-year flood, the return levels are the smallest, for all design floods (Q200, Q1000 and Q10 000). When Storofsen is given the size of a 100-year flood the return levels are highest. Return level discharges estimated excluding Storofsen gives values higher than Storofsen as a 10 000-year flood, but lower when Storofsen is a 100-year flood.

The size Storofsen is given influences the return levels and the differences increase with increasing return interval. The return level of a 10 000-year flood based on Storofsen as a 10 000-year flood is estimated to 3891 m^3/s, which is 359 m^3/s less than the estimation if Storofsen is a 100-year flood. Nevertheless, these differences are not as high as one could expect. There is not much difference in expected return levels if Storofsen is given the size of a 100-, a 1000-year flood or if it is excluded from the flood frequency analysis. The line representing Storofsen as a 100-year flood is not visible on the graph because the line representing when Storofsen is excluded lies over it. That one extreme flood event does not have a huge impact on the flood frequency analysis is somewhat reassuring. Even if Storofsen was as extreme as a 10 000-year flood, the other floods together kind of compensate for single extreme flood.

6.3 Systematic data

Figure 11 and Figure 12 show the AMS-values from Elverum station respectively before and after the regulations. These figures clearly show the effect of the regulations; overall, the AMS-values are higher in the period before Glomma was regulated. Anyway, the large floods are not stopped by these regulations, but they might have been even larger without them. Lundquist and Repp (1997) claims that the 1995-flood would probably have been the same size as Storofsen without these regulations.

Return levels using systematic data are estimated for the period before (Figure 36) and after (Figure 37) the regulations in Glomma. The return level of the 20-year flood is higher using the period before regulations than using the period after (2437 m^3/s compared to 2130 m^3/s). For the larger design floods (Q200 and Q1000) it is the use of systematic data after the regulations that gives the highest return levels (Tables 11 and 12). This indicated that the regulations in Glomma makes the smallest floods smaller, while the larger floods become even a bit larger.

A possible explanation might be that the period after the regulations (after 1936) was a period with larger floods than before. Figure 10 and Figure 12 show that there have been three large floods after 1936; the floods in 1966, 1967 (both characterized as a 100-year flood) and in 1995 (Vesleofsen – which is one of the biggest floods in Norwegian history). These three larger floods might be the cause of the higher estimated return levels using the period after regulations.

Pettersson's (2000) estimates of return levels are summarized in Table 17. The culmination discharges are measured in Glomma at Kongsvinger and the water level is measured in Vingersjøen. These values come from Lars-Evan Pettersson's article about flood estimation for Glomma catchment and the confluence with Vorma (Pettersson, 2000).

Table 17) Return level estimation at Kongsvinger (Pettersson, 2000).

Pettersson's estimations	Culmination discharges (m^3/s), Glomma at Kongsvinger	Vingersjøen, water levels (m)
QM (mean flood)	*1499*	*HM: 145.75*
Q10	2068	H10: 146.77
Q20	2338	H20: 147.13
Q50	2683	H50: 147.57
Q100	2968	H100: 147.88
Q200	3238	H200: 148.18
Q500	3627	H500: 148.55

Pettersson estimated the return level of the 20-year flood to be 2338 m^3/s. This is between the lowest (from paleohydrological data) and the highest (from historical data) return levels for all the cases tested for. Pettersson estimates of the 200-year flood is 3238 m^3/s. This is also between the minimum and maximum return levels for all the cases. Pettersson's estimates of the design floods are close to the estimations in this thesis based on systematic data for the whole period from Elverum.

The value of the length of flood record is somewhat shown in Figures 39 and 40. Figure 39 shows the return levels using the last 60 years of measurements from Elverum and for Figure 40 the last 30 years is used. For both periods, it is the use of historical flood information that gives the highest expected return levels for the design floods, and the paleohydrological flood information that gives the lowest expected return levels. Nevertheless, comparing these two graphs show that the confidence interval for the systematic measurements gets wider when using less years of data. In other words, lengthening the flood record makes the confidence interval narrower. Therefore, it would be reasonable to think that historical flood information, which lengthen the records, improve the flood frequency estimations.

6.4 Combining systematic-, historical- and paleohydrological flood information

Finally, I combined the flood information from all these sources and made return level plots based on this combined information; (i) systematic data, (ii) historical data (nine floods from historical period) and (iii) 155 floods from paleohydrological period. Combining this information with the use of systematic data from Elverum station before the regulations (Table 11), gives the following: the estimated size of the 20-year flood using combined flood information is higher than using paleo-data, but lower than using systematic data or historical data. For the 200-year flood, the return level using combined data is lower than using the estimated magnitudes of the historical floods, but higher than using systematic data, historical floods exceeding a threshold or paleo-data. For the 1000-year flood, the use of combined data gives the highest return level. It seems like the use of this combined flood information gives lower return levels for the smallest floods, and higher return levels for the larger floods.

6.4.1 Comparing 1000-year floods

To design flood estimation varies and depends on the length of the AMS-values used (from systematic data) and the types of information sources used to estimate the design floods. To easier see how these factors affect the design period, the return levels of the 1000-year flood from all the lengths and the different kinds of sources are gathered in Table 18.

*Table 18) Return levels for the 1000-year flood using different length of systematic data and different types of additional flood information sources. The highest values are written in **bold** text, while the lowest values are written in italic.*

2.604 Elverum	Systematic data	Hist. data (threshold)	Hist. data (est. discharge)	Paleo-data	Syst + hist + paleo data
Before regulation	*3083*	3135	3713	3152	**3849**
After regulation	3458	4194	**4298**	*2831*	3217
Whole period	*3372*	3538	3808	3553	**4020**
Last 60 years	3596	4417	**4533**	*3096*	3834
Last 30 years	3735	**4706**	4518	*3093*	4507

Table 18 clearly shows that the return levels of the 1000-year flood vary depending on the flood information type and the length of period for the systematic data the flood frequency is based upon. Looking at the table do not give an immediately relation between the different return levels using different length of data and source of information. For all the periods, except using the period before regulations and the whole period, it is when using paleohydrological data, that the return levels of the 1000-year flood are lowest. The highest return levels of the 1000-year flood vary a lot, depending on the period of systematic data.

The use of different flood information sources and the length of the period with systematic data influence the results of the flood frequency analysis. Generally, the use of historical flood information gives the highest return levels for the design floods, while the use of paleohydrological flood information, on the other hand, gives the lowest return levels for the design flood.

7 Conclusion

The flood frequency analysis today is usually based on systematic flood data from streamflow stations, where limited data is the major drawback. In this study, I have investigated and applied historical- and paleohydrological flood information to lengthen these flood records in a flood frequency analysis. Historical and paleo flood information can be used in two ways; either the number of floods or the magnitude of all floods above a threshold for a specified period. The historical information used in this study is based on flood marks on a flood stone at Elverum. Since streamflows at Glomma exceeding 1500 m^3/s will cause a bifurcation were the flow change direction and cause water to flow from Glomma an into Flyginnsjøen, there is a potential relationship between high streamflows in Glomma at Kongsvinger and dense sediment layers in sediment cores from Flyginnsjøen. Flood counts from these cores have also been added to extend the flood record further. Based on this study, the following conclusions were drawn:

- Historical data can be used to extend the flood records beyond the flood information from systematic data. Historical information adds approximately 200 years (1650-1850) of flood history and nine floods (with decreasing size, in year: 1789, 1675, 1773, 1717, 1724, 1749, 1850, 1827, 1846) to the record.

- Using historical data in flood frequency analysis influences the design flood estimation. The return levels of the design floods (Q20, Q200 and Q1000) are generally higher when adding historical flood information. Ex. the estimated 200-year flood using systematic data from Elverum station before regulations is estimated to have a discharge of 2872 m^3/s. Using the number of floods exceeding a specific threshold during the historical period increases this value to 2930 m^3/s and it further increases to 3277 m^3/s using the estimated magnitudes of these floods.

- There is an added value in using historical information and preferable the magnitude of the historical floods. Using historical flood information extend the flood record and it is especially useful when the length of systematic record is short.

- Paleohydrological information can be used to extend the flood records beyond the information from systematic data. Detailed CT-scan of a 18.0 cm long sediment core, covering the last approximately 65 years) from Flyginnsjøen indicates a link between sediment layers in the core and bifurcation events in Glomma at Kongsvinger (known from instrumental period 1950-2013). 19 of 24 bifurcation events could be linked to a sediment layer, giving a critical success-index of 0.66. This link validates a that a 516 cm long core from the same lake covering the Holocene record could be used to extract flood information for the previous 10 000 years. From this paleohydrological flood information one hundred and fifty-five floods since year 1200 were added to the flood record.

- Using paleohydrological data in flood frequency analysis influences the design flood estimation. The return levels of the design floods (Q20, Q200 and Q1000) are generally lower when using paleohydrological flood information. Ex. the estimated 200-year flood using systematic data from Elverum station before regulations is estimated to have a discharge of 2872 m^3/s. Using paleohydrological flood information decreases this value to 2758 m^3/s

- The use of paleodata in flood frequency analysis is challenging due to non-stationarity caused either by climatic changes – or a change in river geometry.

Suggestions for further research

A major limitation in using historical flood information in the flood frequency analysis is the nature of the flood information available. In this study, water levels on flood monuments are used and stationarity of the river profile is assumed. In other cases, the information about flood damages rather than flood levels is all that is available. In Norway, flood damage information from large floods is typically sourced from either written documents or tax reduction records, which indicate the farms that suffered flood damage. Using this type of historical flood information is more time consuming and requires detailed mapping combined with routing models in order to assess the flood magnitudes which have caused damage.

This propose suggestions for further study of historical flood information. There have not been done much study about the use of historical- and paleohydrological flood information in flood frequency analysis, so there are still a lot to be discovered and studied:

- Investigating more historical flood sources in Norway to obtain even more flood information.

- The CT-scanner I used in my study gave better and more detailed information of a 18 cm long sediment core. A suggestion for future research is to scan more sediment cores with this CT-scanner. It would have been interesting to scan an even longer sediment core in the CT-scanner, and this could be potential topic for another master thesis.

- Another suggestion for further research is to use a longer time (and more floods) from the paleohydrological flood information to extend the flood record further, and do new flood frequency analysis based on this. A huge challenge is then to consider the non-stationarity through Holocene.

- The two different methods the historical data are used in the flood frequency analysis give significantly different results especially considering the period before regulations in Glomma. Further investigation and analysis of these differences could be interesting.

- The use of paleohydrologic data has a potential to find connection between changes in climate and in flood frequency, and this could help us to predict the flood frequency in a future climate. Therefore, the study of paleohydrological sediment cores need to be investigated further.

Appendix

Together with this master thesis there are 5 attachments;

1. CT-scan
   Contains the complete CT-scan of sediment core FLS113.
2. Bifurcation events
   Contain the list of bifurcation events (days and discharge values) from 1950-2013.
3. Age-depth-model
   Contains the age-depth-model based on sediment core FLS213.
4. R-scripts
   Contains the R-script used to make figures and graphs in this study.
5. Data used in R and in flood frequency analysis
   Contains the data used to make figures and to do flood frequency analysis.

References

Appleby, P. G., Piliposian, G. T. (2014) **Radiometric Dating of Lake Sediment Cores from Flyginnsjøen and Vingersjøen, Southern Norway, Provisional Report.** Environmental Radioactivity Research Centre, University of Liverpool, Liverpool.

Bergström, S. (1992) **The HBV-model – its structure and applications**. SMHI RH, No 4. April.

Byggteknisk forskrift (TEK 10), *Direktoratet for byggkvalitet* (2016).

Bøe, A. G., Dahl, S. O., Lie, O. & Nesje, A. (2006) **Holocene River Floods in the Upper Glomma Catchment, Southern Norway: A High-Resolution Multiproxy Record from Lacustrine Sediments.** *The Holocene*, 16, 445-455.

CEH, Center for Ecology & Hydrology, Natural Environment Research Council (w/o. y.) **Flooding** [Internet]. Available from < https://www.ceh.ac.uk/our-science/science-issues/flooding > [Read November 10th. 2016].

CEH, Centre for Ecology & Hydrology, Natural Environment Research Council (2016) **FEH – Flood estimation Handbook** [Internet]. Available from < http://www.ceh.ac.uk/services/flood-estimation-handbook > [Read January 16th. 2017].

Cohn, T.A., Stedinger, J.R. (1987) **Use of historical information in a maximum-likelihood framework.** *J. Hydrol.* 96, 215-223.

Cunnane, C. (1978) **Unbiased plotting positions – A review**: *Journal of Hydrology* 37, May, 205-222.

Dartmouth Flood Observatory Homepage (2006) **1991 Global Register of Major Flood Events** [Internet]. Available from < http://www.dartmouth.edu/~floods/Archives/1991sum.htm > [Read December 11th. 2017].

Dirceu, S. R. Jr., Stedinger, J.R. (2005) **Bayesian MCMC flood frequency analysis with historical information.** *Journal of Hydrology,* 313, 97–116.

Eikenæs, O., Njøs, A., Østdahl, T. & Taugbøl, T. (2000) **Flommen Kommer... Sluttrapport ra HYDRA - et forskningsprogram om flom**. *HYDRA,* NVE, Oslo.

Embrechts, P., Klüppelberg, C., Mikosch, T. (1997) **Modelling Extremal Events for Insurance and Finance.** *Springer International Publishing AG.*

Engeland, K., Wilson, D., Borsányi, P., Roald, L.A., Holmqvist, E. (2017) **Use of historical data in flood frequency analysis – a case study in four catchments in Norway**, *Hydrology Research* (submitted).

Exact Metrology (2017) **Industrial CT-scanning Services** [Internet]. Available from < http://www.exactmetrology.com/3d-scanning-services/industrial-ct-scanning-services > [Read March 3rd. 2017].

Finans Norge (2017) **Naturskadestatistikk (NASK)** [Internet]. Available from < https://www.finansnorge.no/statistikk/skadeforsikring/Naturskadestatistikk-NASK/ > [Read February 25th 2017].

Fisher, R. A., Tippett,L. H. C. (1928) **Limiting forms of the frequency distribution of the largest or smallest member of a sample.** *Proceedings of the Cambridge Philosophical Society,* vol 24, 1928, pp. 180–290.

Flomsteinen ved Norsk Skogbruksmuseum (2017) [Digitalized photography] Available from < https://no.wikipedia.org/wiki/Glomma > [April 18th. 2017].

Gaal, J.L, Szolgay, A., Kohnova, S., Hlavcoc, K. (2010) **Inclusion of historical information in flood frequency analysis using a Bayesian MCMC technique: a case study for the power dam Orl´ık, Czech Republic**. *Contributions to Geophysics and Geodesy,* Vol. 40/2, 121–147.

GEOCACHING (2011) **Hjulstrom Curve – The Power of Water** [Internet]. Available from < https://www.geocaching.com/geocache/GC36PZM_hjulstrom-curve-the-power-of-water?guid=4e69322d-4f34-4fcb-b9aa-3087ee01fb4c > [Read 5th June 2017].

Gilli, A., Anselmetti, F. S., Ariztegui, D., McKenzie, J. A. (2003) **A 600-Year Sedimentary Record of Flood Events from Two Sub-Alpine Lakes (Schwendiseen, Northeastern Switzerland).** *Eclogae Geologicae Helvetiae*, 96**,** S49-S58.

Gilli, A., Anselmetti, F. S., Glur, L., Wirth, S. B. (2013) **Lake Sediments as Archives of Recurrence Rates and Intensities of Past Flood Events.** *Dating Torrential Processes on Fans and Cones.* Volume 47, 225-242.

Giovanoli, F. (1990) **Horizontal Transport and Sedimentation by Interflows and Turbidity Currents in Lake Geneva.** *Large Lakes.* Springer Berlin Heidelberg.

GLB (1947) **Glommens og Laagens Brukseierforening 1918-43**, *Grøndahl & Søns Boktrykkeri*, Oslo.

Goslar, T. (2014) Poznan Radiocarbon Laboratory, Poland. Poznan Radiocarbon Laboratory, Poznan, Polen.

Gnedenko, B (1943) **Sur la distribution limite du terme maximum d'une s´erie al´eatoire.** *Annals of Mathematics,* vol 44, 1943, pp. 423–453.

Grønsten, H. A., Halmrast, K., Hisdal, H., Jensen, T., Melvold, K., Magnussen, I., Midttømme, G. H., Molkersrød, K., Nelson, G. N., Pedersen, T. B., Sommer-Erichson, P. (2015) **NVEs Klimatilpasningsstrategi 2015-2019.** NVE, Oslo.

Hanssen-Bauer, I. & Forland, E. (2000) **Temperature and Precipitation Variations in Norway 1900–1994 and Their Links to Atmospheric Circulation.** *International Journal of Climatology*, 20**,** 1693-1708.

Hanssen-Bauer, I., Forland, E., Haugen, J. & Tveito, O. (2003) **Temperature and Precipitation Scenarios for Norway: Comparison of Results from Dynamical and Empirical Down-Scaling.** *Climate Research*, 25**,** 15-27.

Hanssen-Bauer, I., Forland, E., Roald, L. A., Hisdal, H., Lawrence, D., Drange, H., Nesje, A., Vasskog, K., Sandven, S., Adlandsvik, B. & Sundby, S. (2009) **Klima I Norge I 2100 - Bakgrunnsmateriale Til Nou Klimatilpasning.** *Nou Klimatilpasning.* Norsk Klimasenter, Oslo.

Hanssen-Bauer, I., Førland, E. J., Haddeland, I., Hisdal, H., Mayer, S., Nesje, A., Nilsen, J. E. Ø., Sandven, S., Sandø, A., B., Sorteberg, A., Ådlandsvik, B. (2015) **Klima i Norge 2100. Kunnskapsgrunnlag for klimatilpasning, oppdatert 2015,** *NCCS report* no. 2/2015

Hegge, K. (1968) **Glommas Bifurkasjon Ved Kongsvinger**. Norsk Geografisk Tidsskrift - Norwegian *Journal of Geography*, 22, 166-171.

Hegge, K. (1997) **Vårflommen i Glomma 1995.** Glommens og Laagens Brukseierforening.

Hirsch, R. M., Stedinger, J. R. (1987) **Plotting positions for historical floods and their precision.** *Water Resources Research,* 23(4), 715–727, doi:10.1029/WR023i004p00715

IPCC (2007) **Climate Change 2007 Synthesis Report.** In Barker, T. (ed.). *Intergovernmental Panel on Climate Change*, Valencia, Spania.

IPCC (2012) **Summary for Policymakers In: Managing the Risks of the Extreme Events and Disasters to Advance Climate Change Adaption** In Allen, S. K., Barros, V., Burton, I., Campbell-Lendrum, D., Cardona, O.-D., Cutter, S. L., Dube, O. P., Ebi, K. L., Field, C. B., Handmer, J. W., Lal, P. N., Lavell, A., Mach, K. J., Mastrandrea, M. D., McBean, G. A., Mechler, R., Mitchell, T., Nicholls, N., O'Brien, K. L., Oki, T., Oppenheimer, M., Pelling, M., Plattner, G.-K., Pulwarty, R. S., Seneviratne, S. I., Stocker, T. F., Aalst, M. K. v., Vera, C. S. & Wilbanks, T. J. (eds.). *Intergovernmental Panel on Climate Change, Cambridge,* Storbritannia og New York, USA.

Jarrett, R. D., Tomlinson, E., M. (2000) **Regional interdisciplinary paleoflood approach to assess extreme flood potential**, *Water Resour. Res*., 36(10), 2957–2984, doi:10.1029/2000WR900098.

Killingtveit, A. (1996) **Flood regimes and flood prevention in Norway: Lessons learnt from the 1995 flood.** *Recent trends of floods and their preventive measures.*

Kjeldsen, T.R., Macdonald, N., Lang, M., Mediero, L., Albuquerque, T., Bogdanowicz, E., Brazdil, R., Castellarin, A., David, V., Fleig, A., Gül, G.O., Kriauciuniene, J., Kohnova, S., Merz, B., Nicholson, O., Roald, L.A., Salinas, J.L., Sarauskiene, D., Sraj, M., Strupczewski, W., Szolgay, J., Toumazis, A., Vanneuville, W., Veijalainen, N. & Wilson, D. (2014) **Documentary evidence of past floods in Europe and their utility in flood frequency estimation.** *Journal of Hydrology*, 517, 963–973, doi:10.1016/j.jhydrol.2014.06.038.

Klæboe, H. (1946) **Glommas Bifurkasjon Ved Kongsvinger**. Norsk Geografisk Tidsskrift - Norwegian *Journal of Geography*, 11, 266-275.

Kongsvinger Kommune (2003) **Kommuneplanens arealdel 2003-2014 – planbestemmelser –** *Kommuneplanbestemmelser vedtatt av kommunestyret 4.9.2004*

Lilleengen, A. M., Hagerud, T., Thomassen, H., Delphin, A., Delphin, J. C., Kristiansen, G. (2005) **Kongsvinger Golf Og Friluftspark Liermoen**. In kommune, K. & fylkeskommune, H. (eds.).

Lundquist, D., Repp, K. (1997) **The 1995 flood in southeastern Norway. Operational forecasting, warning and monitoring of a 200-year flood.** *Destructive Water: Water-Caused Natural Disasters, their Abatement and Control (Proceedings of the Conference held at Anaheim, California, June 1996),* IAHS Publ. no. 239.

Lyell, C. (1837) **Principles of Geology: Being an Inquiry How Far the Former Changes of the Earth's Surface Are Referable to Causes Now in Operation***,* J. Kay, jun. & brother.

Midttømme, G.H., Pettersson, L. E., Holmqvist, E., Nøtsund, Ø., Hisdal, H., Sivertsgård, R. (2011) **Retningslinjer for flomberegninger**, NVE, Oslo.

Milly, P. C. D., Betancourt, J., Falkenmark, M., Hirsch, R. M., Kundzewicz, Z. W., Lettenmaier, D. P. & Stouffer, R. J. (2008) **Stationarity Is Dead: Whither Water Management?** *Science*, 319, 573-574.

National Oceanic and Atmospheric Administration's National Weather Service (2015) **Hydrological Information Center – Flood Loss Data** [Internet]. NWS Internet Services Team. Available from < http://www.nws.noaa.gov/hic/ > [Read March 4th. 2017].

NERC (1975), **Flood Studies Report.** *Natur. Environ. Res.* Council, London, Cols 1-5, 1100 pp.

NGU (2017) **Map over soils in Kongsvinger-area** < http://geo.ngu.no/kart/losmasse/?Box=323355:6666003:351420:6683786 >

Nesje, A. (1992) **A Piston Corer for Lacustrine and Marine Sediments**. *Arctic and Alpine Research 24(3)*, 257-259.

Nesje, A. (2009) **Latest Pleistocene and Holocene Alpine Glacier Fluctuations in Scandinavia.** *Quaternary Science Reviews*, 28, 2119-2136.

Nesje, A., Lie, O. & Dahl, S. O. (2000) **Is the North Atlantic Oscillation Reflected in Scandinavian Glacier Mass Balance Records?** *Journal of Quaternary Science*, 15, 587-601.

Nesje, A., Dahl, S. O., Matthews, J. A. & Berrisford, M. S. (2001) **A~ 4500 Yr Record of River Floods Obtained from a Sediment Core in Lake Atnsjoen, Eastern Norway.** *Journal of Paleolimnology*, 25, 329-342.

Nesje, A., Bakke, J., Dahl, S. O., Lie, O. & Matthews, J. A. (2008) **Norwegian Mountain Glaciers in the Past, Present and Future**. *Global and Planetary Change*, 60, 10-27.

Nesje, A., Dahl, S., Thun, T. & Nordli, O. (2008) **The 'Little Ice Age'glacial Expansion in Western Scandinavia: Summer Temperature or Winter Precipitation?** *Climate Dynamics*, 30, 789-801.

NVE (w/o. y.) **Sildre** [Internet] Available from < http://sildre.nve.no > [Read: April 3rd. 2017].

NVE (2014) NVE Atlas. NVE, Oslo.

NVE, Jernbaneverket, Statens vegvesen (2014) **Karakterisering av flomregimer**, *Naturfareprosjektet Dp. 5 Flom og vann på avveie, delprosjekt 5.1.5,* Revisjon av rapport 13-2014

NVE (2016) **1789: Storofsen i Vågå** [Internet]. Available from < https://www.nve.no/om-nve/vassdrags-og-energihistorie/nves-historie/1789-storofsen-i-vaga/ > [Read February 25th. 2017].

NVE (2001) **1789 – Storofsen i Vågå** [Digitalized photography] Available from < https://www.nve.no/om-nve/vassdrags-og-energihistorie/nves-historie/1789-storofsen-i-vaga/ > [February 25th. 2017].

NVE (2017) **NEVINA, NEdbørfelt-Vannføring-INdeks-Analyse** [Internet] Available from < www.nevina.nve.no > [Read June 9th. 2017].

Orsi, T.H., Anderson, A., L. (1999) **Bulk density calibration for X-ray tomographic analysis of marine sediments,** *Geo-Mar. Lett. 19.*

Otnes, J. (1982) **Gamle flommerker langs Glåma**. *Årbok for Glåmdalen.*

Payrastre, O., Gaume, E., Andrieu, H. (2011) **Usefulness of historical information for flood frequency analyses: Developments based on a case study**. *Water Resour. Res.*, 47, W08511, doi:10.1029/2010WR009812.

Pettersson, L. E. (2000) **Flomberegning for Glommavassdraget Oppstrøms Vorma**. NVE, Oslo.

Pettersson, L. E. (2001) **Glommas Bifurkasjon Ved Kongsvinger**. NVE, Oslo.
Payrastre, O., Gaume, E., Andrieu, H. (2011) **Usefulness of historical information for flood frequency analyses: Developments based on a case study**, *Water resources research,* 47, doi:10.1029/2010WR009812

Reis, D. S., Stedinger, J. R. (2005) **Bayesian MCMC flood frequency analysis with historical information,** *Journal of Hydrology* 313, 97-116.

Renberg, I. & Hansson, H. (2008) **The Hth Sediment Corer**. *Journal of Paleolimnology*, 40**,** 655-659.

Roald, L. (2003) **Two Major 18 Th Century Flood Disasters in Norway**. *Palaeofloods, Historical Floods and Climatic Variability: Applications in Flood Risk Assessment (Proceedings of the PHEFRA Workshop, Barcelona, 16-19th October, 2002).*

Roald, L. A. (2013) **Flom I Norge,** Forlaget Tom og Tom 2013 og NVE, Vestfossen.

Roald, L. A., Hisdal, H., Hiltunen, T., Hyvarinen, V., Jutman, T. R., Gudmundsson, K., Jonsson, P. & Ovesen, N. B. (1997) **Historical Runoff Variation in the Nordic Countries**. *IAHS PUBLICATION*, 246, 87-96.

Sandersen, F., Bakkehoi, S., Hestnes, E. & Lied, K. (1997) **The Influence of Meteorological Factors on the Initiation of Debris Flows, Rockfalls, Rockslides and Rockmass Stability**. *Publikasjon-Norges Geotekniske Institutt*, 201**,** 97-114.

Schillereff, D. N., Chiverrell, R. C., Macdonald, N. & Hooke, J. M. (2014) **Flood Stratigraphies in Lake Sediments: A Review.** *Earth Science Reviews, 135, 17-37.*

Sollid, J. L., Kristiansen, K. (1982) **Hedmark Fylke, Kvartærgeologi Og Geomorfologi**. In Geografisk institutt, U. i. O. (ed.). Oslo.

Stedinger, J. R., Cohn, T., A. (1986) **Flood Frequency Analysis With Historical and Paleoflood Information**. *Water Resour. Res.*, 22(5), 785–793, doi:10.1029/WR022i005p00785.

Stenius, S., Glad, P. A., Wilson, D. (2014) **Naturfareprosjektet Dp. 5 Flom og vann på avveie Karakterisering av flomregimer.** Delprosjekt 5.1.5 Revisjon av rapport 13-2014, NVE, Oslo.

Stenius, S., Glad, P. A., Wilson, D. (2014) **Naturfareprosjektet Dp. 5 Flom og vann på avveie Karakterisering av flomregimer.** Delprosjekt 5.1.5 Revisjon av rapport 13-2014, NVE, Oslo. [Digitalized photography] Available from < http://publikasjoner.nve.no/rapport/2014/rapport2014_35.pdf > [January 16th. 2017].

Steffensen, I. G., (2014) **Rekonstruksjon av storflommer i Glomma gjennom holosen – mulige koblinger til naturlig klimavariabilitet og global atmosfærisk sirkulasjon.** UiB, Bergen.

Støren, E. N., Dahl, S. O. & Lie, O. (2008) **Separation of Late-Holocene Episodic Paraglacial Events and Glacier Fluctuations in Eastern Jotunheimen, Central Southern Norway**. *The Holocene*, 18**,** 1179

Støren, E. N., Dahl, S. O., Nesje, A. & Paasche, O. (2010) **Identifying the Sedimentary Imprint of High-Frequency Holocene River Floods in Lake Sediments: Development and Application of a New Method.** *Quaternary Science Reviews*, 29, 3021-3033.

Støren, E. N., Kolstad, E. W. & Paasche, O. (2011) **Linking Past Flood Frequencies in Norway to Regional Atmospheric Circulation Anomalies**. *Journal of Quaternary Science, 27(1), 71-80*.

Støren, E. N., Paasche, O. (2014) **Scandinavian Floods: From Past Observations to Future Trends.** *Global and Planetary Change*, 113, 34-43.

Støren, E. N., Bakke, J., Engeland, K., E. W. Kolstad, Paasche, Ø., Aano, A. (modified from Hegge, K., 1968) (2017) **Integrating lake sediment paleoflood reconstructions in Norwegian flood frequency scenarios.** Pages 5th Open Science Meeting; Zaragosa, Spain, 2017-05-09 - 2017-05-13.

Sælthun, N. R. (1997) **Regional flomfrekvensanalyse for norske vassdrag**. Rapport nr. 14-97, NVE.

Sælthun, N. R. (1999) **Flommer og flomberegninger.** Institutt for geofysikk, Universitetet i Oslo, Oslo.

Sælthun, N. R. (2016) **Flomstøtte Grindalen** [Digitized photography] Available from < https://wiki.uio.no/mn/geo/hydro/index.php/Flomst%C3%B8tte_Grindalen > [April 18th 2017].

Thompson, R., Battarbee, R., O'Sulliuan, P. & Oldfield, F. (1975) **Magnetic Susceptibility of Lake Sediments.** *Limnology and Oceanography, 20(5), 687-698*.

Thorndycraft, V., Hu, Y., Oldfield, F., Crooks, P. & Appleby, P. (1998) **Individual Flood Events Detected in the Recent Sediments of the Petit Lac D'annecy, Eastern France**. *The Holocene*, 8, 741-746.

Thorndycraft, V., Benito, G., Rico, M., Sopena, A., Sanchez-Moya, Y. & Casas, A. (2005) **A Long-Term Flood Discharge Record Derived from Slackwater Flood Deposits of the Llobregat River, Ne Spain**. *Journal of Hydrology*, 313, 16-31.

Thorndycraft, V. & Benito, G. (2006) **Late Holocene Fluvial Chronology of Spain: The Role of Climatic Variability and Human Impact.** *Catena*, 66, 34-41.

Uvo, C. B. (2003) **Analysis and Regionalization of Northern European Winter Precipitation Based on Its Relationship with the North Atlantic Oscillation**. *International Journal of Climatology*, 23, 1185-1194.

Vanniere, B., Magny, M., Joannin, S., Simonneau, A., Wirth, S., Hamann, Y., Chapron, E., Gilli, A., Desmet, M., Anselmetti, F. (2013) **Orbital Changes, Variation in Solar Activity and Increased Anthropogenic Activities: Controls on the Holocene Flood Frequency in the Lake Ledro Area, Northern Italy**. *Climate of the Past*, 9, 1193-1209.

Vasskog, K., Nesje, A., Storen, E. N., Waldmann, N., Chapron, E. & Ariztegui, D. (2011) **A Holocene Record of Snow-Avalanche and Flood Activity Reconstructed from a Lacustrine Sedimentary Sequence in Oldevatnet, Western Norway**. *The Holocene*, 21, 597-614.

Viglione, A., Castellarin, A., Rogger, M., Merz, R., Blöschl, G. (2012) **Extreme rainstorms: Comparing regional envelope curves to stochastically generated events**, *Water Resources Res.*, 48, W01509, doi:10.1029/2011WR010515.

Viglione, A., Merz, R., Salinas, J.L., Blöschl, G. (2013) **Flood frequency hydrology: 3. A Bayesian analysis**, *Water resources research, vol. 49,* 675-692.

Vormoor, K., Lawrence, D., Schlichting, L., Wilson, D., Wong, W. K. (2016) Evidence for changes in the magnitude and frequency of observed rainfall vs. snowmelt driven floods in Norway, *J. Hydrol.,* 538, 33–48.

Walker, M. J. C. (2005) Quaternary Dating Methods, Wiley.

Wilson, D., Fleig, A. K., Lawrence, D., Hisdal, H., Pettersson, L. E., Holdmqvist E. (2011) A review of NVE's flood frequency estimation procedures, *NVE report*, NVE, Oslo.

Wilhelm, B., Arnaud, F., Sabatier, P., Magand, O., Chapron, E., Courp, T., Tachikawa, K., Fanget, B., Malet, E., Pignol, C. (2013) Palaeoflood Activity and Climate Change over the Last 1400 Years Recorded by Lake Sediments in the North-West European Alps. *Journal of Quaternary Science*, 28, 189-199.

Yen, C. Y. (1933) The 1931 Flood in China: An Economic Survey by the Department of Agricultural Economics, College of Agriculture and Forestry, the University of Nanking, in Co-Operation with the National Flood Relief Commission. *American Journal of Sociology 39, no. 1 (Jul., 1933): 152.*

Østmoe, A. (1985) Stor-Ofsen 1789. *Oversiktsregisteret, Ski*.